

# Sticky Prices for Inflationary Economies: A Tractable Linear Approximation to Menu Cost Models with Trend Inflation

JONATHAN J. ADAMS\*

Federal Reserve Bank of Kansas City

March 13, 2026

WORKING PAPER

[Link to Most Current Version](#)

## Abstract

When inflation is low, the Calvo model is a good approximation of sticky prices. But when inflation is high, menu costs matter for macroeconomics. Drawing from recent work on mean field games, I derive an analytical solution to the menu cost model with trend inflation in response to small shocks. The solution includes dynamics of the value function, distribution of price gaps, and aggregate variables. Then, I consider a discrete time approximation that is tractable enough for use in standard DSGE models. Menu costs modify the usual Calvo Phillips curve with a single variable: the *frequency of price adjustment*. Accounting for the frequency matters in an inflationary economy; when trend inflation is zero, the term disappears. But surprisingly, the effect of trend inflation on the Phillips curve is first-order. The modified system is a function of the microfoundations and can be calibrated to match pricing statistics, a useful result even without trend inflation. Finally, I embed the price-setting block in an otherwise standard New Keynesian model and show how menu costs and trend inflation affect monetary policy.

**Keywords:** State-dependent pricing, menu costs, inflation, Phillips curve, mean field games, optimal monetary policy

**JEL-Codes:** C60, E31, E52

---

\*email: [adamsjonathanj@gmail.com](mailto:adamsjonathanj@gmail.com), website: [jonathanjadams.com](http://jonathanjadams.com). First public version: February 15 2026. I am grateful for feedback from seminar participants at the BLS and Kansas City Fed. The views expressed are those of the author and do not necessarily reflect the positions of the Federal Reserve Bank of Kansas City or the Federal Reserve System.

# 1 Introduction

Do menu costs or other models of state-dependent pricing matter for macroeconomics? The answer depends on the inflation environment. When trend inflation is close to zero, the Calvo (1983) model of random adjustment opportunities gives an accurate approximation of the Phillips curve, if correctly parameterized (Auclert et al., 2024). On the other hand, when trend inflation is high, state-dependent price setting is fundamentally different than the Calvo model, and menu costs matter for macroeconomic dynamics. However, menu cost models are not well understood in this case. Most well-known theoretical results are derived under zero trend inflation, because it is precisely the edge case where the endogenous frequency of price adjustment is irrelevant, and the model simplifies (Alvarez and Lippi, 2022). Therefore, high inflation settings are both where menu costs matter most, and where economists understand them the least.

This paper addresses this gap with three main contributions. First, I derive an analytical solution to the mean field game (MFG) for a menu cost model with trend inflation. Addressing the entire MFG allows me to characterize how the value function, pricing decisions, inaction region, and distribution of prices evolve in response to shocks. With low trend inflation, some of these features are not quantitatively important; Alvarez and Lippi (2014) and Cavallo et al. (2024) show that a fixed inaction region is an accurate approximation. But when there is non-trivial trend inflation, the firm’s value and decisions are more elastic, so the entire MFG is needed. To derive the solution, I draw on insights from Alvarez et al. (2023), who give a linear representation of the MFG in response to small shocks. Their assumption of zero trend inflation implies that they can ignore the “reinjection” of price-resetting firms to the distribution of price gaps, which allows for a simple solution to the Kolmogorov Forward Equation (KFE). However when there is trend inflation, this reinjection matters. To handle it, I apply results from Adams (2025), which illustrates how the dynamic distribution determines the endogenous reinjection process.

Second, I tackle another challenge facing menu cost models: they are relatively intractable. Their relevant state variable is an infinite-dimensional distribution of price gaps, which means that they are usually solved numerically and analyzed in partial equilibrium. To be useful for policy analysis, it would be valuable to have a representation that fits neatly in existing general equilibrium models, without introducing too much additional complexity.<sup>1</sup> To this end, I derive a low-dimensional discrete time approximation to the MFG solution: the *primary eigenvalue decomposition* (PED). Each component of the full solution is associated with a particular eigenvalue in the KFE, but in practice only a few eigenvalues matter quantitatively. I show that the PED, which uses just the most important eigenvalue, is a reasonably accurate approximation to the full solution.

The PED is much more tractable, while retaining the realism and interesting features of the full solution. In particular, the PED implies a dynamic Phillips curve that nests the traditional New Keynesian Phillips

---

<sup>1</sup>Indeed, this is why the Calvo model became popular, compared to alternative models of staggered price-setting such as Taylor (1980).

curve:

$$\pi_t = \underbrace{\Lambda mc_t + \beta \mathbb{E}_t[\pi_{t+1}]}_{\text{Calvo term}} + \underbrace{\epsilon(\theta^{-1} F_t - \beta \mathbb{E}_t[F_{t+1}])}_{\text{FPA correction}} \quad (1)$$

The ‘‘Calvo term’’ is standard, except that the slope  $\Lambda$  is not given by the usual Calvo calibration. Menu costs however introduce an additional term, which depends on the *Frequency of Price Adjustment* (FPA). When there is zero trend inflation, the correction coefficient  $\epsilon$  is also zero, and equation (1) reduces to the New Keynesian Phillips curve, validating the numerical findings from Auclert et al. (2024). However, when trend inflation is nontrivial, the FPA dynamics matter for inflation dynamics. This is consistent with existing knowledge: empirical and simulation results agree that the correlation between inflation and the FPA is much stronger at high inflation rates.<sup>2</sup>

Why does the FPA show up in the Phillips curve? Because of the price-setting selection effect (Goloso and Lucas Jr., 2007): economy-wide inflation depends on the distribution of firms that change prices. Adams (2025) shows that the path of the FPA encodes all of the relevant features of the distribution of firms. Thus FPA dynamics are sufficient to capture time-variation in the selection effect.

Third, because the PED is so tractable, I show that it can be easily embedded in general equilibrium models and used for policy analysis. Since the PED equations’ coefficients are known analytically from the model’s microfoundations, they can be easily calibrated using pricing statistics. Doing so does not require solving the full non-linear dynamic model. This result is valuable even for practitioners studying low-inflation economies: while it was already known that the Calvo Phillips curve was an accurate approximation of a low-inflation menu cost economy, it was unclear how to calibrate it. After calibrating the PED, I embed it in an otherwise textbook New Keynesian model, in order to analyze dynamics and monetary policy in general equilibrium.

The PED reveals how menu costs amplify inflationary shocks relative to a Calvo structure. They do so through two channels: increasing the slope of the Phillips curve, and increasing the direct effect of the FPA on inflation. The Phillips curve effect is second-order when trend inflation is zero, consistent with the wide acceptance of using zero trend to approximate relatively low inflation economies.<sup>3</sup> However, the effect of trend inflation on the FPA coefficient is *first-order* at zero. This is because while trend inflation has second-order effects on firms’ decisions, it has first-order effects on aggregation. Therefore, in general equilibrium, modest rates of trend inflation lead to substantially amplified dynamics relative to the driftless calibration. For example, in the simple New Keynesian-style model, raising the annual trend inflation rate from 0% to 5% increases the CIR of inflation to cost shocks by roughly one fourth.

The PED easily demonstrates how menu costs affect optimal monetary policy. Consistent with the (Goloso and Lucas Jr., 2007) story, menu costs cause the economy to act as if price are more flexible

<sup>2</sup>See for example Gagnon (2009); Nakamura et al. (2018); Alvarez et al. (2019); Montag and Villar (2025); Gagliardone et al. (2025).

<sup>3</sup>For example, Nakamura et al. (2018) and Alvarez et al. (2019) correctly argue that zero trend inflation accurately approximates the Phillips curve under the low inflation rates experienced by rich countries at the beginning of the 21st century, because the effects on firms’ decision rules are second-order.

than in a Calvo model. This yields a textbook implication: monetary policy optimally becomes more aggressive, because real shocks have larger effects on inflation. But trend inflation changes the calculus. As trend inflation increases, the Phillips curve slope increases, so optimal policy becomes even more aggressive. Moreover, trend inflation amplifies the inflationary feedback through the FPA. Thus accounting for the endogenous price adjustment increases the optimal monetary policy response even further.

Within the extensive menu cost literature, this paper is closely related to a few ongoing lines of inquiry. Blanco et al. (2024) work to address the tractability of menu cost models by developing a theory in which multi-product firms choose how many (but not which) of their prices to adjust. This assumption eliminates the need to track the distribution of firms, allowing for exact aggregation with a simple non-linear Phillips curve, in which the FPA appears. As an alternative to approximating or simplifying the model, Karadi et al. (2025) study optimal monetary policy in the full nonlinear menu cost setting, focusing on the response to large shocks. They also find that the endogenous FPA affects optimal policy; when inflation is high and the Phillips curve is steep, it is optimal for monetary policy to take advantage of the heightened slope and respond aggressively.<sup>4</sup>

The remainder of the paper is organized as follows. Section 2 lays out the model. Section 3 derives the analytical solution to the pricing block. Readers who prefer to avoid the partial differential equations should skip to Section 4, which introduces the PED. Section 5 evaluates the approximation accuracy quantitatively. If the reader is a practitioner who simply wants to see the approximation summarized and embedded in a linear general equilibrium model, they should skip to Section 6, which studies the quantitative effects of menu costs and trend inflation on dynamics and monetary policy. Section 7 concludes.

## 2 General Equilibrium Model

I consider a general equilibrium model most similar to Alvarez et al. (2024), where firms face menu costs and idiosyncratic shocks, leading to state-dependent price adjustments. The economy consists of a representative household, a central bank that conducts monetary policy, and firms facing price-setting frictions.

### 2.1 Households and Monetary Policy

The representative household maximizes lifetime utility:

$$\int_0^\infty e^{-\rho t} \left[ \frac{C(t)^{1-\sigma_C} - 1}{1-\sigma_C} - \varkappa \frac{\sigma_L}{1+\sigma_L} L(t)^{\frac{1+\sigma_L}{\sigma_L}} \right] dt, \quad (2)$$

where  $C(t)$  is consumption and  $L(t)$  is labor supply. Consumption is a CES aggregate of differentiated goods:

$$C(t) = \left( \int_0^1 A_i(t) C_i(t)^{\frac{\eta-1}{\eta}} di \right)^{\frac{\eta}{\eta-1}} \quad (3)$$

---

<sup>4</sup>Beyond menu costs, this paper also contributes to a related literature exploring how trend inflation affects dynamics and monetary policy in New Keynesian models; Ascari and Sbordone (2014) provide a survey.

where  $A_i(t)$  is a stochastic preference shifter, and  $\eta > 1$  is the elasticity of substitution.

The household's budget constraint is given by

$$M(0) + \int_0^\infty Q(t) [W(t)L(t) + D(t) - P(t)C(t) - R(t)M(t)] dt \geq 0. \quad (4)$$

where  $W(t)$  is the nominal wage,  $D(t)$  are firms' profits paid as dividends,  $P(t)$  is the price level,  $R(t)$  is the nominal interest rate, and  $Q(t) = e^{-\int_0^t R(s)ds}$  is the price of a nominal bond.

The first order conditions for the household's problem are

$$e^{-\rho t} C(t)^{-\sigma_C} = \lambda_{HH} Q(t) P(t) \quad e^{-\rho t} \varkappa L(t)^{\frac{1}{\sigma_L}} = \lambda_{HH} Q(t) W(t) \quad (5)$$

where  $\lambda_{HH}$  is the household's Lagrange multiplier for the budget constraint. These first order conditions imply an intratemporal labor supply equation:

$$P(t) \varkappa L(t)^{\frac{1}{\sigma_L}} C(t)^{\sigma_C} = W(t) \quad (6)$$

and an intertemporal Euler equation

$$R(t) - \pi(t) - \rho = \sigma_C \frac{\dot{C}(t)}{C(t)} \quad (7)$$

where  $\pi(t) = \frac{\dot{P}(t)}{P(t)}$  denotes the inflation rate.

A central bank sets the nominal interest rate  $R(t)$  by a Taylor-type rule, as a function of the state of the economy.

The household and monetary policy side of the model is standard, and will be discussed further in Section 6 when the general equilibrium economy is analyzed. The firm side of the model is discussed in detail next.

## 2.2 Firms

Firms produce differentiated goods using labor as the only input:

$$Y_i(t) = \frac{1}{Z_i(t)} L_i(t) \quad (8)$$

where  $Z_i(t)$  represents stochastic idiosyncratic inverse productivity.  $Z_i(t)$  represents a quality shifter, so it is assumed to be perfectly correlated with the preference shifter, i.e.  $Z_i(t) = A_i(t)$ .<sup>5</sup>  $Z_i(t)$  is i.i.d. across firms, following a Brownian motion with variance  $2\nu$ .

Firms are monopolistic, so they set prices, but face menu costs. It is common to represent the firm's problem using a second order approximation around their frictionless optimal price. In this case, the profit

<sup>5</sup>As in Midrigan (2011), this assumption conveniently reduces the state space relative to Golosov and Lucas Jr. (2007).

lost in every period is the quadratic  $\mathbf{B}g_i(t)^2$ , where  $\mathbf{B} = \frac{\eta(\eta-1)}{2}$  and  $\eta$  is the price elasticity of demand. I adopt the language of Alvarez et al. (2024):<sup>6</sup>  $g_i(t)$  denotes the log “markup gap”, which is given by

$$g_i(t) \equiv \log \frac{P_i(t)}{Z_i(t)W(t)} - \mu \quad (9)$$

where  $\mu$  is the frictionless optimal markup. From this markup gap, it is useful to construct the firm’s state variable as a log “price gap”  $x_i(t)$ :

$$x_i(t) \equiv \log P_i(t) - \log Z_i(t) - \log \bar{W}(t) - \mu \quad (10)$$

where  $\bar{W}(t)$  is the long-run wage trend. In the inaction region  $\log P_i(t)$  is constant,  $\log Z_i(t)$  has no drift, and  $\log \bar{W}(t)$  grows at rate  $\bar{\pi}$ , so  $x_i(t)$  will have drift  $\mathbb{E}[dx_i(t)] = -\bar{\pi}dt$ .

Thus the markup gap is related to the price gap by

$$g_i(t) = x_i(t) - MC(t) \quad (11)$$

where  $MC(t) \equiv \log W(t) - \log \bar{W}(t)$  is the deviation from trend for the average log marginal cost across firms, because  $\log Z_i(t)$  is mean zero. To a first order approximation,<sup>7</sup> the economy-wide price index is  $\log P(t) = \int_0^1 \log P_i(t) di$ , so the price level can be written from the average price gap  $X(t) \equiv \int_0^1 \log x_i(t) di$  as

$$\log P(t) = X(t) + \log \bar{W}(t) + \mu \quad (12)$$

### 2.3 The Price Setting Problem

The firm faces a “Calvo-plus” pricing problem (Nakamura and Steinsson, 2010), which nests the simple menu cost case (Golosov and Lucas Jr., 2007).

If the firm wishes to change its price, it must pay real cost  $\Psi$ . However, it also receives Calvo-style free adjustment opportunities at rate  $\zeta$ . With this setup, the firm’s problem is characterized by its idiosyncratic state variable – the price gap  $x_i(t)$  – and the aggregate marginal cost  $MC(t)$ . From here on, I will drop the  $i$  subscripts.

As usual, menu costs imply an inaction region for firms. The firm chooses lower and upper bounds for the price gap  $\underline{x}(t)$  and  $\bar{x}(t)$ . Whenever its price gap  $x(t)$  reaches these bounds, or if the firm receives a random free adjustment, then it resets its price gap to some optimal  $x^*(t)$ . The firm’s problem is to choose the profit-maximizing path for  $x^*(t)$ ,  $\underline{x}(t)$ , and  $\bar{x}(t)$ .

<sup>6</sup>Reader beware: many papers refer to  $g_i(t)$  as the price gap, and treat it as the firm’s state variable.

<sup>7</sup>The true CES price index is  $P(t)^{1-\eta} = \int_0^1 \log P_i(t)^{1-\eta} di$ .

Inside the inaction region, the firm's Hamilton-Jacobi-Bellman (HJB) equation is given by

$$\rho v(x, t) = -\mathbf{B}(x - MC(t))^2 + \partial_t v(x, t) - \bar{\pi} \partial_x v(x, t) + \nu \partial_x^2 v(x, t) + \zeta (v(x^*(t), t) - v(x, t)) \quad (13)$$

where  $\bar{\pi}$  is the trend inflation rate, and  $2\nu$  is the variance of the productivity process. The boundary conditions for this problem are:

Value-matching	$v(\underline{x}(t), t) = v(x^*(t), t) + \Psi = v(\bar{x}(t), t)$
Reset optimality	$\partial_x v(x^*(t), t) = 0$
Smooth-pasting	$\partial_x v(\underline{x}(t), t) = 0 = \partial_x v(\bar{x}(t), t)$
Terminal condition	$v(x, T) = \phi_{term.}(x)$

## 2.4 The Kolmogorov Forward Equation (KFE)

When marginal costs are constant, the distribution of price gaps  $h(x, t)$  evolves according to the Kolmogorov forward equation:

$$\partial_t h(x, t) = \nu \partial_x^2 h(x, t) + \bar{\pi} \partial_x h(x, t) - \zeta h(x, t) + F(t) \delta(x - x^*(t)) \quad (14)$$

where  $F(t)$  is the *frequency of price adjustment* (FPA), and  $\delta(\cdot)$  is the Dirac delta. The boundary conditions for this PDE are:

Absorbing boundaries	$h(\underline{x}(t), t) = 0$	$h(\bar{x}(t), t) = 0$
FPA determination	$F(t) = \nu \partial_x h(\underline{x}(t), t) + \bar{\pi} h(\underline{x}(t), t) - \nu \partial_x h(\bar{x}(t), t) - \bar{\pi} h(\bar{x}(t), t) + \zeta$	
Initial condition	$h(x, 0) = \phi_{init.}(x)$	

Finally, there is an aggregation equation:

$$X(t) = \int_{\underline{x}(t)}^{\bar{x}(t)} x h(x, t) dx \quad (15)$$

which determines the average price gap  $X(t)$ .

## 3 The Mean Field Game

This section derives the equations governing the pricing mean field game in response to small shocks, and solves them.

### 3.1 Derivation of the Mean Field Game for Small Shocks

Consider the standard aggregate nominal cost shock: raising every firm's marginal cost enters the mean field game (MFG) through the profit function in the HJB. This is a distinction between the price gap and markup gap representations; the latter is common and is how Alvarez et al. (2023) represent the model. When the markup gap defined in equation (9) is used as a state variable, then a nominal cost shock shifts the distribution of state variables directly. In that case, a permanent marginal cost shock will enter the KFE instead of the HJB.<sup>8</sup>

Specifically, I consider a small unanticipated change to the path of aggregate nominal marginal costs  $MC(t)$  modified by a small scalar  $\kappa$ . This shock affects the HJB through the profit function:

$$\rho v(x, t) = \mathbf{B}(x - \kappa MC(t))^2 + \partial_t v(x, t) - \bar{\pi} \partial_x v(x, t) + \nu \partial_x^2 v(x, t) + \zeta(v(x^*(t), t) - v(x, t))$$

The shock does not affect the distribution  $h(x, t)$  directly. Instead, the distribution evolves according to the KFE, respecting the boundary conditions. This evolution depends on the critical points  $\underline{x}(t)$ ,  $\bar{x}(t)$ , and  $x^*(t)$ , which are endogenous responses to the shock through the HJB.

Denote the solution to the MFG with steady state initial condition and the  $\kappa$ -scaled path of aggregate shocks as the functions  $h(x, t, \kappa)$ ,  $v(x, t, \kappa)$ ,  $\underline{x}(t, \kappa)$ ,  $\bar{x}(t, \kappa)$ , and  $x^*(t, \kappa)$ .

To study small shocks analytically, we will solve for the derivative of the MFG solution with respect to the shock. When the solution functions are written with hats, they denote derivatives around the no-shock steady state:

$$\hat{h}(x, t) \equiv \partial_\kappa h(x, t, 0) \quad \hat{v}(x, t) \equiv \partial_\kappa v(x, t, 0) \quad \hat{\underline{x}}(t) \equiv \partial_\kappa \underline{x}(t, 0) \quad \hat{\bar{x}}(t) \equiv \partial_\kappa \bar{x}(t, 0) \quad \hat{x}^*(t) \equiv \partial_\kappa x^*(t, 0)$$

Proposition 1 shows that the derivative functions are themselves solutions to a MFG with a convenient form. Throughout, I denote steady-state values with a subscript  $ss$ : the steady-state distribution is  $h_{ss}(x)$ , the value function  $v_{ss}(x)$ , the frequency of price adjustment  $F_{ss}$ , and the critical points  $x_{ss}^*$ ,  $\underline{x}_{ss}$ ,  $\bar{x}_{ss}$ . For brevity, in integration limits, domain specifications, eigenfunction arguments, and coefficient subscript labels, I suppress the subscript and write  $\underline{x}$ ,  $\bar{x}$ , etc.

**Proposition 1.** *The derivative functions corresponding to the MFG with small aggregate shocks are themselves solutions to the following MFG:*

$$\rho \hat{v}(x, t) = 2\mathbf{B}x(-MC(t)) + \partial_t \hat{v}(x, t) - \bar{\pi} \partial_x \hat{v}(x, t) + \nu \partial_x^2 \hat{v}(x, t) + \zeta(\hat{v}(x^*, t) - \hat{v}(x, t)) \quad (16)$$

$$\hat{v}(\underline{x}, t) = \hat{v}(\bar{x}, t) = \hat{v}(x^*, t) \quad (17)$$

$$\partial_x \hat{v}(\underline{x}, t) + \partial_x^2 v_{ss}(\underline{x}) \hat{\underline{x}}(t) = \partial_x \hat{v}(\bar{x}, t) + \partial_x^2 v_{ss}(\bar{x}) \hat{\bar{x}}(t) = \partial_x \hat{v}(x^*, t) + \partial_x^2 v_{ss}(x^*) \hat{x}^*(t) = 0 \quad (18)$$

---

<sup>8</sup>A disadvantage of using the markup gap as a state variable is that transitory marginal cost shocks affect both the HJB and KFE, complicating the analysis. This is why I adopt the price gap as the state variable.

$$\hat{v}(x, T) = 0 \quad (19)$$

$$\partial_t \hat{h}(x, t) = \nu \partial_x^2 \hat{h}(x, t) + \bar{\pi} \partial_x \hat{h}(x, t) - \zeta \hat{h}(x, t) + \hat{F}(t) \delta(x - x_{ss}^*) - F_{ss} \delta'(x - x_{ss}^*) \hat{x}^*(t) \quad (20)$$

$$\hat{h}(\underline{x}, t) + h'_{ss}(\underline{x}) \hat{x}(t) = \hat{h}(\bar{x}, t) + h'_{ss}(\bar{x}) \hat{x}(t) = 0 \quad (21)$$

$$\hat{F}(t) = \nu \partial_x \hat{h}(\underline{x}, t) + \bar{\pi} \hat{h}(\underline{x}, t) - \nu \partial_x \hat{h}(\bar{x}, t) - \bar{\pi} \hat{h}(\bar{x}, t) \quad (22)$$

$$\hat{h}(x, 0) = 0 \quad x \in (\underline{x}, \bar{x}) \quad (23)$$

$$\hat{X}(t) = \int_{\underline{x}(t)}^{\bar{x}(t)} x \hat{h}(x, t) dx \quad (24)$$

*Proof:* Appendix A.1

### 3.2 Conditional Solutions to the MFG

This section derives the distribution  $\hat{h}(x, t)$  and value function  $\hat{v}(x, t)$  as *conditional* solutions to the MFG. Lemma 1 solves the HJB PDE conditional on the path of aggregate prices, while Lemma 2 solves the KFE PDE conditional on firms' pricing decisions. The complete solution will necessarily combine these two conditional solutions; they are valuable intermediate steps that are straightforward to derive.

**Lemma 1.** *The conditional solution to the HJB is the infinite sum*

$$\hat{v}(x, t) = \sum_{n=1}^{\infty} \hat{v}_n(x, t)$$

where

$$\hat{v}_n(x, t) = \Theta_{MC,n}(x) \int_t^T e^{-\lambda_{HJB,n}(\tau-t)} (-MC(\tau)) d\tau + \Theta_{v,n}(x) \int_t^T e^{-\lambda_{HJB,n}(\tau-t)} \hat{v}(x^*, \tau) d\tau$$

and

$$\lambda_{HJB,n} = \rho + \zeta + \frac{\bar{\pi}^2}{4\nu} + \frac{\nu n^2 \pi^2}{(\bar{x} - \underline{x})^2}$$

$$\gamma_{HJB,n}(x, y) \equiv \frac{2}{\bar{x} - \underline{x}} e^{\frac{-\bar{\pi}}{2\nu}(y-x)} \sin\left(\frac{n\pi(x - \underline{x})}{\bar{x} - \underline{x}}\right) \sin\left(\frac{n\pi(y - \underline{x})}{\bar{x} - \underline{x}}\right)$$

$$\Theta_{MC,n}(x) \equiv -2\mathbf{B} \int_{\underline{x}}^{\bar{x}} \gamma_{HJB,n}(x, y) y dy$$

$$\Theta_{v,n}(x) \equiv -\zeta \int_{\underline{x}}^{\bar{x}} \gamma_{HJB,n}(x, y) dy + \nu \partial_y \gamma_{HJB,n}(x, \underline{x}) - \nu \partial_y \gamma_{HJB,n}(x, \bar{x})$$

*Proof:* Appendix A.2

The conditional solution to the KFE is more complicated. This is because Property 3 only gives a direct solution for the distribution  $\hat{h}(x, t)$  on the *interior* of the inaction region. But the distribution depends on the FPA, and the FPA depends on properties of the distribution at the *boundaries*. This is because the

Green's function always satisfies the zero boundary conditions.

To address this, I follow a standard “lifting function” strategy. Because the KFE is linear, it is possible to separate into components that solve each non-homogeneous term in the PDE. First, an “interior” term  $\hat{h}_{\text{int}}$  is the component of the distribution that responds to the flow of resetting firms and satisfies the zero boundary conditions. Second, a “critical-point” term  $\hat{h}_{\text{crit}}$  is the component that satisfies the non-homogeneous boundary conditions and is unaffected by the FPA. This second term also includes the effects of the reset point changing over time, which is useful to address without the Green's function for computational reasons.

To state the KFE solution, define the lifting functions (derived in Appendix D):

$$H_{\underline{x}}(x) \equiv \frac{e^{r_2(x-\bar{x})} - e^{r_1(x-\bar{x})}}{e^{-r_2\ell} - e^{-r_1\ell}}, \quad H_{\bar{x}}(x) \equiv \frac{e^{r_1(x-\underline{x})} - e^{r_2(x-\underline{x})}}{e^{r_2\ell} - e^{r_1\ell}} \quad (25)$$

$$J_{x^*}(x) \equiv \begin{cases} -\frac{\psi_R(x^*)}{\nu W_N(x^*)} \psi'_L(x) & x < x^* \\ -\frac{\psi_L(x^*)}{\nu W_N(x^*)} \psi'_R(x) & x > x^* \end{cases} \quad (26)$$

where  $\ell \equiv \bar{x} - \underline{x}$  is the length of the inaction region. The characteristic roots are

$$r_{1,2} = (-\bar{\pi} \pm \sqrt{\bar{\pi}^2 + 4\nu\zeta})/(2\nu)$$

and the auxiliary functions are

$$\begin{aligned} \psi_L(x) &= r_2 e^{r_1(x-\underline{x})} - r_1 e^{r_2(x-\underline{x})} & \psi_R(x) &= r_2 e^{r_1(x-\bar{x})} - r_1 e^{r_2(x-\bar{x})} \\ W_N(x^*) &= \psi_L(x^*)\psi'_R(x^*) - \psi'_L(x^*)\psi_R(x^*) \end{aligned}$$

**Lemma 2.** *The conditional solution to the KFE is*

$$\hat{h}(x, t) = \hat{h}_{\text{crit}}(x, t) + \hat{h}_{\text{int}}(x, t)$$

where the critical-point component is

$$\hat{h}_{\text{crit}}(x, t) = -h'_{ss}(\underline{x})\hat{x}(t)H_{\underline{x}}(x) + h'_{ss}(\bar{x})\hat{x}(t)H_{\bar{x}}(x) - F_{ss}\hat{x}^*(t)J_{x^*}(x) \quad (27)$$

with  $H_{\underline{x}}$ ,  $H_{\bar{x}}$ , and  $J_{x^*}$  defined in (25)–(26), and the interior component is

$$\hat{h}_{\text{int}}(x, t) = \sum_{n=1}^{\infty} \hat{h}_{\text{int},n}(x, t)$$

$$\begin{aligned} \hat{h}_{\text{int},n}(x,t) &= e^{-\lambda_{KFE,n}t} \left( h'_{ss}(\underline{x})\hat{x}(0)\varpi_{H,\underline{x},n}(x) - h'_{ss}(\bar{x})\hat{x}(0)\varpi_{H,\bar{x},n}(x) + F_{ss}\hat{x}^*(0)\varpi_{J,n}(x) \right) \\ &+ \int_0^t e^{-\lambda_{KFE,n}(t-\tau)} \left( \varpi_{F,n}(x)\hat{F}(\tau) + F_{ss}\hat{x}^*(\tau)\varpi_{J,n}(x) + h'_{ss}(\underline{x})\hat{x}'(\tau)\varpi_{H,\underline{x},n}(x) - h'_{ss}(\bar{x})\hat{x}'(\tau)\varpi_{H,\bar{x},n}(x) \right) d\tau \end{aligned} \quad (28)$$

and

$$\begin{aligned} \lambda_{KFE,n} &\equiv \zeta + \frac{\bar{\pi}^2}{4\nu} + \frac{\nu n^2 \pi^2}{\ell^2}, \quad \ell \equiv \bar{x} - \underline{x} \\ \gamma_{KFE,n}(x,y) &\equiv \frac{2}{\ell} e^{\frac{\bar{\pi}}{2\nu}(y-x)} \sin\left(\frac{n\pi(x-\underline{x})}{\ell}\right) \sin\left(\frac{n\pi(y-\underline{x})}{\ell}\right) \\ \varpi_{F,n}(x) &\equiv \gamma_{KFE,n}(x,x^*) \quad \varpi_{J,n}(x) \equiv \int_{\underline{x}}^{\bar{x}} \gamma_{KFE,n}(x,y) J_{x^*}(y) dy \\ \varpi_{H,\underline{x},n}(x) &\equiv \frac{\nu}{\lambda_{KFE,n}} \partial_y \gamma_{KFE,n}(x,\underline{x}) \quad \varpi_{H,\bar{x},n}(x) \equiv \frac{\nu}{\lambda_{KFE,n}} \partial_y \gamma_{KFE,n}(x,\bar{x}) \end{aligned} \quad (29)$$

*Proof:* Appendix A.3

### 3.3 Aggregate Solution to the MFG

This section derives the integral equations describing the dynamics for aggregate variables solving the MFG.

The frequency of price adjustment  $\hat{F}(t)$  decomposes into *critical-point* and *interior* components:

$$\hat{F}(t) = \hat{F}_{\text{crit}}(t) + \hat{F}_{\text{int}}(t) \quad (30)$$

The critical-point component depends on the *levels* of the boundary locations  $\hat{x}^*(t)$ ,  $\hat{x}(t)$ ,  $\hat{\bar{x}}(t)$ . The interior component depends on the *time derivatives* (or in discrete time, *differences*) of these boundaries, and further decomposes into eigenfunctions:  $\hat{F}_{\text{int}}(t) = \sum_{n=1}^{\infty} \hat{F}_{\text{int},n}(t)$ . The aggregate gap  $\hat{X}(t)$  is expressed directly in terms of levels without this decomposition.

The critical-point coefficients for  $\hat{F}$  (no  $n$  subscript) are defined from the lifting functions in Lemma 2:

$$\varphi_{x^*} \equiv -F_{ss}\nu(J'_{x^*}(\underline{x}) - J'_{x^*}(\bar{x})) \quad \varphi_{\underline{x}} \equiv h'_{ss}(\underline{x})\nu(H'_{\underline{x}}(\underline{x}) - H'_{\underline{x}}(\bar{x})) \quad \varphi_{\bar{x}} \equiv h'_{ss}(\bar{x})\nu(H'_{\bar{x}}(\underline{x}) - H'_{\bar{x}}(\bar{x}))$$

The interior coefficients for  $\hat{F}$  depend on the eigenfunction index  $n$ , and are defined from the corresponding  $\varpi_{\cdot,n}(x)$  function (defined in Lemma 2):

$$\begin{aligned} \varphi_{x^*,n} &\equiv F_{ss}\nu(\varpi'_{J,n}(\underline{x}) - \varpi'_{J,n}(\bar{x})) \quad \varphi_{\underline{x},n} \equiv h'_{ss}(\underline{x})\nu(\varpi'_{H,\underline{x},n}(\underline{x}) - \varpi'_{H,\underline{x},n}(\bar{x})) \\ \varphi_{\bar{x},n} &\equiv h'_{ss}(\bar{x})\nu(\varpi'_{H,\bar{x},n}(\underline{x}) - \varpi'_{H,\bar{x},n}(\bar{x})) \quad \varphi_{F,n} \equiv \nu(\varpi'_{F,n}(\underline{x}) - \varpi'_{F,n}(\bar{x})) \end{aligned}$$

The coefficients for  $\hat{X}$  in the levels representation depend on the eigenfunction index  $n$  and are derived from

the Green's function (see Lemma 3):

$$\xi_{F,n} \equiv \int_{\underline{x}}^{\bar{x}} x \gamma_{KFE,n}(x, x^*) dx \quad (31)$$

$$\xi_{x^*,n} \equiv F_{ss} \int_{\underline{x}}^{\bar{x}} x \partial_y \gamma_{KFE,n}(x, x^*) dx \quad (32)$$

$$\xi_{\underline{x},n} \equiv -\nu h'_{ss}(\underline{x}) \int_{\underline{x}}^{\bar{x}} x \partial_y \gamma_{KFE,n}(x, \underline{x}) dx \quad (33)$$

$$\xi_{\bar{x},n} \equiv -\nu h'_{ss}(\bar{x}) \int_{\underline{x}}^{\bar{x}} x \partial_y \gamma_{KFE,n}(x, \bar{x}) dx \quad (34)$$

The remaining coefficients for the value function and boundary dynamics are:

$$\chi_{x^*,n} \equiv -\frac{1}{\partial_x^2 v_{ss}(x^*)} \Theta'_{MC,n}(x^*) \quad \Xi_{x^*,n} \equiv -\frac{1}{\partial_x^2 v_{ss}(x^*)} \Theta'_{v,n}(x^*)$$

$$\chi_{\underline{x},n} \equiv -\frac{1}{\partial_x^2 v_{ss}(\underline{x})} \Theta'_{MC,n}(\underline{x}) \quad \Xi_{\underline{x},n} \equiv -\frac{1}{\partial_x^2 v_{ss}(\underline{x})} \Theta'_{v,n}(\underline{x})$$

$$\chi_{\bar{x},n} \equiv -\frac{1}{\partial_x^2 v_{ss}(\bar{x})} \Theta'_{MC,n}(\bar{x}) \quad \Xi_{\bar{x},n} \equiv -\frac{1}{\partial_x^2 v_{ss}(\bar{x})} \Theta'_{v,n}(\bar{x})$$

**Theorem 1.** *In a solution to the MFG, the aggregate variables are characterized by the following integral equations.*

*The value function at any point  $x$  is given by backward integrals in the HJB eigenfunctions:*

$$\hat{v}(x, t) = \sum_{n=1}^{\infty} \hat{v}_n(x, t) \quad (35)$$

$$\hat{v}_n(x, t) = \Theta_{MC,n}(x) \int_t^T e^{-\lambda_{HJB,n}(\tau-t)} (-MC(\tau)) d\tau + \Theta_{v,n}(x) \int_t^T e^{-\lambda_{HJB,n}(\tau-t)} \hat{v}(x^*, \tau) d\tau \quad (36)$$

*The optimal reset point  $\hat{x}^*(t)$  follows from smooth pasting and decomposes into eigenfunction components:*

$$\hat{x}^*(t) = \sum_{n=1}^{\infty} \hat{x}_n^*(t) \quad \hat{x}_n^*(t) = \chi_{x^*,n} \int_t^T e^{-\lambda_{HJB,n}(\tau-t)} (-MC(\tau)) d\tau + \Xi_{x^*,n} \int_t^T e^{-\lambda_{HJB,n}(\tau-t)} \hat{v}(x^*, \tau) d\tau \quad (37)$$

*The other critical points  $\hat{\underline{x}}(t) = \sum_n \hat{\underline{x}}_n(t)$  and  $\hat{\bar{x}}(t) = \sum_n \hat{\bar{x}}_n(t)$  have analogous forms with coefficients  $\chi_{\underline{x},n}$ ,  $\Xi_{\underline{x},n}$ ,  $\chi_{\bar{x},n}$ ,  $\Xi_{\bar{x},n}$ .*

*The aggregate price gap is given by a forward integral in levels of the boundary locations:*

$$\hat{X}(t) = \sum_{n=1}^{\infty} \hat{X}_n(t) \quad (38)$$

$$\hat{X}_n(t) = \int_0^t e^{-\lambda_{KFE,n}(t-\tau)} \left( \xi_{F,n} \hat{F}(\tau) + \xi_{x^*,n} \hat{x}^*(\tau) + \xi_{\underline{x},n} \hat{\underline{x}}(\tau) - \xi_{\bar{x},n} \hat{\bar{x}}(\tau) \right) d\tau \quad (39)$$

where the coefficients  $\xi_{F,n}$ ,  $\xi_{x^*,n}$ ,  $\xi_{\underline{x},n}$ , and  $\xi_{\bar{x},n}$  are defined in equations (31)–(34).

The FPA decomposes into critical-point and interior components:

$$\hat{F}_{\text{crit}}(t) = \varphi_{x^*} \hat{x}^*(t) + \varphi_{\underline{x}} \hat{\underline{x}}(t) - \varphi_{\bar{x}} \hat{\bar{x}}(t) \quad (40)$$

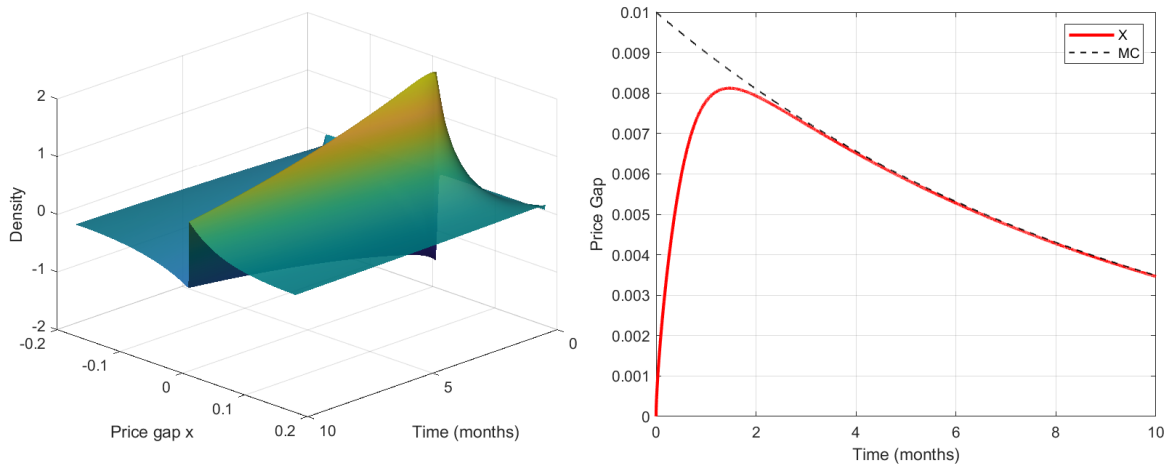
$$\begin{aligned} \hat{F}_{\text{int},n}(t) = & e^{-\lambda_{KFE,n}t} (\varphi_{x^*,n} \hat{x}^*(0) + \varphi_{\underline{x}',n} \hat{\underline{x}}(0) - \varphi_{\bar{x}',n} \hat{\bar{x}}(0)) \\ & + \int_0^t e^{-\lambda_{KFE,n}(t-\tau)} (\varphi_{F,n} \hat{F}(\tau) + \varphi_{x^*,n} \hat{x}^*(\tau) + \varphi_{\underline{x}',n} \hat{\underline{x}}'(\tau) - \varphi_{\bar{x}',n} \hat{\bar{x}}'(\tau)) d\tau \quad (41) \end{aligned}$$

Note that the FPA interior component depends on the time derivatives of the critical points ( $\hat{x}^*$ ,  $\hat{\underline{x}}'$ ,  $\hat{\bar{x}}'$ ) rather than their levels. The aggregate gap  $\hat{X}$  uses a direct levels representation.

*Proof:* Appendix A.4

The integral equations in Theorem 1 can be solved directly in “sequence space.” Alternatively, by the Fundamental Theorem of Calculus, these integral equations imply differential equations for the  $n$ -indexed components which can be solved recursively subject to initial and terminal conditions using a standard method such as Sims (2002). Either way, the aggregate quantities of interest are recovered by summing:  $\hat{x}^*(t) = \sum_{n=1}^{\infty} \hat{x}^*(t)$ ,  $\hat{X}(t) = \sum_{n=1}^{\infty} \hat{X}_n(t)$ , and similarly for the other variables.

To build more intuition for how the aggregate price gap responds to shocks in the menu cost model, Figure 1 pairs the impulse response of the aggregate price gap  $X_t$  (right panel) with the underlying distribution perturbation  $\hat{h}(x, t)$  (left panel). The distribution perturbation shows how a marginal cost shock propagates through the cross-sectional distribution of price gaps. As firms with large price gaps adjust, mass flows from the tails back toward the reset point, and the aggregate price gap decays.



*Notes:* The left panel plots the distribution perturbation  $\hat{h}(x, t)$  after a marginal cost shock. The right panel plots the aggregate price gap response  $\hat{X}(t)$  and the exogenous marginal cost path  $MC(t)$ .

Figure 1: Analytical Perturbation to the Distribution and Aggregate Price Gap

Figure 1 demonstrates Theorem 1's solution with a simple example. Firms face an unexpected increase in nominal marginal costs that decays slowly over time. The left panel plots the perturbed distribution  $\hat{h}(x, t)$ , which represents the marginal change in the firms' distribution from the shock. On impact, there is a marginal increase in all critical points. This means that on the steady-state interval  $[\underline{x}_{ss}, \bar{x}_{ss}]$  where  $\hat{h}(x, t)$  is defined, the initial density changes precisely at the original critical points and is flat everywhere else. The density  $\hat{h}(x, 0)$  is negative at  $\underline{x}$ , because additional firms leave the interval and reset prices when the critical point rises. Analogously, the density is positive at  $\bar{x}$ , because firms that would have reset no longer do so. The density is unusual at the critical point  $x^*$ : it is dipole-like, with a negative jump immediately followed by a positive jump, matching the shape of the  $-\delta'(x - x^*)$  term.<sup>9</sup> Despite this non-continuous initial condition,  $\hat{h}(x, t)$  evolves smoothly for  $t > 0$ , with mass accumulating in the positive region as firms choose higher prices, raising the average price gap (right panel). Over time, the function converges back to zero, consistent with the full distribution returning to the steady state.

### 3.4 Discrete Time Approximation

The true continuous time model is valuable for analytical characterization, but a discrete time model is often more tractable for many applications. This section derives a discrete time approximation of the continuous time solution by discretizing the integrals in Theorem 1. Throughout,  $\Delta t$  denotes the time step size for the approximation, which I set to  $\Delta t = 1$  in the final representation. The approximation treats time-varying terms (marginal costs, boundary locations, aggregate values) as constant on each time step, and integrates the exponential kernel  $e^{-\lambda_n \tau}$  exactly. Define the *exact integration weight* for eigenvalue  $\lambda$  at step size  $\Delta t$  as

$$\varsigma(\lambda) \equiv \int_0^{\Delta t} e^{-\lambda \tau} d\tau = \frac{1 - e^{-\lambda \Delta t}}{\lambda} \quad (42)$$

When  $\Delta t = 1$ , let  $\varsigma_{HJB, n} \equiv \varsigma(\lambda_{HJB, n})$  and  $\varsigma_{KFE, n} \equiv \varsigma(\lambda_{KFE, n})$ .<sup>10</sup>

In Proposition 2,  $\hat{V}_t^*$  denotes the discrete time approximation of the reset value  $\hat{v}(x^*, t)$ . Values at the other boundaries  $\hat{V}_t$  and  $\hat{\bar{V}}_t$  are similarly defined. Written in terms of these discrete time values, the derivative value-matching conditions (17) are

$$\hat{V}_t^* = \hat{\underline{V}}_t = \hat{\bar{V}}_t \quad (43)$$

As before, these values are sums of  $n$ -indexed components for each eigenvalue, as are the other variables:

$$\hat{V}_t^* = \sum_{n=1}^{\infty} \hat{V}_{n,t}^* \quad \hat{\underline{V}}_t = \sum_{n=1}^{\infty} \hat{\underline{V}}_{n,t} \quad \hat{\bar{V}}_t = \sum_{n=1}^{\infty} \hat{\bar{V}}_{n,t}$$

<sup>9</sup>Appendix F.1 describes this initial condition in greater detail.

<sup>10</sup>The exact integration weight is approximately equivalent to the familiar Riemann weight  $\Delta t$ , because for small  $\lambda$ ,  $\varsigma(\lambda) \approx \Delta t$ . However, the exact integration weight is more accurate for larger  $\lambda$ , where exponential decay over the  $\Delta t$  time interval is nontrivial. This distinction matters for large  $n$ , so using exact integration weights is useful for both accuracy and numerical stability.

$$\hat{x}_t^* = \sum_{n=1}^{\infty} \hat{x}_{n,t}^* \quad \hat{x}_t = \sum_{n=1}^{\infty} \hat{x}_{n,t} \quad \hat{\underline{x}}_t = \sum_{n=1}^{\infty} \hat{\underline{x}}_{n,t}$$

The aggregate gap is a sum of eigenfunction components, while the FPA decomposes into critical-point and interior components:

$$\hat{X}_t = \sum_{n=1}^{\infty} \hat{X}_{n,t} \quad \hat{F}_t = \hat{F}_{\text{crit},t} + \sum_{n=1}^{\infty} \hat{F}_{\text{int},n,t}$$

As in the continuous time case,  $\vec{z}_t$  is a vector of the aggregate variables,  $\vec{z}_{\text{crit},t}$  contains the critical-point components (for  $\hat{F}$ ),  $\vec{z}_{n,t}$  contains the  $n$ th eigenfunction components, and  $\mathbf{z}_t$  is a vector stacking these in ascending order.

**Proposition 2** (Discrete time MFG dynamics). *The discrete time approximation satisfies the system of equations*

$$\hat{V}_{n,t}^* = \varsigma_{HJB,n} \left( \Theta_{MC,n}(x^*) (-MC_{t+1}) + \Theta_{v,n}(x^*) \hat{V}_{t+1}^* \right) + e^{-\lambda_{HJB,n}} \hat{V}_{n,t+1}^* \quad (44)$$

$$\hat{V}_{n,t} = \varsigma_{HJB,n} \left( \Theta_{MC,n}(\underline{x}) (-MC_{t+1}) + \Theta_{v,n}(\underline{x}) \hat{V}_{t+1}^* \right) + e^{-\lambda_{HJB,n}} \hat{V}_{n,t+1} \quad (45)$$

$$\hat{V}_{n,t} = \varsigma_{HJB,n} \left( \Theta_{MC,n}(\bar{x}) (-MC_{t+1}) + \Theta_{v,n}(\bar{x}) \hat{V}_{t+1}^* \right) + e^{-\lambda_{HJB,n}} \hat{V}_{n,t+1} \quad (46)$$

$$\hat{x}_{n,t}^* = \varsigma_{HJB,n} \left( \chi_{x^*,n} (-MC_{t+1}) + \Xi_{x^*,n} \hat{V}_{t+1}^* \right) + e^{-\lambda_{HJB,n}} \hat{x}_{n,t+1}^* \quad (47)$$

$$\hat{\underline{x}}_{n,t} = \varsigma_{HJB,n} \left( \chi_{\underline{x},n} (-MC_{t+1}) + \Xi_{\underline{x},n} \hat{V}_{t+1}^* \right) + e^{-\lambda_{HJB,n}} \hat{\underline{x}}_{n,t+1} \quad (48)$$

$$\hat{\bar{x}}_{n,t} = \varsigma_{HJB,n} \left( \chi_{\bar{x},n} (-MC_{t+1}) + \Xi_{\bar{x},n} \hat{V}_{t+1}^* \right) + e^{-\lambda_{HJB,n}} \hat{\bar{x}}_{n,t+1} \quad (49)$$

$$\hat{X}_{n,t} = \varsigma_{KFE,n} \left( \xi_{F,n} \hat{F}_t + \xi_{x^*,n} \hat{x}_t^* + \xi_{\underline{x},n} \hat{\underline{x}}_t - \xi_{\bar{x},n} \hat{\bar{x}}_t \right) + e^{-\lambda_{KFE,n}} \hat{X}_{n,t-1} \quad (50)$$

$$\hat{F}_{\text{crit},t} = \varphi_{x^*} \hat{x}_t^* + \varphi_{\underline{x}} \hat{\underline{x}}_t - \varphi_{\bar{x}} \hat{\bar{x}}_t \quad (51)$$

$$\hat{F}_{\text{int},n,t} = \varsigma_{KFE,n} \left( \varphi_{F,n} \hat{F}_t + \varphi_{x^*,n} \Delta \hat{x}_t^* + \varphi_{\underline{x}',n} \Delta \hat{\underline{x}}_t - \varphi_{\bar{x}',n} \Delta \hat{\bar{x}}_t \right) + e^{-\lambda_{KFE,n}} \hat{F}_{\text{int},n,t-1} \quad (52)$$

where  $\Delta \hat{x}_t^* \equiv \hat{x}_t^* - \hat{x}_{t-1}^*$ ,  $\Delta \hat{\underline{x}}_t \equiv \hat{\underline{x}}_t - \hat{\underline{x}}_{t-1}$ , and  $\Delta \hat{\bar{x}}_t \equiv \hat{\bar{x}}_t - \hat{\bar{x}}_{t-1}$  are discrete time approximations to  $\hat{x}'(t)$ ,  $\hat{\underline{x}}'(t)$ , and  $\hat{\bar{x}}'(t)$ .

*Proof:* Appendix A.5

Together, the dynamic equations in Propositions 2 define a partial equilibrium for firms and their pricing decisions, which Definition 1 formalizes.

**Definition 1.** *A discrete time partial equilibrium of the pricing side of the economy is a bounded infinite sequence of price gaps  $\hat{X}_t$ , boundaries  $\hat{x}_t^*, \hat{\underline{x}}_t, \hat{\bar{x}}_t$ , values  $\hat{V}_t^*, \hat{V}_t, \hat{V}_t$ , and flows  $\hat{F}_t$ , that satisfy the dynamic equations in Proposition 2, given a path for marginal costs  $MC_t$ .*

In practical terms, Proposition 2 shows that the pricing problem and associated dynamics are entirely characterized by a *system of linear dynamic equations* in discrete time. While PDEs may be uncomfortable, systems of dynamic linear equations are bread-and-butter for macroeconomists. The system is infinite

dimensional, but with a large truncation on the eigenseries index  $n$ , and a sufficiently small time step  $\Delta t$ , the system can be solved to find the analytical solution with arbitrary precision.<sup>11</sup> Moreover, this can be done with standard macroeconomic model solvers using simple matrix algebra.

Still, an arbitrarily large system of equations is unwieldy. Next, I show that the system can be well represented by only a few dimensions, and that this approximation is relatively accurate under a standard calibration.

## 4 The Primary Eigenfunction Discretization

The analytical solution to the mean field game is infinite-dimensional. This section shows how the true solution can be easily reduced to a low-dimensional discrete time approximation, the *Primary Eigenfunction Discretization* (PED).

Each eigenvalue indexed by  $n$  is associated with an eigenfunction. These eigenfunctions form a basis for functions on the interval  $[\underline{x}, \bar{x}]$ . Thus, the distribution  $\hat{h}(x, t)$  can be written as a linear combination of these eigenfunctions. Each eigenfunction explains a share of the behavior of  $\hat{h}(x, t)$  over time. The *primary eigenfunction* explains the most. This eigenfunction is not necessarily associated with the “dominant eigenvalue” (Hansen and Scheinkman, 2009), i.e. the largest eigenvalue which describes dynamics at the longest horizons.<sup>12</sup>

The PED is an approximation of the true solution. Before defining it, let us ask: What properties should the PED have in order to be a good approximation?

### 4.1 Desirable Properties of an Approximate Solution

Consider any finite-dimensional approximation to the true solution. There are many ways to craft such a thing, but in order to accurately approximate the true solution, it should inherit a number of salient features. Imposing these properties will discipline the approximation.

First, a crucial property of the true solution is the long-run neutrality of monetary shocks. In the model, a permanent increase in nominal marginal costs should increase nominal prices one-for-one in the long run. I formalize this property as follows:

**Definition 2.** *An approximation to the model solution satisfies **long-run neutrality** if, in response to a*

<sup>11</sup>For further guidance, see the Computational Appendix H.

<sup>12</sup>Indeed, in the case of zero trend inflation, Alvarez and Lippi (2022) and Alvarez et al. (2023) show that the dominant eigenvalue is irrelevant for the aggregate effects of cost shocks, because it describes symmetric (even) changes in the value function, while a cost shock induces an anti-symmetric (odd) change.

permanent marginal cost shock  $MC(t) = \kappa$  for  $t \geq 0$ , the following limits hold:

$$\lim_{t \rightarrow \infty} \hat{X}_t = \kappa \quad (53)$$

$$\lim_{t \rightarrow \infty} \hat{x}_t^* = \kappa \quad (54)$$

$$\lim_{t \rightarrow \infty} \hat{\underline{x}}_t = \kappa \quad (55)$$

$$\lim_{t \rightarrow \infty} \hat{\bar{x}}_t = \kappa \quad (56)$$

Second, the model also has a number of implications for the dynamics of the FPA. These are more mathematical. Let  $\mathbf{n}_{\text{approx}}$  denote a finite set of eigenvalue indices that are used to approximate the full solution. In such an approximation, let the FPA be given by

$$\begin{aligned} \hat{F}_t &= \hat{F}_{\text{crit},t} + \sum_{n \in \mathbf{n}_{\text{approx}}} \hat{F}_{\text{int},n,t} \\ \hat{F}_{\text{int},n,t} &= \varsigma_{KFE,n} \left( \tilde{\varphi}_{F,n} \hat{F}_t + \varphi_{x^*,n} \Delta \hat{x}_t^* + \varphi_{\underline{x},n} \Delta \hat{\underline{x}}_t - \varphi_{\bar{x},n} \Delta \hat{\bar{x}}_t \right) + e^{-\lambda_{KFE,n}} \hat{F}_{\text{int},n,t-1} \end{aligned} \quad (57)$$

where

$$\tilde{\varphi}_{F,n} = \alpha_\varphi \varphi_{F,n} \quad \forall n$$

Equation (57) only differs from equation (52) by replacing  $\varphi_{F,n}$  with  $\tilde{\varphi}_{F,n}$ , which allows for control of the feedback of the aggregate FPA  $\hat{F}_t$  to the finite components  $\hat{F}_{\text{int},n,t}$ . With this notation, desirable full solution properties of the FPA are:

**Definition 3.** An approximation to the model solution satisfies **FPA-consistency** if, in response to a permanent marginal cost shock  $MC(t) = \kappa$  for  $t \geq 0$ , the following hold:

$$\lim_{t \rightarrow \infty} \hat{F}_t = 0 \quad (58)$$

$$\hat{F}_1 = \left( 2\sqrt{\frac{\nu}{\pi \Delta t}} (h'_{ss}(\underline{x}) + h'_{ss}(\bar{x})) + \frac{\bar{\pi}}{2} (h'_{ss}(\bar{x}) - h'_{ss}(\underline{x})) \right) \kappa \quad (59)$$

and if in general the aggregate feedback is

$$\sum_{n \in \mathbf{n}_{\text{approx}}} \tilde{\varphi}_{F,n} = \sum_{n=1}^{\infty} \varphi_{F,n} = 0 \quad (60)$$

Equation (58) is simply long-run neutrality for the FPA. Equation (59) says that the discrete time impact effect is approximately equal to the continuous time impact effect. Corollary 1 derives the given expression from the integrated average FPA over the initial time period; it is an approximation of the true effect, most accurate when the time interval and  $\bar{\pi}$  are small. Lastly, equation (60) imposes that finite-dimensional approximation does not alter the aggregate feedback effect of the FPA, which could be

potentially destabilizing, especially because  $\varphi_{F,n}$  is not a convergent series.

## 4.2 Defining the Primary Eigenfunction Discretization

Before finding the PED, I must first define what it means to approximate the solution with a single eigenfunction. The discrete-time equilibrium relations collected in Proposition 2 are not all satisfied when restricting to one eigenfunction. But the full proposition is broken down into subcomponents associated with each  $n$ -indexed eigenvalue. A single-eigenfunction approximation satisfies the relevant  $n$ th subcomponent equation for the chosen eigenfunction.

In order to clean up notation, if a variable is written with a time subscript but without a hat, then it denotes the PED. Additionally, to comport with convention, I use  $p$ 's to denote PED price gap variables. Thus  $p_t$  denotes the (log) deviation of the price level from trend. To be specific:

**Definition 4.** *A discrete time single-eigenfunction approximation of the pricing side of the economy is an infinite sequence of price gaps  $p_t$ , boundaries  $p_t^*, \underline{p}_t, \bar{p}_t$ , values  $V_t^*, \underline{V}_t, \bar{V}_t$ , and flows  $F_t$  such that for eigenfunction index  $n$*

$$\begin{aligned} p_t &\propto \hat{X}_{n,t} \\ p_t^* &\propto \hat{x}_{n,t}^* & \underline{p}_t &\propto \hat{x}_{n,t} & \bar{p}_t &\propto \hat{x}_{n,t} \\ V_t^* &= \hat{V}_{n,t}^* & \underline{V}_t &= \hat{V}_{n,t} & \bar{V}_t &= \hat{V}_{n,t} \\ F_t &= \hat{F}_{\text{crit},t} + \hat{F}_{\text{int},n,t} \end{aligned}$$

which also: satisfy the dynamic equations, (43), (45), and (46); satisfy the dynamic equations (47), (48), (49), (50), (51), and (57) up to scale; and obey the long-run limits (53), (54), (55), (56); given a path for nominal marginal costs  $MC_t$ .

Definition 4 only imposes that Proposition 2's dynamic equations determining nominal variables only hold up to scale, which introduces enough degrees of freedom in order to ensure that long-run neutrality is satisfied. This is because any discrete-time approximation of the continuous-time model will not precisely satisfy long-run neutrality, even when all eigenvalues are accounted for. Scaling aside, Definition 4 has the same number of equations as unknowns, but hides a shortcut: I do not impose that the dynamic equation (44) associated with  $V_t^*$  holds. This is because the approximation is *over-determined*. Of course it is: otherwise it would be a complete solution. Specifically, the equations describing the values at the boundaries ((44), (45), (46)) cannot generally all hold while also respecting the value-matching condition (43). Thus there is flexibility in choosing which equations should hold in the approximation. This decision is innocuous when there is zero trend inflation, in which case any three of these equations imply the fourth (Alvarez et al., 2023, Lemma 4), but when  $\bar{\pi} \neq 0$ , a selection must be made. I choose to enforce value-matching but not equation (44) for two reasons. First, this choice is more tractable, as dropping the value-matching condition would

introduce an additional forward-looking equation to the PED system in Theorem 2. Second, this choice is consistent with the validation exercises conducted in Section 5.

To determine the primary eigenfunction and eigenvalue, a criterion is needed in order to determine how well the choice of a particular eigenfunction approximates the true solution. To do so, let  $\mathbf{C}$  denote a criterion vector, which is some lag operator polynomial mapping some type of process into an equilibrium outcome in the discrete time representation of the true model. For example, in the true model there is some lag-operator polynomial  $\mathbf{IRF}_P(L)$  which represents the impulse response function (IRF) mapping an unanticipated real marginal cost shock to the price level by  $p_t = \mathbf{IRF}_P(L)mc_t$ . If the PED is judged by how accurately it approximates this IRF, then the criterion vector would be  $\mathbf{C} = \mathbf{IRF}_P(L)$ .

To judge how well a particular eigenfunction approximates the true model, let  $\mathbf{C}_n$  denote the appropriate criterion vector implied by the eigenfunction approximation indexed by  $n$ . Lag operator polynomials can be represented as infinite vectors, so define the approximation error by

$$[\text{Approximation error}] : \quad \|\mathbf{C}_n - \mathbf{C}\|$$

where  $\|\cdot\|$  denotes some function that quantifies the error. Then, the PED is the discretization minimizing this error:

**Definition 5.** *The **primary eigenfunction discretization (PED)**, indexed by **primary index**  $\hat{n}$ , is the discrete time single-eigenfunction approximation such that*

$$\hat{n} = \arg \min_{n \in \mathbb{Z}} \|\mathbf{C}_n - \mathbf{C}\|$$

for some criterion vector  $\mathbf{C}$ .

When trend inflation is reasonably small, the *second* eigenfunction ( $n = 2$ ) is the *primary eigenfunction*. I demonstrate this in Section 5, but it is consistent with known properties of the menu cost model: with zero trend inflation, the deviation in the value function (Alvarez et al., 2023, Lemma 4) and price gap distribution (Alvarez et al., 2023, Lemma 6) are both anti-symmetric, i.e. spanned by only the eigenfunctions with even index  $n$ .<sup>13</sup> Among these, the lowest order eigenfunction is by far the most important; for  $n = 4, 6, 8, \dots$  the contribution decays to zero rapidly.

**Theorem 2.** *The primary eigenfunction discretization (PED) is described by three equations:*

<i>Optimal Price Setting</i>	$p_t^* = (1 - \theta\beta)MC_t + \theta\beta p_{t+1}^*$
<i>Price Level Law of Motion</i>	$p_t = \epsilon F_t + (1 - \theta)p_t^* + \theta p_{t-1}$
<i>Frequency of Price Adjustment Determination</i>	$F_t = \psi_{p^*}(p_t^* - p_{t-1}^*) + \theta F_{t-1}$

---

<sup>13</sup>Irritatingly, eigenfunctions that are *odd* around  $x^*$  have *even* indices, so I prefer the less common “anti-symmetric” terminology.

where, given primary eigenvalue index  $\hat{n}$ , the coefficients are defined:

$$\begin{aligned}\beta &\equiv e^{-\rho} & \theta &\equiv e^{-\lambda_{KFE, \hat{n}}} \\ \epsilon &\equiv (1 - \theta) \frac{\xi_{F, \hat{n}}}{\xi_{p^*, \hat{n}}} \\ \xi_{p^*, \hat{n}} &\equiv \xi_{x^*, \hat{n}} + \xi_{\bar{x}, \hat{n}} - \xi_{\bar{x}, \hat{n}} \\ \psi_{p^*} &= 2\sqrt{\frac{\nu}{\pi\Delta t}} (h'_{ss}(\underline{x}) + h'_{ss}(\bar{x})) + \frac{\bar{\pi}}{2} (h'_{ss}(\bar{x}) - h'_{ss}(\underline{x}))\end{aligned}$$

*Proof:* Appendix A.6

Theorem 2 gives a concise, linear representation of the model in terms of the FPA  $F_t$  and two price variables  $p_t$  and  $p_t^*$ . However, like the Calvo model, this representation is not always the most practical. This is because the reset price  $p_t^*$  does not have a clear empirical counterpart, and also because both price level variables tend to be non-stationary in general equilibrium models with real shocks. This is why New Keynesian models are typically written in terms of inflation  $\pi_t$ , rather than the price level. With Calvo pricing, doing so gives a New Keynesian Phillips Curve.

This transformation is possible for the PED as well. Proposition 3 provides a ‘‘Menu Cost New Keynesian’’ (MCNK) Phillips curve, which modifies the familiar Calvo equation with a correction term that accounts for the endogenous FPA. The Proposition also provides a transformation of Theorem 2’s FPA Determination equation that gives  $F_t$  in terms of inflation.

**Proposition 3.** *Under the primary eigenfunction discretization, the New Keynesian Phillips Curve is modified by*

$$\begin{aligned}\text{MCNK Phillip Curve} & & \pi_t &= \Lambda mc_t + \beta\pi_{t+1} + \underbrace{\frac{\epsilon}{\theta}(F_t - \theta\beta F_{t+1})}_{\text{FPA correction}} \\ \text{MCNK FPA Determination} & & F_t &= \psi_\pi (\pi_t - \theta\pi_{t-1}) + (\theta + (1 - \theta)\psi_\pi\epsilon) F_{t-1}\end{aligned}$$

where  $\Lambda \equiv \frac{(1-\theta)(1-\theta\beta)}{\theta}$  is the New Keynesian slope parameter and

$$\psi_\pi \equiv \frac{\psi_{p^*}}{1 - \theta + \psi_{p^*}\epsilon}$$

*Proof:* Appendix A.7

Proposition 3 reveals that menu costs modify the traditional New Keynesian Phillips curve in two ways. First, the slope  $\Lambda = \frac{(1-\theta)(1-\theta\beta)}{\theta}$  is affected through  $\theta$ : the endogenous pricing decision substantially lowers  $\theta$ , raising the ‘‘slope’’ of the Phillips curve, consistent with findings by Gertler and Leahy (2008), Alvarez et al. (2017), and Auclert et al. (2024). Second, the curve is modified by a new dynamic term, the ‘‘FPA correction’’, which depends on the frequency of price adjustment. The Proposition also shows that menu

costs introduce a new internal propagation mechanism:  $F_t$  is a persistent state variable in the MCNK FPA Determination equation. This is noteworthy because the textbook New Keynesian model features no internal propagation; the Calvo pricing structure alone delivers no persistence (Galí, 2008).

Together, Proposition 3's equations pin down paths for the inflation rate  $\pi_t$  and FPA  $F_t$  in terms of the real marginal cost  $mc_t$ . This system is easily embedded in general equilibrium models, replacing the usual Phillips curve. I do so in Section 6. But first, some quantitative tests are needed to validate that the PED is not just a reasonable dimensionality reduction, but an accurate approximation of the true solution.

## 5 Validating the Primary Eigenfunction Discretization

Is the PED a reasonable approximation of the true solution? This section answers: yes. I show that the PED satisfies known theoretical properties in Section 5.1, and is quantitatively accurate in Section 5.2.

### 5.1 PED Validation: Theoretical Properties

This section gives two theoretical results validating the primary eigenvalue approach. The first shows that it nests the usual Calvo linearization as a special case. The second shows that it is consistent with a known result: without trend inflation, the menu cost model is closely approximated by the New Keynesian Phillips Curve.

**Property 1.** *With zero trend inflation ( $\bar{\pi} = 0$ ), the textbook Calvo model is given by*

$$\begin{aligned} \text{Optimal Price Setting} & & p_t^* &= (1 - \theta_{Calvo}\beta)(mc_t + p_t) + \theta_{Calvo}\beta p_{t+1}^* \\ \text{Price Level Law of Motion} & & p_t &= (1 - \theta_{Calvo})p_t^* + \theta_{Calvo}p_{t-1} \end{aligned}$$

where  $\theta_{Calvo} \equiv e^{-\zeta}$  is the Calvo parameter consistent with the random reset rate  $\zeta$  for small time steps.

#### 5.1.1 The PED of the Calvo Model is the Textbook Calvo Model

This section shows that the primary eigenvalue approximation nests the trend-less Calvo model as a special case. This is a desirable property of a useful approximation. When the inaction region becomes large, the  $\theta$  coefficient on the law of motion converges to  $e^{-\zeta}$ , which represents the share of firms receiving random resets in the discrete time approximation. Proposition 4 gives the result:

**Proposition 4.** *If trend inflation is zero ( $\bar{\pi} = 0$ ), the PED of the Calvo model is equivalent to the textbook Calvo model from Property 1.*

*Proof:* Appendix A.8

Proposition 4 is specific to the zero trend inflation. When trend inflation is non-zero, Property 1 does not hold exactly, unless prices are indexed. Without indexing, Ascari (2004) shows that the New Keynesian Phillips curve (61) depends on additional future inflation and marginal cost terms. This is true in the continuous time model’s full solution as well, but not captured by the low-dimensional PED.

### 5.1.2 Same Old Phillips Curve?

Auclert et al. (2024) showed numerically that a menu cost model without trend inflation is, for a particular calibration, very closely approximated by a Calvo model.<sup>14</sup> They also found that this approximation breaks down when trend inflation gets sufficiently large. Proposition 3 demonstrated that with trend inflation, the PED Phillips curve does not hold, and is affected by the FPA. But in this section, I show that the PED is consistent with the established numerical finding: with zero trend inflation, the PED implies the standard New Keynesian Phillips Curve.

**Proposition 5.** *With zero trend inflation ( $\bar{\pi} = 0$ ), the PED implies the standard New Keynesian Phillips Curve:*

$$\pi_t = \Lambda mc_t + \beta \pi_{t+1} \tag{61}$$

where  $\Lambda = \frac{(1-\theta)(1-\theta\beta)}{\theta}$ .

*Proof:* Appendix A.9

## 5.2 PED Validation: Quantitative Properties

This section quantitatively evaluates the PED approximation accuracy. Under a standard calibration, it is relatively accurate, and much more so than the Calvo model, although the accuracy of both decreases when the trend inflation rate becomes especially large.

### 5.2.1 Calibration

This section describes a standard calibration based on the micro pricing statistics measured in Alvarez et al. (2024) for the French economy. As a baseline, I set trend inflation to be  $\bar{\pi} = 0.02$ , matching the French experience from the 1994-2019 sample. In various experiments, I will change  $\bar{\pi}$  while keeping unchanged the other structural parameters, such as the menu cost.

The model has three key parameters that govern the distribution of price changes: the menu cost  $\Psi$ , the diffusion variance  $\nu$ , and the random reset rate  $\zeta$ . These parameters are not directly observable, so they must be inferred from the price adjustment statistics. I calibrate the parameters to match three moments: the frequency of price adjustment  $F_{ss}$ , the standard deviation of price changes, and the kurtosis of price

---

<sup>14</sup>Auclert et al show this result for the full impulse of marginal cost shocks. This builds on an earlier result by Alvarez et al. (2017), who demonstrate the equivalence for the cumulative impulse response function.

changes. In all cases I use the CPI-based statistics, and the kurtosis measure that adjusts for heterogeneity (Alvarez et al., 2022). Table 1 (right panel) reports these three values for the French economy.

Parameter	Symbol	Value
Trend inflation	$\bar{\pi}$	0.02
Discount rate	$\rho$	0.04
Elasticity of substitution	$\eta$	6

(a) Fixed parameters

Model	Parameters			Targeted Moments		
	$\zeta$	$\nu$	$\psi$	$F$	std	kurtosis
Calvo	1.2600	—	—	1.2600	—	—
Golosov-Lucas	0	0.003713	0.011842	1.2600	0.0759	—
Calvo-plus	1.1469	0.003580	0.165623	1.2600	0.0759	3.413

(b) Calibrated parameters and targeted moments

Table 1: Model calibration. Panel (a) reports fixed parameters that are held constant across calibrations. Panel (b) reports three calibrations of the price adjustment parameters ( $\zeta, \nu, \Psi$ ) to match moments from French CPI microdata (Alvarez et al., 2024). The Calvo model matches only frequency. The Golosov-Lucas model ( $\zeta = 0$ ) matches frequency and standard deviation. The Calvo-plus model matches all three moments.

Table 1 presents three calibrations. The first is a pure Calvo model, which has no inaction region and serves as a classic comparison.  $\zeta$  is chosen to match the measured FPA, I interpret to approximate the instantaneous frequency.<sup>15</sup> The second is a Golosov-Lucas model, which sets  $\zeta = 0$  so that all adjustments occur at the boundaries; this model can match the frequency and standard deviation but not kurtosis. The third is a “Calvo-plus” model that includes all three parameters and matches all three moments.

The price change statistics are nonlinear functions of the three parameters ( $\Psi, \nu, \zeta$ ). Appendix G derives expressions for the statistics, given in terms of features of the stationary distribution. Typically the stationary distribution is solved numerically, but it is known in closed-form for the special case of zero trend inflation.<sup>16</sup> Given  $\nu$  and  $\zeta$ , there is a one-to-one mapping between the menu cost  $\Psi$  and the inaction region width  $\ell$ . This allows for Proposition 6, which gives the pricing statistics analytically from  $(\ell, \nu, \zeta)$  under zero trend inflation.

**Proposition 6.** *If trend inflation is zero ( $\bar{\pi} = 0$ ), then the steady-state frequency of price adjustment is*

$$F_{ss} = \frac{\zeta \cosh(s_{zd}\ell/2)}{\cosh(s_{zd}\ell/2) - 1}.$$

<sup>15</sup>In reality, the frequency is measured at the monthly level as 10.5%, which is annualized to 1.26.

<sup>16</sup>My calibration procedure features an inner and outer loop algorithm. For a given guess of  $(\Psi, \nu, \zeta)$ , the inner loop solves the steady-state value function to obtain the inaction region boundaries  $(\underline{x}_{ss}, x_{ss}^*, \bar{x}_{ss})$ . Given the boundaries, the stationary distribution  $h_{ss}(x)$  is computed from the KFE, and the price change moments follow from Appendix G. The outer loop adjusts  $(\Psi, \nu, \zeta)$  until the computed moments match the targets.

The standard deviation of (log) price changes conditional on adjustment  $\Delta p \equiv x_{ss}^* - x$  is

$$Std(\Delta p) = \left[ \frac{2\nu}{\zeta} (1 - \text{sech}(s_{zd}\ell/2)) \right]^{1/2}$$

The kurtosis of conditional price changes is

$$Kurt(\Delta p) = \frac{6}{1 - \text{sech}(s_{zd}\ell/2)} - \frac{3\ell^2\zeta}{4\nu \cosh(s_{zd}\ell/2) (1 - \text{sech}(s_{zd}\ell/2))^2}$$

where  $s_{zd} \equiv \sqrt{\zeta/\nu}$  and  $\ell \equiv \bar{x}_{ss} - \underline{x}_{ss}$  is the steady state inaction region width.

*Proof.* See Appendix G. □

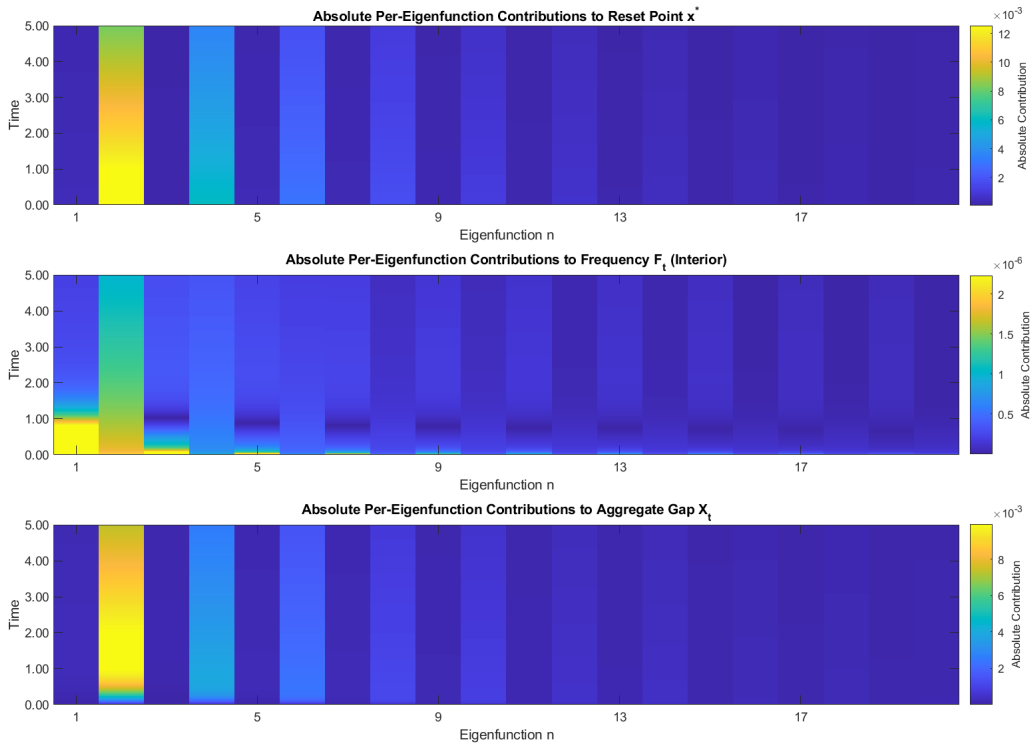
Proposition 6 is valuable for practitioners who may want to use the Calvo Phillips curve as an approximation of the menu cost model under low inflation. Doing so requires a method to calibrate it because, while the Calvo Phillips curve matches the functional form of the menu cost model, the Phillips curve *slope* does not match (Auclert et al., 2024). The typical Calvo calibration (where  $1 - \theta$  is equivalent to the FPA) is an inaccurate approximation, so it is crucial to have a microfounded value for  $\theta$  that captures the menu cost model's inflation dynamics.

### 5.2.2 Choosing the Primary Eigenvalue

The PED approximates the full eigenfunction expansion with a single term, indexed by  $\hat{n}$ . Which eigenfunction should be chosen? The answer depends on which eigenfunction contributes most to the aggregate price gap dynamics. In this section I show that choosing  $\hat{n} = 2$  is appropriate for the PED.

The second eigenfunction ( $n = 2$ ) is overwhelmingly important under the baseline calibration. Figure 2 displays the absolute contribution of each eigenfunction to the reset point  $x^*$ , the frequency of price adjustment  $F$ , and the aggregate gap  $X$ , as a function of time and eigenfunction index. The heatmaps reveal that for all variables, the second eigenfunction ( $n = 2$ ) explains the most variation. For both  $x^*$  and  $X$ , the even-indexed eigenfunctions are most important, consistent with Alvarez et al. (2023). However the FPA  $\hat{F}_t$  also depends noticeably on odd-indexed eigenfunctions,  $n = 1$  in particular.

To ascertain how the PED index affects the approximation, I compare the accuracy of several index choices in Figure 3. Specifically, the criterion is the accuracy of the aggregate gap IRF to a nominal marginal cost shock with annual autocorrelation 0.9. The left panel reports the relative mean squared error between the PED and full-solution IRFs. When these are the criterion and error function, the Definition 5 implies that the  $\hat{n} = 2$  approximation is the PED. Panel 3a shows that this choice (plotted in purple triangles) minimizes the MSE across all trend inflation rates. The next most relevant eigenfunctions ( $n = 4, 6$ ) are less accurate, and higher indices are even worse. I also consider an approximation where the FPA is allowed to use a different eigenfunction, and choose  $n = 1$  the FPA equation alone, given its relevance in Figure 2. This asymmetric case is plotted in yellow diamonds; it performs almost as well as the uniform  $\hat{n} = 2$  PED, which



Notes: Heatmaps show absolute contributions by eigenfunction index  $n$  (horizontal axis) and time (vertical axis) for  $x_t^*$ ,  $F_t$ , and  $X_t$  after a slow-decaying marginal cost shock with 0.9 annualized autocorrelation.

Figure 2: Eigenfunction Contributions to Aggregate Dynamics.

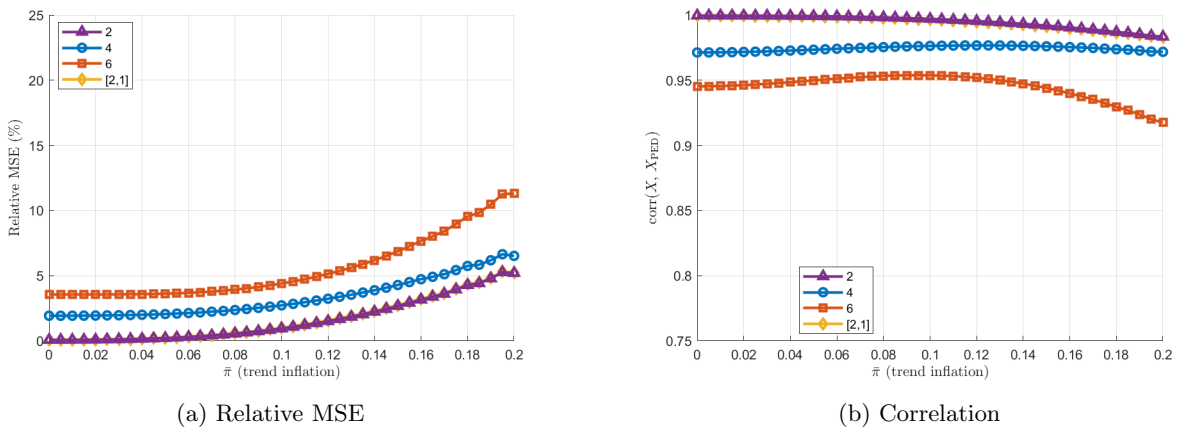


Figure 3: PED Approximation Quality by Eigenfunction Index Choice

Notes: The left panel reports the relative mean squared error (MSE) of the aggregate gap IRF, and the right panel reports the correlation between the PED and full-solution aggregate gap IRFs, across candidate PED indices. The baseline choice  $\hat{n} = 2$  (purple triangles) is most accurate and most correlated with the true solution. The [2, 1] case (yellow diamonds) uses separate indices for prices ( $n = 2$ ) and flow dynamics ( $n = 1$ ).

is why the curve is obscured, although it is slightly less accurate. Thus for parsimony, choosing a single common  $\hat{n} = 2$  is appropriate.

The approximation error begins to rise when trend inflation increases. For hyperinflationary economies, the PED may not be an accurate approximation, and Theorem 1’s full solution should be consulted. However, for the moderate trend inflation rates up to at least 20%, the PED is a good approximation. Panel 3b shows the correlation coefficient between the PED and full-solution IRFs. Even when trend inflation is high and errors start to increase, the PED remains highly correlated with the true solution. And again, the  $\hat{n} = 2$  PED is the most accurate across all trend inflation rates when judged by the correlation.

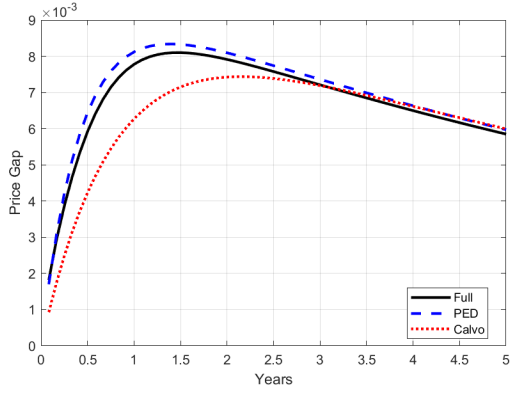
### 5.3 PED vs Calvo

How well does the PED approximate the full solution compared to Calvo? To concretely illustrate the approximation quality, Figure 4 plots impulse response functions for the aggregate price gap (top row) and the frequency of price adjustment (bottom row) to a persistent nominal marginal cost shock. In each subfigure, the full continuous time solution is plotted in black, aggregated up to a monthly frequency. The dashed blue line denotes the  $\hat{n} = 2$  PED, while the dotted red line is the calibrated Calvo model.

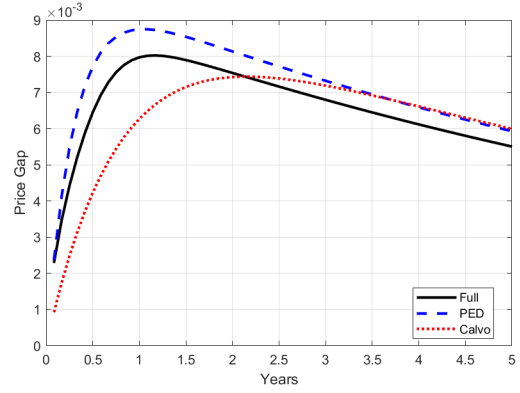
The PED closely approximates the full solution in the baseline calibration ( $\bar{\pi} = .02$ ). Figure 4a shows that the PED price gap is nearly exactly the same, because the  $n = 2$  eigenvalue explains most of the behavior of the full solution’s aggregate price gap. The PED price gap is just slightly larger, because it features a slightly higher FPA (Figure 4c). The impact FPA is larger than under the full solution, because it is normalized to exactly match the impact effect of a permanent marginal cost shock, but in this example the shock is transitory.

In contrast, the Calvo model badly approximates the dynamics. On impact, the Calvo price level jumps by too little, because it misses the contribution from the endogenous FPA. With menu costs, the FPA jumps on impact because the density of firms is most perturbed near the boundaries; this dynamic is entirely missing in the Calvo model. As a result, Figure 4a shows that the price increase is too small and too slow. Moreover, the Calvo-plus model is the best possible case for the performance of the Calvo approximation, because nearly all resets are random (see Table 1:  $\zeta \sim F_{ss}$ ). This means that the Calvo model will miss the short run price response but match the long-run decay ( $\theta_{Calvo} \sim \theta_{\hat{n}}$ ).

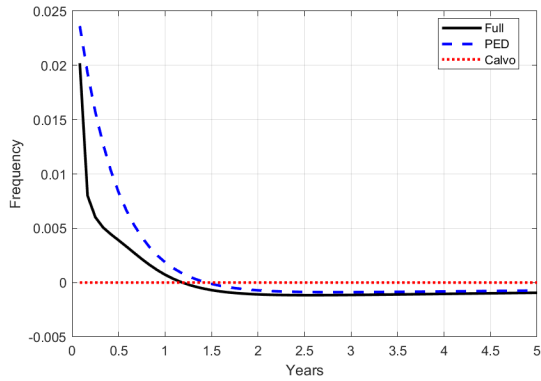
When trend inflation is higher, both approximations are worse (Figure 4b). The PED is still more accurate than Calvo because it more closely matches the short run price response, while both perform similarly in the long-run. But consistent with the Figure 3 results, PED accuracy declines with trend inflation. Figure 4d reveals that this is due to a worse match with the FPA behavior. The PED still has qualitatively the correct shape, but it overstates the FPA on impact, and does not sufficiently capture the negative FPA perturbation in the medium-run. Above 10% trend inflation, it may be wise to simply use the full solution if high accuracy is needed.



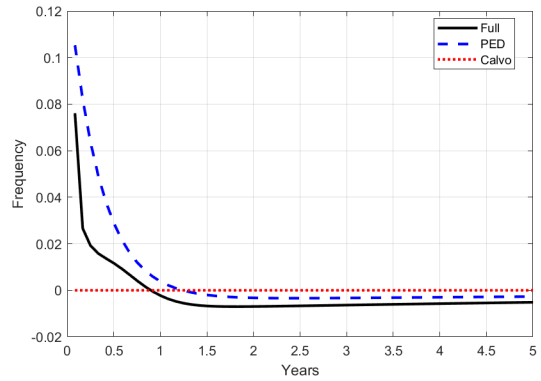
(a) Aggregate Price Gap,  $\bar{\pi} = 2\%$



(b) Aggregate Price Gap,  $\bar{\pi} = 10\%$



(c) Frequency of Price Adjustment,  $\bar{\pi} = 2\%$



(d) Frequency of Price Adjustment,  $\bar{\pi} = 10\%$

Figure 4: IRFs to Marginal Cost Shock: PED vs Calvo.

*Notes:* Responses are to a 0.01 marginal cost shock with annual persistence 0.9. Columns compare  $\bar{\pi} = 2\%$  and  $\bar{\pi} = 10\%$ . The top row reports aggregate price gap responses and the bottom row reports frequency responses. Black line is the full solution (aggregated to monthly), blue dashed line is the monthly PED ( $n = 2$ ), and red dotted line is Calvo.

## 6 The Menu Cost New Keynesian Model

This section embeds the menu cost pricing block into an otherwise standard New Keynesian model; I refer to the resulting system as a “Menu Cost New Keynesian” (MCNK) model. I show how the model dynamics are affected by the inclusion of menu costs and the value of the trend inflation rate. Then I calculate the implications for optimal monetary policy.

### 6.1 The Linear General Equilibrium Model

The textbook New Keynesian model is a three-equation system including the Calvo pricing block:

**Property 2.** *With zero trend inflation ( $\bar{\pi} = 0$ ), the textbook New Keynesian model is given by*

$$\begin{array}{ll}
 \text{NK Phillips Curve} & \pi_t = \Lambda(\alpha y_t + z_t^c) + \beta \mathbb{E}_t[\pi_{t+1}] \\
 \text{Euler Equation} & \sigma y_t = \sigma \mathbb{E}_t[y_{t+1}] - i_t + \mathbb{E}_t[\pi_{t+1}] + z_t^d \\
 \text{Taylor Rule} & i_t = \phi_\pi \pi_t + \phi_y y_t + z_t^r
 \end{array}$$

The New Keynesian model adds an Euler equation (which follows from differentiating w.r.t. time the household’s consumption first order condition in equation (5)) and a monetary policy rule for the nominal interest rate  $i_t$ . Imposing market clearing gives that consumption must equal output  $y_t$ , and the labor supply equation implies that real marginal costs satisfy  $mc_t = \alpha y_t + z_t^c$ .<sup>17</sup>  $z_t^c$  adds an exogenous cost shock which controls how real marginal costs differ from those implied by labor supply alone.

Proposition 7 gives the MCNK model, which replaces the Phillips curve with Proposition 3’s pricing block. This representation modifies the PED in two ways: forward-looking variables are only known in expectation, and the real marginal cost  $mc_t$  is determined in general equilibrium.

**Proposition 7.** *The linear Menu Cost New Keynesian Model is given by*

$$\begin{array}{ll}
 \text{MCNK Phillips Curve} & \pi_t = \Lambda(\alpha y_t + z_t^c) + \beta \mathbb{E}_t[\pi_{t+1}] + \frac{\epsilon}{\theta}(F_t - \theta \beta \mathbb{E}_t[F_{t+1}]) \\
 \text{MCNK FPA Determination} & F_t = \psi_\pi (\pi_t - \theta \pi_{t-1}) + (\theta + (1 - \theta)\psi_\pi \epsilon) F_{t-1} \\
 \text{Euler Equation} & \sigma y_t = \sigma \mathbb{E}_t[y_{t+1}] - i_t + \mathbb{E}_t[\pi_{t+1}] + z_t^d \\
 \text{Taylor Rule} & i_t = \phi_\pi \pi_t + \phi_y y_t + z_t^r
 \end{array}$$

In the analysis that follows, I will assume the cost, demand, and monetary policy shocks are independent AR(1) processes:

$$z_t^c = \rho_c z_{t-1}^c + \varepsilon_t^c \quad z_t^d = \rho_d z_{t-1}^d + \varepsilon_t^d \quad z_t^r = \rho_r z_{t-1}^r + \varepsilon_t^r$$

<sup>17</sup>See Galí (2008) for a clear textbook treatment. In this Property 2 representation, the natural rate of interest is fixed.

In the exercises that follow, I adopt the Calvo-plus calibration reported in Table 1, which imply the PED coefficients  $(\theta, \Lambda, \epsilon, \psi_\pi)$  reported in Table 2. I set the remaining parameters to typical values.

Parameter	Value	Description
$\bar{\pi}$	.02	Baseline trend inflation (annual)
$\beta$	.997	Discount factor (monthly)
$\sigma$	1	Inverse IES
$\alpha$	8	Marginal cost-output elasticity
$\theta$	.825	MCNK price-stickiness coefficient
$\Lambda$	.0378	MCNK Phillips-curve slope
$\epsilon$	.000683	FPA correction coefficient
$\psi_\pi$	13.894	Inflation feedback to FPA
$\phi_\pi$	1.5	Taylor-rule inflation coefficient
$\phi_y$	.125	Taylor-rule output coefficient
$\rho_r$	.5	Monetary shock persistence
$\rho_c$	.5	Cost shock persistence
$\rho_d$	.5	Demand shock persistence
$\sigma_r$	.01	Monetary shock innovation std. dev.
$\sigma_{cp}$	.01	Effective cost-push innovation std. dev.
$\sigma_d$	.01	Demand shock innovation std. dev.

*Notes:* Tabel reports the baseline calibration for the 4-equation general equilibrium model. PED coefficients  $(\theta, \Lambda, \epsilon, \psi_\pi)$  are determined from the pricing parameters in Table 1, and the expressions in Theorem 2 and Proposition 3.

Table 2: Baseline Calibration of the Menu Cost New Keynesian Model

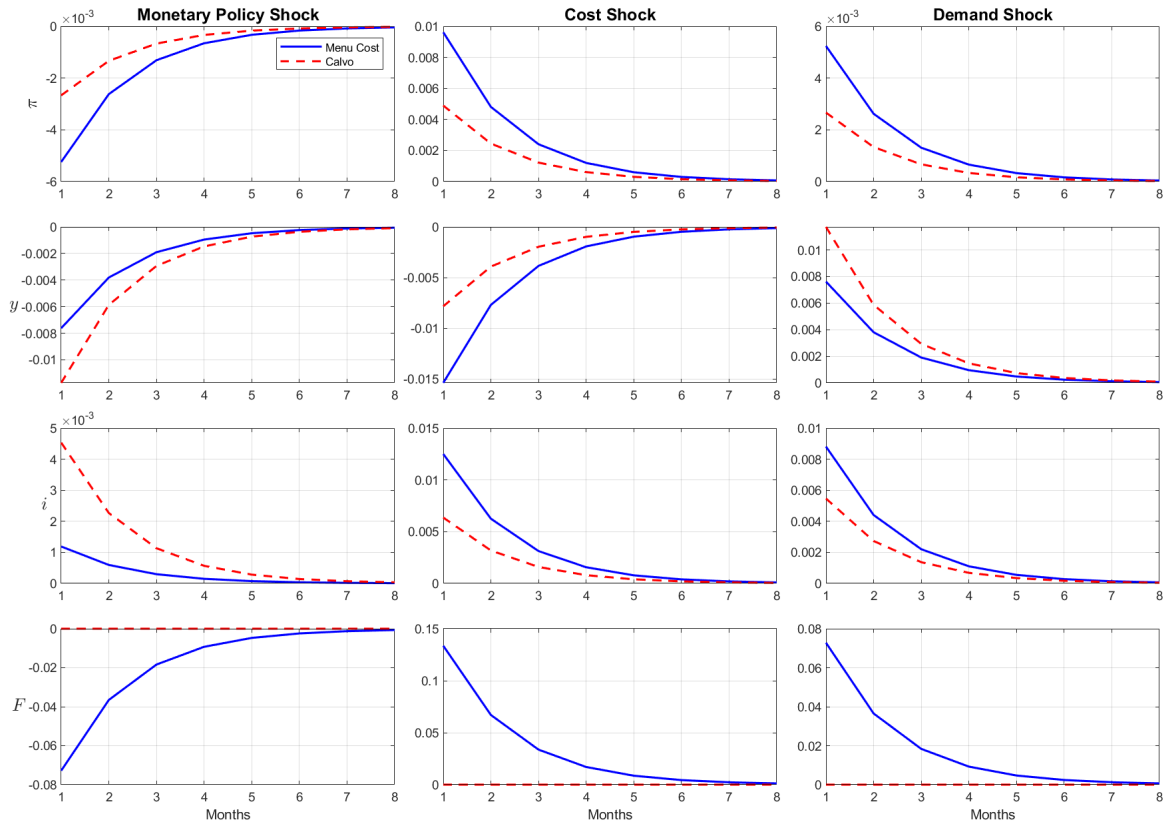
## 6.2 MCNK vs Calvo: Impulse Responses

How does the MCNK model differ from the textbook Calvo formulation? The key distinction is the endogenous frequency of price adjustment. In the Calvo model, the fraction of firms adjusting prices each period is fixed at  $1 - \theta_{Calvo}$ . In the MCNK model, this fraction responds to the aggregate state through the FPA equation.

Figure 5 compares impulse responses to a monetary policy shock, a cost shock, and a demand shock. Rows show inflation, output, the nominal interest rate, and the FPA. In all cases, the MCNK and Calvo models produce qualitatively similar dynamics, but the magnitudes differ.

The gaps between IRFs are due to two model differences. First, menu costs imply that the Phillips curve slope  $\Lambda = \frac{(1-\theta)(1-\theta\beta)}{\theta}$  is much steeper. This is the well-established *steady-state* selection effect: menu costs imply that firms with prices further away from their optimum are more likely to change prices, so real shocks have larger price effects, as if prices overall were more flexible than under Calvo pricing. Second, menu costs imply that the endogenous FPA distorts the Phillips curve. This is the *time-varying* selection effect, because aggregate shocks shift the distribution, which is captured by the FPA path.<sup>18</sup> Figure 5 shows that the endogenous FPA response amplifies the inflationary effects of shocks: when a monetary policy, cost, or

<sup>18</sup>Adams (2025) shows how the path of the flow of resets encodes all of the relevant information in the dynamic distribution.



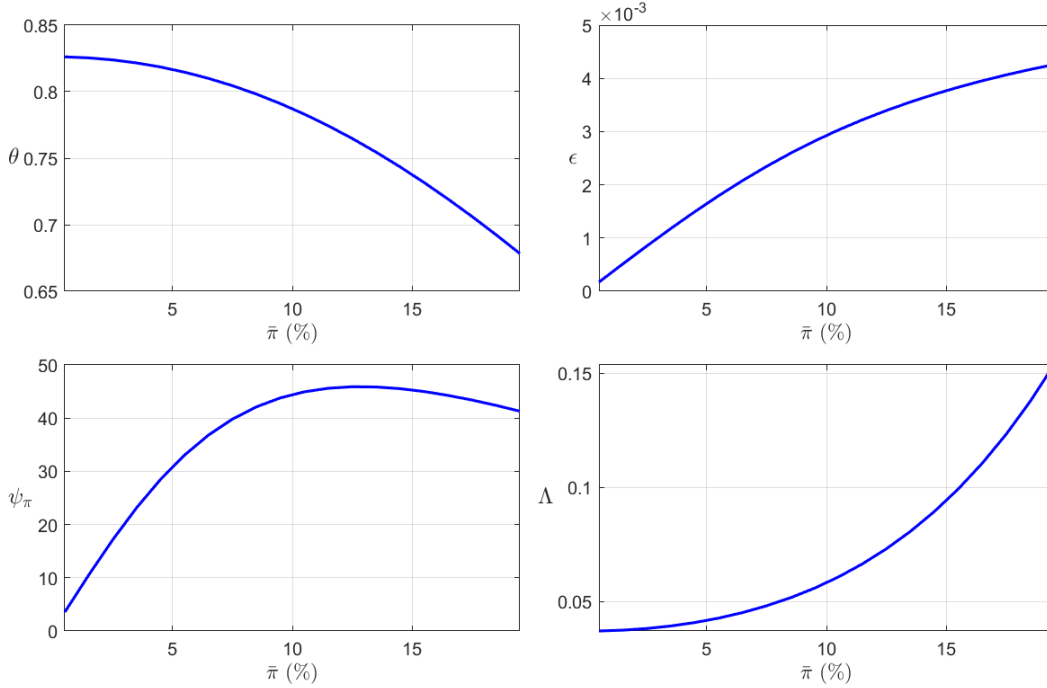
*Notes:* Both models use the Calvo-plus calibration reported in Table 2. Columns correspond to monetary policy, cost, and demand shocks. Rows report inflation, output, nominal interest rate, and the frequency of price adjustment (FPA). Blue solid is MCNK; red dashed is Calvo.

Figure 5: Impulse Responses: MCNK vs Calvo

demand shock increases inflation, the FPA moves in the same direction, acting as an “inflation accelerator”.<sup>19</sup>

### 6.3 Trend Inflation and the PED Coefficients

Trend inflation affects the MCNK model through several channels. The PED coefficients  $\theta$ ,  $\epsilon$ , and  $\psi_\pi$  vary with  $\bar{\pi}$ , while  $b_{p^*} = 1 - \theta$  and  $\phi_F = \theta$  follow directly from the PED Theorem. Figure 6 plots  $\theta$ ,  $\epsilon$ ,  $\psi_\pi$ , and the implied Phillips curve slope  $\Lambda = \frac{(1-\theta)(1-\theta\beta)}{\theta}$ .



*Notes:* The figure reports how PED coefficients vary with trend inflation  $\bar{\pi}$ . In particular, it traces  $\theta$ ,  $\epsilon$ ,  $\psi_\pi$ , and the implied Phillips-curve slope  $\Lambda = \frac{(1-\theta)(1-\theta\beta)}{\theta}$ .

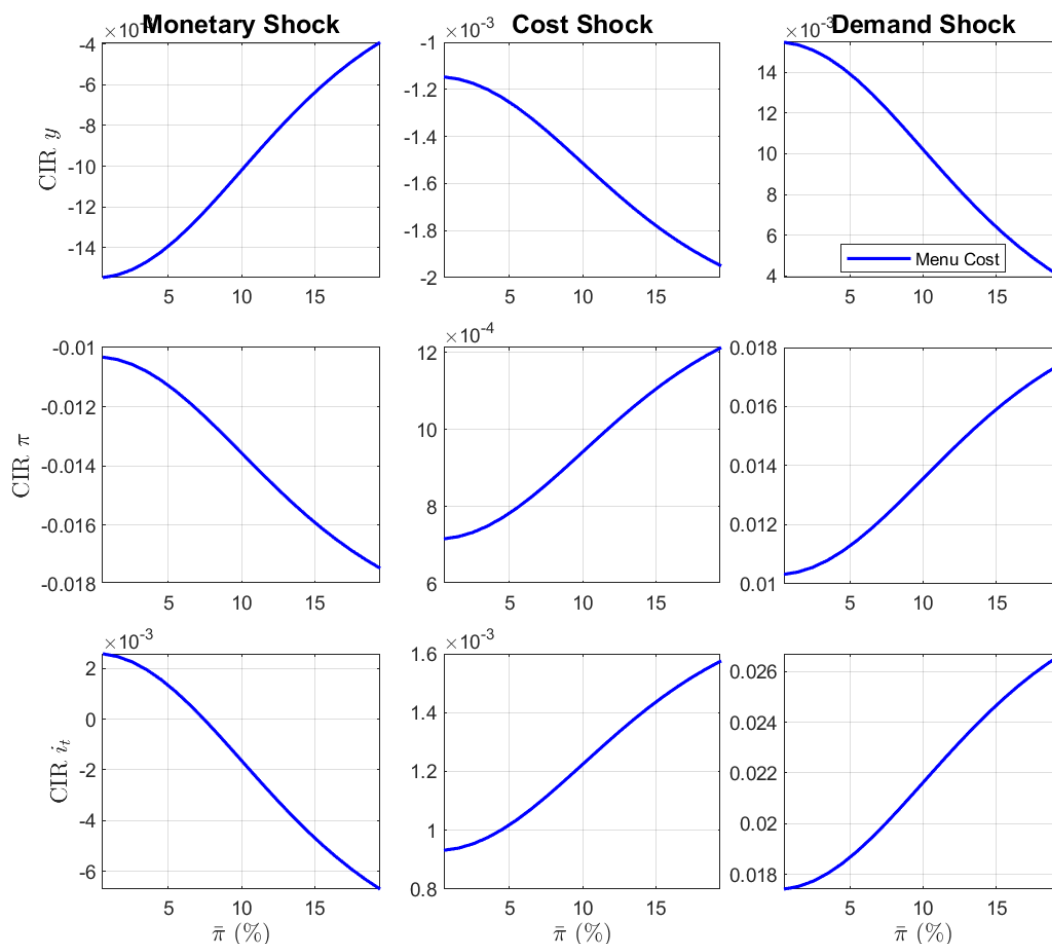
Figure 6: PED Coefficients vs Trend Inflation

Three patterns emerge. First,  $\theta$  increases with trend inflation: higher drift pushes mass toward the boundaries more quickly, but also widens the inaction region asymmetrically, with an ambiguous net effect on the decay rate. Second, the FPA impact coefficient  $\psi_{p^*}$  varies with trend inflation, reflecting how boundary conditions change as the inaction region becomes asymmetric. Third, the implied Phillips curve slope  $\Lambda$  moves nonlinearly with  $\theta$ , changing how marginal costs map into inflation.<sup>20</sup> This effect on the slope is a distinct feature of endogenous price adjustment; in contrast, trend inflation reduces the slope in the Calvo model, effectively making prices more rigid (Ascari, 2004).

<sup>19</sup>Blanco et al. (2024) coined this term; they study how price adjustment amplifies the inflation response in a nonlinear Phillips curve.

<sup>20</sup>This positive association between the slope and inflation rate is observed in the data (Ball and Mazumder, 2011; Hazell et al., 2022; Costain et al., 2022) and is a feature of other types of menu cost models beyond Golosov-Lucas or Calvo-plus (Blanco et al., 2024; Morales-Jiménez and Stevens, 2024).

These coefficient changes alter the general equilibrium dynamics. Figure 7 demonstrates how the dynamics depend on the trend inflation rate by plotting cumulative impulse responses (CIRs) for output, inflation, and the nominal interest rate  $i_t$  as a function of  $\bar{\pi}$ . The left column shows responses to a monetary policy shock, the middle column to a cost shock, and the right column to a demand shock.



*Notes:* The panels report MCNK cumulative impulse responses as  $\bar{\pi}$  varies. The left column corresponds to monetary policy shocks, the middle column to cost shocks, and the right column to demand shocks. Reported outcomes are output, inflation, and nominal interest responses.

Figure 7: Cumulative Impulse Responses vs Trend Inflation

The main lesson revealed by Figure 7 is that increasing trend inflation acts as if prices in the economy become more flexible. In New Keynesian models, more flexible prices imply a steeper Phillips curve, which is also the effect documented in Figure 6. The full dynamics captured by the CIR further include the endogenous FPA behavior, but these effects are reinforcing. After a contractionary cost shock, inflation rises; when  $\bar{\pi}$  is large, inflation rises by much more.<sup>21</sup> After a monetary contraction, inflation falls; when  $\bar{\pi}$  is large, inflation falls by much more. After an expansionary demand shock, inflation rises; when  $\bar{\pi}$  is large,

<sup>21</sup>For cost shocks, it is crucial that the shock has a direct effect that is immediately scaled by the slope of the Phillips curve. In a textbook “cost-push” shock, there is no such scaling, and  $\bar{\pi}$  would not have such an amplifying effect on the inflation CIR.

inflation rises by much more.

At what point is trend inflation non-trivial? It is common to justify a zero trend calibration as a reasonable approximation of small inflation economies because firms' decisions are second-order in the inflation rate; this is clear in Figure 6, where the Phillips curve slope  $\Lambda$  is unchanging in trend inflation at  $\bar{\pi} = 0$ . However the figure also shows that trend inflation has *first-order* effects on the FPA coefficient  $\epsilon$ . As a result, trend inflation affects the general equilibrium response even at low values. Figure 7 shows that the inflation CIR is already substantially amplified at 5% trend inflation, and the effect quickly gets larger from there.

## 6.4 Optimal Monetary Policy

How should monetary policy respond to shocks in the MCNK model? To calculate optimal policy, I apply the textbook method typically used to analyze the New Keynesian model, and illustrate how it is affected by the inclusion of menu costs.<sup>22</sup>

As in Woodford (2003), I consider a central bank that commits to a Taylor rule of the form  $i_t = \phi_\pi \pi_t + \phi_y y_t + z_t^r$ , and chooses their optimal  $\phi_\pi$ , keeping  $\phi_y$  fixed for this simple example. The central bank minimize a quadratic loss function,

$$\mathcal{L} = \text{Var}(\pi) + \lambda_y \text{Var}(y)$$

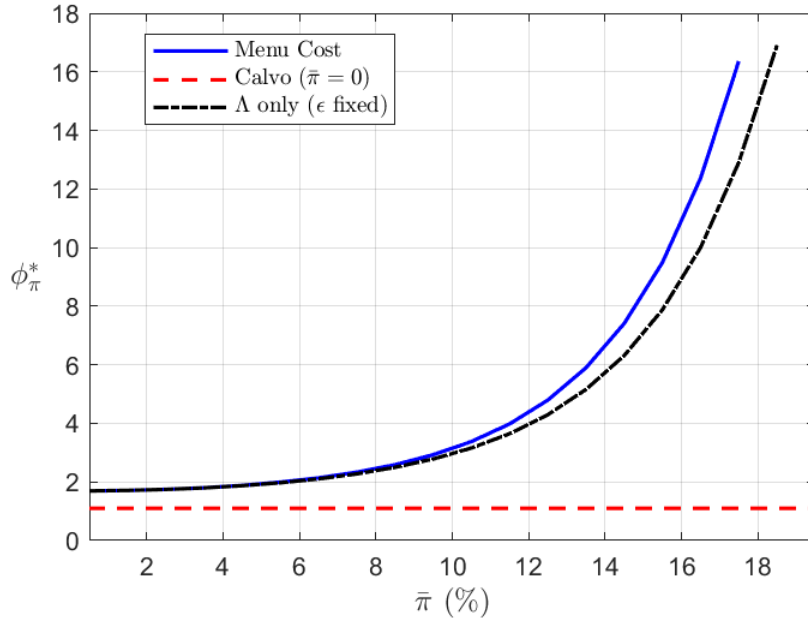
where  $\lambda_y \geq 0$  is the relative weight on output gap variability. The weight  $\lambda_y$  is typically calibrated to be small, but Pfajfar and Winkler (2024) finds that equal weights more closely match public preferences, so I choose  $\lambda_y = 1$  in the baseline. Because the cost shock enters the Phillips curve as  $\Lambda z_t^c$ , the effective cost-shock disturbance to inflation varies with the slope of the Phillips curve. To isolate the role of  $\Lambda$  in propagation from its role in scaling the cost shock, I hold the cost-push variance  $(\Lambda \sigma_c)^2$  constant across models and inflation rates, where  $\sigma_c$  is the standard deviation of the cost shock innovation.

Figure 8 plots the optimal policy coefficient as a function of trend inflation. Optimal policy in the menu cost model (solid blue line) responds more aggressively to inflation than in the Calvo model (dashed red line, only calculated for  $\bar{\pi} = 0$ ) because the slope of the Phillips curve is steeper. This is a standard result; at zero-trend inflation, the menu cost PED is equivalent to a Calvo model with more flexible prices, which requires more aggressive monetary policy because real shocks have larger inflationary effects.

The menu cost model's prescription for aggressive monetary policy is strengthened as trend inflation increases. This is for two reasons: first, higher trend inflation raises the Phillips curve slope (see Figure 6) increasing the optimal  $\phi_\pi$  for the standard reason. The dashed black line isolates this channel: only the slope  $\Lambda$  is reparameterized with  $\bar{\pi}$ . The second reason is that the endogenous FPA amplifies inflationary effects. Absent when trend inflation is zero, the FPA contribution becomes large; at 18.5% trend inflation, the optimal  $\phi_\pi$  coefficient is one third larger in the full menu cost PED (solid blue line) as it is when only

---

<sup>22</sup>A fuller treatment that does not depend on approximations and that considers questions of commitment versus discretion would be desirable for serious quantitative analysis; see Karadi et al. (2025). I apply this textbook approach in order to demonstrate the tractability of the PED and to quickly draw qualitative conclusions. The tractability will be particularly valuable if additional realism is added to the general equilibrium model.



*Notes:* The figure compares optimal policy coefficient ( $\phi_{\pi}^*$ ) across trend inflation levels in MCNK and Calvo. Solid blue line denotes MCNK, dashed black line uses the MCNK slope  $\Lambda$  but fixes  $\epsilon = 0$ , and dashed red line denotes Calvo (calculated only for  $\bar{\pi} = 0$ ).

Figure 8: Optimal Taylor Rule Coefficients vs Trend Inflation

accounting for the effect on  $\Lambda$  (dashed black line).

## 7 Conclusion

Menu costs matter the most when trend inflation is sizeable. And yet this is also when they are least understood. This paper works to resolve this tension by deriving the analytical solution to the firm's MFG under trend inflation. Then I derived a tractable linear discrete time representation, the PED. I showed how the PED can be calibrated and inserted into a standard DSGE framework for optimal policy analysis.

But these methods apply more broadly. The menu cost model is one example of  $(s, S)$  inaction behavior, but it features prominently in many settings. And most cases, drift in the state variable (akin to trend inflation) is standard. For example, drift matters for investment fixed cost problems when there is productivity growth or depreciation (Caballero and Engel, 1999; Baley and Blanco, 2021), portfolio management when illiquid assets have large excess returns (Alvarez et al., 2012), or consumer durables when there is income growth (Attanasio, 2000).

In such cases, the MFG can be linearized and solved following the same steps as in Section 3. Then it can be approximated with a PED as in Section 4. And finally it can be analyzed in tractable macroeconomic models as in Section 6. Thus these methods will be useful for future macroeconomic research.

## References

- Adams, Jonathan J.**, “The Dynamic Distribution in the Fixed Cost Model: An Analytical Solution,” *Available at SSRN 4988128*, 2025.
- Alvarez, Fernando and Francesco Lippi**, “Price Setting With Menu Cost for Multiproduct Firms,” *Econometrica*, 2014, *82* (1), 89–135.
- and – , “The Analytic Theory of a Monetary Shock,” *Econometrica*, 2022, *90* (4), 1655–1680.
- , **Andrea Ferrara, Erwan Gautier, Hervé Le Bihan, and Francesco Lippi**, “Empirical Investigation of a Sufficient Statistic for Monetary Shocks,” *The Review of Economic Studies*, August 2024, p. rdae082.
- , **Francesco Lippi, and Aleksei Oskolkov**, “The Macroeconomics of Sticky Prices with Generalized Hazard Functions\*,” *The Quarterly Journal of Economics*, May 2022, *137* (2), 989–1038.
- , – , and **Juan Passadore**, “Are State- and Time-Dependent Models Really Different?,” *NBER Macroeconomics Annual*, January 2017, *31*, 379–457. Publisher: The University of Chicago Press.
- , – , and **Panagiotis Souganidis**, “Price Setting With Strategic Complementarities as a Mean Field Game,” *Econometrica*, 2023, *91* (6), 2005–2039.
- , **Luigi Guiso, and Francesco Lippi**, “Durable Consumption and Asset Management with Transaction and Observation Costs,” *American Economic Review*, May 2012, *102* (5), 2272–2300.
- , **Martin Beraja, Martín Gonzalez-Rozada, and Pablo Andrés Neumeyer**, “From Hyperinflation to Stable Prices: Argentina’s Evidence on Menu Cost Models,” *The Quarterly Journal of Economics*, February 2019, *134* (1), 451–505.
- Ascari, Guido**, “Staggered prices and trend inflation: some nuisances,” *Review of Economic Dynamics*, July 2004, *7* (3), 642–667.
- and **Argia M. Sbordone**, “The Macroeconomics of Trend Inflation,” *Journal of Economic Literature*, September 2014, *52* (3), 679–739.
- Attanasio, Orazio P.**, “Consumer Durables and Inertial Behaviour: Estimation and Aggregation of (S, s) Rules for Automobile Purchases,” *The Review of Economic Studies*, October 2000, *67* (4), 667–696.
- Auclert, Adrien, Rodolfo Rigato, Matthew Rognlie, and Ludwig Straub**, “New Pricing Models, Same Old Phillips Curves?,” *The Quarterly Journal of Economics*, February 2024, *139* (1), 121–186.
- Baley, Isaac and Andrés Blanco**, “Aggregate Dynamics in Lumpy Economies,” *Econometrica*, 2021, *89* (3), 1235–1264.

- Ball, Laurence and Sandeep Mazumder**, “Inflation Dynamics and the Great Recession,” *Brookings Papers on Economic Activity*, March 2011, pp. 337–381. Publisher: Johns Hopkins University Press.
- Blanco, Andrés, Corina Boar, Callum J Jones, and Virgiliu Midrigan**, “The inflation accelerator,” Technical Report, National Bureau of Economic Research 2024.
- Caballero, Ricardo J. and Eduardo M. R. A. Engel**, “Explaining Investment Dynamics in U.S. Manufacturing: A Generalized (S, s) Approach,” *Econometrica*, 1999, 67 (4), 783–826.
- Calvo, Guillermo A.**, “Staggered prices in a utility-maximizing framework,” *Journal of Monetary Economics*, September 1983, 12 (3), 383–398.
- Carslaw, H. S. and J. C. Jaeger**, *Conduction of Heat in Solids*, second edition, second edition ed., Oxford, New York: Oxford University Press, 1959.
- Cavallo, Alberto, Francesco Lippi, and Ken Miyahara**, “Large Shocks Travel Fast,” *American Economic Review: Insights*, 2024.
- Costain, James, Anton Nakov, and Borja Petit**, “Flattening of the Phillips Curve with State-Dependent Prices and Wages,” *The Economic Journal*, February 2022, 132 (642), 546–581.
- Gagliardone, Luca, Mark Gertler, Simone Lenzu, and Joris Tielens**, “Micro and Macro Cost-Price Dynamics in Normal Times and During Inflation Surges,” February 2025.
- Gagnon, Etienne**, “Price Setting during Low and High Inflation: Evidence from Mexico,” *The Quarterly Journal of Economics*, August 2009, 124 (3), 1221–1263.
- Galí, Jordi**, *Monetary policy, inflation, and the business cycle: an introduction to the new Keynesian framework and its applications*, Princeton University Press, 2008.
- Gertler, Mark and John Leahy**, “A Phillips Curve with an Ss Foundation,” *Journal of Political Economy*, June 2008, 116 (3), 533–572. Publisher: The University of Chicago Press.
- Golosov, Mikhail and Robert E. Lucas Jr.**, “Menu Costs and Phillips Curves,” *Journal of Political Economy*, April 2007, 115 (2), 171–199. Publisher: The University of Chicago Press.
- Hansen, Lars Peter and José A. Scheinkman**, “Long-Term Risk: An Operator Approach,” *Econometrica*, 2009, 77 (1), 177–234.
- Hazell, Jonathon, Juan Herreño, Emi Nakamura, and Jón Steinsson**, “The Slope of the Phillips Curve: Evidence from U.S. States\*,” *The Quarterly Journal of Economics*, August 2022, 137 (3), 1299–1344.

- Karadi, Peter, Anton Nakov, Galo Nuño, Ernesto Pasten, and Dominik Thaler**, “Strike while the iron is hot: optimal monetary policy with a nonlinear Phillips curve,” 2025. Publisher: Banco de Espana Working Paper.
- Midrigan, Virgiliu**, “Menu Costs, Multiproduct Firms, and Aggregate Fluctuations,” *Econometrica*, 2011, 79 (4), 1139–1180.
- Montag, Hugh and Daniel Villar**, “Post-Pandemic Price Flexibility in the U.S.: Evidence and Implications for Price Setting Models,” March 2025.
- Morales-Jiménez, Camilo and Luminita Stevens**, “Price rigidities in US business cycles,” *Manuscript, University of Maryland*, 2024.
- Nakamura, Emi and Jón Steinsson**, “Monetary Non-neutrality in a Multisector Menu Cost Model,” *The Quarterly Journal of Economics*, August 2010, 125 (3), 961–1013.
- , —, **Patrick Sun, and Daniel Villar**, “The Elusive Costs of Inflation: Price Dispersion during the U.S. Great Inflation\*,” *The Quarterly Journal of Economics*, November 2018, 133 (4), 1933–1980.
- Pfajfar, Damjan and Fabian Winkler**, “Households’ Preferences Over Inflation and Monetary Policy Tradeoffs,” *FEDS Working Paper*, May 2024.
- Polyanin, Andrei D.**, *Handbook of Linear Partial Differential Equations for Engineers and Scientists*, New York: Chapman and Hall/CRC, November 2001.
- Sims, Christopher A.**, “Solving Linear Rational Expectations Models,” *Computational Economics*, October 2002, 20 (1-2), 1–20. Num Pages: 1-20 Place: Dordrecht, Netherlands Publisher: Springer Nature B.V.
- Taylor, John B.**, “Aggregate Dynamics and Staggered Contracts,” *Journal of Political Economy*, February 1980, 88 (1), 1–23. Publisher: The University of Chicago Press.
- Uhlig, Harald**, “A Toolkit for Analysing Nonlinear Dynamic Stochastic Models Easily,” in Ramon Marimon and Andrew Scott, eds., *Computational Methods for the Study of Dynamic Economies*, Oxford University Press, October 2001, p. 0.
- Woodford, Michael**, *Interest and Prices: Foundations of a Theory of Monetary Policy*, Princeton University Press, 2003.

## A Proofs

This section collects proofs of the main results. Proofs of additional results in other appendices are included where their results are stated.

### A.1 Proof of Proposition 1

*Proof.* With the marginal cost function scaled by  $\kappa$ , the HJB is

$$\rho v(x, t, \kappa) = \mathbf{B} (x - \kappa MC(t))^2 + \partial_t v(x, t, \kappa) - \bar{\pi} \partial_x v(x, t, \kappa) + \nu \partial_x^2 v(x, t, \kappa) + \zeta (v(x^*(t), t, \kappa) - v(x, t, \kappa))$$

Taking derivatives with respect to  $\kappa$  at  $\kappa = 0$ , the value function  $v(x, t, \kappa)$  and HJB become

$$\rho \hat{v}(x, t) = 2\mathbf{B}x (-MC(t)) + \partial_t \hat{v}(x, t) - \bar{\pi} \partial_x \hat{v}(x, t) + \nu \partial_x^2 \hat{v}(x, t) + \zeta (\hat{v}(x^*(t), t) + \partial_x \hat{v}(x^*, t) \hat{x}^*(t) - \hat{v}(x, t)) \quad (62)$$

where terms without  $t$  arguments such as  $x^*$  and  $w$  denote steady state values. The steady state value of the marginal cost deviation  $MC(t)$  is zero. The reset condition at the steady state is  $\partial_x \hat{v}(x^*, t) = 0$ , which gives equation (16).

The value-matching conditions are

$$\hat{v}(\underline{x}, t) + \partial_x v_{ss}(\underline{x}) \hat{x}(t) = \hat{v}(\bar{x}, t) + \partial_x v_{ss}(\bar{x}) \hat{x}(t) = \hat{v}(x^*(t), t) + \partial_x v_{ss}(x^*) \hat{x}^*(t)$$

and the steady state smooth pasting and reset conditions imply that  $\partial_x v_{ss}(\underline{x}) = \partial_x v_{ss}(\bar{x}) = \partial_x v_{ss}(x^*) = 0$ . Therefore, the value-matching conditions become

$$\hat{v}(\underline{x}, t) = \hat{v}(\bar{x}, t) = \hat{v}(x^*, t)$$

The smooth-pasting and reset-optimality conditions are

$$\partial_x \hat{v}(\underline{x}, t) + \partial_x^2 v_{ss}(\underline{x}) \hat{x}(t) = \partial_x \hat{v}(\bar{x}, t) + \partial_x^2 v_{ss}(\bar{x}) \hat{x}(t) = \partial_x \hat{v}(x^*(t), t) + \partial_x^2 v_{ss}(x^*) \hat{x}^*(t) = 0$$

and the terminal condition is

$$\hat{v}(x, T) = 0$$

The derivative of the KFE (14) becomes

$$\partial_t \hat{h}(x, t) = \nu \partial_x^2 \hat{h}(x, t) + \bar{\pi} \partial_x \hat{h}(x, t) - \zeta \hat{h}(x, t) + \hat{F}(t) \delta(x - x_{ss}^*) - F_{ss} \delta'(x - x_{ss}^*) \hat{x}^*(t) \quad (63)$$

$\delta'(\cdot)$  denotes the derivative of the Dirac delta function, which is not everywhere defined, but is well behaved when integrated against a smooth function, as will be the case in the MFG solution.

The absorbing boundary conditions become

$$\hat{h}(\underline{x}, t) + h'_{ss}(\underline{x})\hat{x}(t) = \hat{h}(\bar{x}, t) + h'_{ss}(\bar{x})\hat{x}(t) = 0$$

The FPA is given by

$$\hat{F}(t) = \nu\partial_x\hat{h}(\underline{x}, t) + \bar{\pi}\hat{h}(\underline{x}, t) - \nu\partial_x\hat{h}(\bar{x}, t) - \bar{\pi}\hat{h}(\bar{x}, t) + (\nu h''_{ss}(\underline{x}) + \bar{\pi}h'_{ss}(\underline{x}))\hat{x}(t) - (\nu h''_{ss}(\bar{x}) + \bar{\pi}h'_{ss}(\bar{x}))\hat{x}(t)$$

The latter terms simplify; the steady state KFE implies that away from the reset point:

$$[x \neq x_{ss}^*] : \quad \zeta h_{ss}(x) = \nu h''_{ss}(x) + \bar{\pi}h'_{ss}(x)$$

therefore the boundary conditions  $h_{ss}(\underline{x}) = 0 = h_{ss}(\bar{x})$  imply  $\nu h''_{ss}(\underline{x}) + \bar{\pi}h'_{ss}(\underline{x}) = 0 = \nu h''_{ss}(\bar{x}) + \bar{\pi}h'_{ss}(\bar{x})$ , and the FPA equation simplifies to

$$\hat{F}(t) = \nu\partial_x\hat{h}(\underline{x}, t) + \bar{\pi}\hat{h}(\underline{x}, t) - \nu\partial_x\hat{h}(\bar{x}, t) - \bar{\pi}\hat{h}(\bar{x}, t)$$

Finally, the initial condition on the interior is given by the derivative of the initial steady state distribution, which is fixed:

$$\hat{h}(x, 0) = 0 \quad \text{for } x \in (\underline{x}, \bar{x})$$

At the boundaries, the absorbing conditions imply  $\hat{h}(\underline{x}, 0) = -h'_{ss}(\underline{x})\hat{x}(0)$  and  $\hat{h}(\bar{x}, 0) = -h'_{ss}(\bar{x})\hat{x}(0)$ , which are possibly non-zero.  $\square$

## A.2 Proof of Lemma 1

*Proof.* By Lemma 5, the solution to the derivative HJB (16) is

$$\begin{aligned} \hat{v}(x, t) = & -2\mathbf{B} \int_t^T \int_{\underline{x}}^{\bar{x}} G_{HJB}(x, y, \tau - t) y(-MC(\tau)) dy d\tau - \zeta \int_t^T \int_{\underline{x}}^{\bar{x}} G_{HJB}(x, y, \tau - t) \hat{v}(x^*, \tau) dy d\tau \\ & + \nu \int_t^T \partial_y G_{HJB}(x, \underline{x}, \tau - t) \hat{v}(x^*, \tau) d\tau - \nu \int_t^T \partial_y G_{HJB}(x, \bar{x}, \tau - t) \hat{v}(x^*, \tau) d\tau \quad (64) \end{aligned}$$

The derivative value matching condition (17) gives the Dirichlet boundary conditions.  $G_{HJB}(x, y, t)$  denotes the appropriately parameterized Green's function per equation (69), shifted to the interval  $[\underline{x}, \bar{x}]$ . Written in the typical heat equation form, the HJB is

$$\partial_t \hat{v}(x, t) = -\nu \partial_x^2 \hat{v}(x, t) + \bar{\pi} \partial_x \hat{v}(x, t) + (\rho + \zeta) \hat{v}(x, t) - 2\mathbf{B}x(-MC(t)) - \zeta \hat{v}(x^*, t)$$

so by Lemma 5 the Green's function is

$$G_{HJB}(x, y, t) = \frac{2}{\bar{x} - \underline{x}} e^{\left(\frac{-\bar{x}}{2\nu}(y-x) + (-\rho + \zeta) - \frac{\bar{x}^2}{4\nu}\right)t} \sum_{n=1}^{\infty} \sin\left(\frac{n\pi(x - \underline{x})}{\bar{x} - \underline{x}}\right) \sin\left(\frac{n\pi(y - \underline{x})}{\bar{x} - \underline{x}}\right) e^{-\frac{\nu n^2 \pi^2}{(\bar{x} - \underline{x})^2} t} \quad (65)$$

which can be written concisely in terms of the eigenfunctions and eigenvalues:

$$G_{HJB}(x, y, t) = \sum_{n=1}^{\infty} \gamma_{HJB,n}(x, y) e^{-\lambda_{HJB,n} t}$$

With this notation, equation (64) can be written as

$$\hat{v}(x, t) = \sum_{n=1}^{\infty} \hat{v}_n(x, t)$$

where

$$\begin{aligned} \hat{v}_n(x, t) = & -2\mathbf{B} \int_t^T \int_{\underline{x}}^{\bar{x}} \gamma_{HJB,n}(x, y) e^{-\lambda_{HJB,n}(\tau-t)} y (-MC(\tau)) dy d\tau \\ & + \int_t^T \left( -\zeta \int_{\underline{x}}^{\bar{x}} \gamma_{HJB,n}(x, y) dy + \nu \partial_y \gamma_{HJB,n}(x, \underline{x}) - \nu \partial_y \gamma_{HJB,n}(x, \bar{x}) \right) e^{-\lambda_{HJB,n}(\tau-t)} \hat{v}(x^*, \tau) d\tau \end{aligned}$$

which gives the desired expression once the definitions of  $\Theta_{MC,n}(x)$  and  $\Theta_{v,n}(x)$  are used.  $\square$

### A.3 Proof of Lemma 2

*Proof.* The linearized KFE has time-varying boundary conditions  $\hat{h}(\underline{x}, t) = -h'_{ss}(\underline{x})\hat{x}(t)$  and  $\hat{h}(\bar{x}, t) = -h'_{ss}(\bar{x})\hat{x}(t)$ , and two forcing terms:  $\hat{F}(t)\delta(x - x_{ss}^*)$  and  $-F_{ss}\delta'(x - x_{ss}^*)\hat{x}^*$ .

Decompose  $\hat{h} = \hat{h}_{\text{crit}} + \hat{h}_{\text{int}}$  where  $\hat{h}_{\text{crit}}$  captures the singular components (boundary conditions and  $\delta'$  forcing) and  $\hat{h}_{\text{int}}$  satisfies zero boundary conditions with smooth forcing.

Lemma 8 implies that  $-h'_{ss}(\underline{x})\hat{x}(t)H_{\underline{x}}(x) + h'_{ss}(\bar{x})\hat{x}(t)H_{\bar{x}}(x)$  solves the KFE with zero forcing and the time-varying boundary conditions. Lemma 6 says that  $-F_{ss}\hat{x}^*(t)J_{x^*}(x)$  solves the KFE with zero boundary conditions and forcing  $-F_{ss}\delta'(x - x_{ss}^*)\hat{x}^*(t)$ . Combining these gives the critical-point component  $\hat{h}_{\text{crit}}$  in (27).

Since  $\hat{h}(x, 0) = 0$ , the interior component must satisfy the initial condition

$$\hat{h}_{\text{int}}(x, 0) = -\hat{h}_{\text{crit}}(x, 0) = h'_{ss}(\underline{x})\hat{x}(0)H_{\underline{x}}(x) - h'_{ss}(\bar{x})\hat{x}(0)H_{\bar{x}}(x) + F_{ss}\hat{x}^*(0)J_{x^*}(x)$$

By Property 3 with Green's function  $G_{KFE}(x, y, t) = \sum_n \gamma_{KFE,n}(x, y) e^{-\lambda_{KFE,n} t}$ , the solution decomposes into  $\hat{h}_{\text{int}} = \sum_n \hat{h}_{\text{int},n}$ .  $\square$

## A.4 Proof of Theorem 1

*Proof.* The value function at  $x$  is determined by the HJB solution (64), which gives equations (35)–(36) directly.

I prove the result for  $\hat{x}^*(t)$ ; the other boundaries follow the same logic. The optimal reset point is given by the smooth-pasting condition 18:

$$\hat{x}^*(t) = -\frac{1}{\partial_x^2 v_{ss}(x^*)} \partial_x \hat{v}(x^*, t)$$

which is determined by future aggregate price gaps, marginal costs, and the value function at the boundaries through the HJB solution (64):

$$\hat{x}^*(t) = -\frac{1}{\partial_x^2 v_{ss}(x^*)} \sum_{n=1}^{\infty} \partial_x \hat{v}_n(x^*, t)$$

Decompose  $\hat{x}^*(t) = \sum_{n=1}^{\infty} \hat{x}_n^*(t)$  into a sum of terms associated with each eigenvalue:

$$\begin{aligned} \hat{x}_n^*(t) &= -\frac{1}{\partial_x^2 v_{ss}(x^*)} \partial_x \hat{v}_n(x^*, t) \\ &= -\frac{1}{\partial_x^2 v_{ss}(x^*)} \left( \Theta'_{MC,n}(x^*) \int_t^T e^{-\lambda_{HJB,n}(\tau-t)} (-MC(\tau)) d\tau + \Theta'_{v,n}(x^*) \int_t^T e^{-\lambda_{HJB,n}(\tau-t)} \hat{v}(x^*, \tau) d\tau \right) \end{aligned}$$

by Lemma 1. Using the coefficient definitions  $\chi_{x^*,n} = -\frac{1}{\partial_x^2 v_{ss}(x^*)} \Theta'_{MC,n}(x^*)$  and  $\Xi_{x^*,n} = -\frac{1}{\partial_x^2 v_{ss}(x^*)} \Theta'_{v,n}(x^*)$  gives equation (37).

Decompose the FPA  $\hat{F}(t) = \hat{F}_{\text{crit}}(t) + \hat{F}_{\text{int}}(t)$  into critical-point and interior components, where  $\hat{F}_{\text{int}}(t) = \sum_{n=1}^{\infty} \hat{F}_{\text{int},n}(t)$ . The interior component  $\hat{F}_{\text{int},n}(t)$  is computed from  $\hat{h}_{\text{int},n}(x, t)$  using the flux formula. Since  $\hat{h}_{\text{int},n}(x, t)$  satisfies zero boundary conditions, Lemma 2 and the flux formula give equation (41). The critical-point component  $\hat{F}_{\text{crit}}(t)$  is computed from the lifting functions in Lemma 2, giving equation (40).

The conditional path for the average gap  $X(t)$  is given by integrating the conditional solution to the KFE:

$$\hat{X}(t) = \int_{\underline{x}}^{\bar{x}} x \hat{h}(x, t) dx = \int_{\underline{x}}^{\bar{x}} \sum_{n=1}^{\infty} x h_n(x, t) dx = \sum_{n=1}^{\infty} \hat{X}_n(t)$$

where  $\hat{X}_n(t) \equiv \int_{\underline{x}}^{\bar{x}} x h_n(x, t) dx$ . The average gap does not require the lifting function solution of Lemma 2; Lemma 3 gives a simpler solution that follows directly from the Green's function approach (Property 3):  $\hat{h}(x, t) = \sum_{n=1}^{\infty} \hat{h}_n(x, t)$  where

$$\hat{h}_n(x, t) = \int_0^t e^{-\lambda_{KFE,n}(t-\tau)} \left( \varpi_{F,n}(x) \hat{F}(\tau) + \varpi_{x^*,n}(x) \hat{x}^*(\tau) + \varpi_{\underline{x},n}(x) \hat{\underline{x}}(\tau) - \varpi_{\bar{x},n}(x) \hat{\bar{x}}(\tau) \right) d\tau$$

$$\varpi_{F,n}(x) \equiv \gamma_{KFE,n}(x, x^*)$$

$$\varpi_{x^*,n}(x) \equiv \partial_y \gamma_{KFE,n}(x, x^*) F_{ss} \quad \varpi_{\underline{x},n}(x) \equiv -\nu \partial_y \gamma_{KFE,n}(x, \underline{x}) h'_{ss}(\underline{x}) \quad \varpi_{\bar{x},n}(x) \equiv -\nu \partial_y \gamma_{KFE,n}(x, \bar{x}) h'_{ss}(\bar{x})$$

therefore each  $\hat{X}_n(t)$  term is given by

$$\hat{X}_n(t) = \int_{\underline{x}}^{\bar{x}} \int_0^t e^{-\lambda_{KFE,n}(t-\tau)} x \left( \varpi_{F,n}(x) \hat{F}(\tau) + \varpi_{x^*,n}(x) \hat{x}^*(\tau) + \varpi_{\underline{x},n}(x) \hat{\underline{x}}(\tau) - \varpi_{\bar{x},n}(x) \hat{\bar{x}}(\tau) \right) d\tau dx$$

Substitute using the coefficient definitions to yield the desired expression.  $\square$

The proofs the following intermediate result, while solves the KFE for the perturbed distribution without the lifting functions:

**Lemma 3.** *The conditional solution to the KFE is the infinite sum*

$$\hat{h}(x, t) = \sum_{n=1}^{\infty} \hat{h}_n(x, t)$$

where

$$\hat{h}_n(x, t) = \int_0^t e^{-\lambda_{KFE,n}(t-\tau)} \left( \varpi_{F,n}(x) \hat{F}(\tau) + \varpi_{x^*,n}(x) \hat{x}^*(\tau) + \varpi_{\underline{x},n}(x) \hat{\underline{x}}(\tau) - \varpi_{\bar{x},n}(x) \hat{\bar{x}}(\tau) \right) d\tau$$

and

$$\begin{aligned} \lambda_{KFE,n} &\equiv \zeta + \frac{\bar{\pi}^2}{4\nu} + \frac{\nu n^2 \pi^2}{(\bar{x} - \underline{x})^2} \\ \gamma_{KFE,n}(x, y) &\equiv \frac{2}{\bar{x} - \underline{x}} e^{\frac{\bar{\pi}}{2\nu}(y-x)} \sin\left(\frac{n\pi(x - \underline{x})}{\bar{x} - \underline{x}}\right) \sin\left(\frac{n\pi(y - \underline{x})}{\bar{x} - \underline{x}}\right) \\ \varpi_{F,n}(x) &\equiv \gamma_{KFE,n}(x, x^*) \end{aligned}$$

$$\varpi_{x^*,n}(x) \equiv \partial_y \gamma_{KFE,n}(x, x^*) F_{ss} \quad \varpi_{\underline{x},n}(x) \equiv -\nu \partial_y \gamma_{KFE,n}(x, \underline{x}) h'_{ss}(\underline{x}) \quad \varpi_{\bar{x},n}(x) \equiv -\nu \partial_y \gamma_{KFE,n}(x, \bar{x}) h'_{ss}(\bar{x})$$

*Proof.* By Property 3, the conditional solution to the derivative KFE (20) is

$$\begin{aligned} \hat{h}(x, t) &= - \int_{\underline{x}}^{\bar{x}} \int_0^t G_{KFE}(x, y, t - \tau) \hat{F}(\tau) \delta(y - x^*) d\tau dy + \int_{\underline{x}}^{\bar{x}} \int_0^t G_{KFE}(x, y, t - \tau) F_{ss} \delta'(y - x^*) \hat{x}^*(\tau) d\tau dy \\ &\quad - \nu \int_0^t \partial_y G_{KFE}(x, \underline{x}, t - \tau) h'_{ss}(\underline{x}) \hat{\underline{x}}(\tau) d\tau + \nu \int_0^t \partial_y G_{KFE}(x, \bar{x}, t - \tau) h'_{ss}(\bar{x}) \hat{\bar{x}}(\tau) d\tau \quad (66) \end{aligned}$$

where  $G_{KFE}(x, y, t)$  is the appropriately parameterized Green's function per equation (69), albeit shifted to the interval  $[\underline{x}, \bar{x}]$ :

$$G_{KFE}(x, y, t) = \frac{2}{\bar{x} - \underline{x}} e^{\left(\frac{\bar{\pi}}{2\nu}(y-x) + \left(-\zeta - \frac{\bar{\pi}^2}{4\nu}\right)t\right)} \sum_{n=1}^{\infty} \sin\left(\frac{n\pi(x - \underline{x})}{\bar{x} - \underline{x}}\right) \sin\left(\frac{n\pi(y - \underline{x})}{\bar{x} - \underline{x}}\right) e^{-\frac{\nu n^2 \pi^2}{(\bar{x} - \underline{x})^2} t} \quad (67)$$

The Green's function (67) terms can be neatly separated by

$$G_{KFE}(x, y, t) = \sum_{n=1}^{\infty} \gamma_{KFE,n}(x, y) e^{-\lambda_{KFE,n} t} \quad (68)$$

With this notation, the solution (66) becomes

$$\hat{h}(x, t) = \sum_{n=1}^{\infty} \hat{h}_n(x, t)$$

where

$$\begin{aligned} \hat{h}_n(x, t) &= \int_{\underline{x}}^{\bar{x}} \int_0^t \gamma_{KFE,n}(x, y) e^{-\lambda_{KFE,n}(t-\tau)} \hat{F}(\tau) \delta(y-x^*) d\tau dy - \int_{\underline{x}}^{\bar{x}} \int_0^t \gamma_{KFE,n}(x, y) e^{-\lambda_{KFE,n}(t-\tau)} F_{ss} \delta'(y-x^*) \hat{x}^*(\tau) d\tau dy \\ &\quad - \nu \int_0^t \partial_y \gamma_{KFE,n}(x, \underline{x}) e^{-\lambda_{KFE,n}(t-\tau)} h'_{ss}(\underline{x}) \hat{x}(\tau) d\tau + \nu \int_0^t \partial_y \gamma_{KFE,n}(x, \bar{x}) e^{-\lambda_{KFE,n}(t-\tau)} h'_{ss}(\bar{x}) \hat{x}(\tau) d\tau \end{aligned}$$

Simplify the Dirac terms:

$$\begin{aligned} &= \int_0^t \gamma_{KFE,n}(x, x^*) e^{-\lambda_{KFE,n}(t-\tau)} \hat{F}(\tau) d\tau + \int_0^t \partial_y \gamma_{KFE,n}(x, x^*) e^{-\lambda_{KFE,n}(t-\tau)} F_{ss} \hat{x}^*(\tau) d\tau \\ &\quad - \nu \int_0^t \partial_y \gamma_{KFE,n}(x, \underline{x}) e^{-\lambda_{KFE,n}(t-\tau)} h'_{ss}(\underline{x}) \hat{x}(\tau) d\tau + \nu \int_0^t \partial_y \gamma_{KFE,n}(x, \bar{x}) e^{-\lambda_{KFE,n}(t-\tau)} h'_{ss}(\bar{x}) \hat{x}(\tau) d\tau \\ &= \int_0^t e^{-\lambda_{KFE,n}(t-\tau)} \left( \gamma_{KFE,n}(x, x^*) \hat{F}(\tau) + \partial_y \gamma_{KFE,n}(x, x^*) F_{ss} \hat{x}^*(\tau) \right. \\ &\quad \left. - \nu \partial_y \gamma_{KFE,n}(x, \underline{x}) h'_{ss}(\underline{x}) \hat{x}(\tau) + \nu \partial_y \gamma_{KFE,n}(x, \bar{x}) h'_{ss}(\bar{x}) \hat{x}(\tau) \right) d\tau \end{aligned}$$

which gives the intended expression.  $\square$

## A.5 Proof of Proposition 2

*Proof.* The approach is to approximate the forcing in each integral of Theorem 1 as constant on intervals of width  $\Delta t$ , and integrate the exponential kernel exactly. For any eigenvalue  $\lambda$ , the exact integral of the kernel over one time step is given by equation (42).

For the value function component at  $x^*$  (and similarly for the boundary points) a discrete time approximation of the integral in equation (36) treats the forcing as constant at its right-endpoint value on each interval of width  $\Delta t$ , and integrates the exponential kernel exactly:

$$\hat{v}_n(x^*, t) \approx \sum_{k=1}^{\infty} (\Theta_{MC,n}(x^*) (-MC(t+k\Delta t)) + \Theta_{v,n}(x^*) \hat{v}(x^*, t+k\Delta t)) \int_{(k-1)\Delta t}^{k\Delta t} e^{-\lambda_{HJB,n}\tau} d\tau$$

The integral evaluates to  $e^{-\lambda_{HJB,n}(k-1)\Delta t} \zeta(\lambda_{HJB,n})$ . Because of the exponential function, this equation is recursive forwards:

$$\hat{v}_n(x^*, t) \approx (\Theta_{MC,n}(x^*) (-MC(t+\Delta t)) + \Theta_{v,n}(x^*) \hat{v}(x^*, t+\Delta t)) \zeta(\lambda_{HJB,n}) + e^{-\lambda_{HJB,n}\Delta t} \hat{v}_n(x^*, t+\Delta t)$$

For  $\hat{x}_n^*(t)$  (and similarly for the boundary points) a discrete time approximation of the forward-looking integral in equation (37) follows the same procedure.<sup>23</sup>

$$\hat{x}_n^*(t) \approx \sum_{k=1}^{\infty} (\chi_{x^*,n}(-MC(t+k\Delta t)) + \Xi_{x^*,n}\hat{v}(x^*,t+k\Delta t)) e^{-\lambda_{HJB,n}(k-1)\Delta t} \varsigma(\lambda_{HJB,n})$$

Because of the exponential function, this equation is recursive forwards:

$$\hat{x}_n^*(t) \approx (\chi_{x^*,n}(-MC(t+\Delta t)) + \Xi_{x^*,n}\hat{v}(x^*,t+\Delta t)) \varsigma(\lambda_{HJB,n}) + e^{-\lambda_{HJB,n}\Delta t} \hat{x}_n^*(t+\Delta t)$$

For the interior component  $\hat{F}_{\text{int},n}(t)$ , a discrete time approximation of the integral in equation (41) treats the forcing as constant on each interval of width  $\Delta t$ , and integrates the kernel exactly. Note that this involves  $\hat{x}'(\tau)$ ,  $\hat{\underline{x}}'(\tau)$ , and  $\hat{\bar{x}}'(\tau)$ , which are approximated by the discrete differences  $\Delta\hat{x}^*(\tau) \equiv \hat{x}^*(\tau) - \hat{x}^*(\tau - \Delta t)$ ,  $\Delta\hat{\underline{x}}(\tau) \equiv \hat{\underline{x}}(\tau) - \hat{\underline{x}}(\tau - \Delta t)$ , and similarly for  $\hat{\bar{x}}$ . Since  $\hat{x}'(\tau) \approx \Delta\hat{x}^*(\tau)/\Delta t$ , the derivative terms receive a factor  $\varsigma(\lambda_{KFE,n})/\Delta t$  while the  $\hat{F}$  term receives  $\varsigma(\lambda_{KFE,n})$ . The economy is in steady state for  $t < 0$ , so the initial condition term is absorbed into the  $\tau = 0$  term:

$$\hat{F}_{\text{int},n}(t) \approx \sum_{j=0}^{\lfloor t/\Delta t \rfloor} e^{-\lambda_{KFE,n}(t-j\Delta t-\Delta t)} \varsigma(\lambda_{KFE,n}) \left( \varphi_{F,n}\hat{F}(j\Delta t) + \varphi_{x^*,n} \frac{\Delta\hat{x}^*(j\Delta t)}{\Delta t} + \varphi_{\underline{x},n} \frac{\Delta\hat{\underline{x}}(j\Delta t)}{\Delta t} - \varphi_{\bar{x},n} \frac{\Delta\hat{\bar{x}}(j\Delta t)}{\Delta t} \right)$$

using  $\Delta\hat{x}^*(0) = \hat{x}^*(0)$ ,  $\Delta\hat{\underline{x}}(0) = \hat{\underline{x}}(0)$ , and  $\Delta\hat{\bar{x}}(0) = \hat{\bar{x}}(0)$  to combine the initial condition term with the  $\tau = 0$  flow term. Because of the exponential function, this equation is recursive backwards:<sup>24</sup>

$$\hat{F}_{\text{int},n}(t) \approx \varsigma(\lambda_{KFE,n}) \left( \varphi_{F,n}\hat{F}(t) + \varphi_{x^*,n} \frac{\Delta\hat{x}^*(t)}{\Delta t} + \varphi_{\underline{x},n} \frac{\Delta\hat{\underline{x}}(t)}{\Delta t} - \varphi_{\bar{x},n} \frac{\Delta\hat{\bar{x}}(t)}{\Delta t} \right) + e^{-\lambda_{KFE,n}\Delta t} \hat{F}_{\text{int},n}(t-\Delta t)$$

For the critical-point component  $\hat{F}_{\text{crit}}(t)$ , equation (40) gives directly:

$$\hat{F}_{\text{crit}}(t) = \varphi_{x^*}\hat{x}^*(t) + \varphi_{\underline{x}}\hat{\underline{x}}(t) - \varphi_{\bar{x}}\hat{\bar{x}}(t)$$

The total FPA is  $\hat{F}(t) = \hat{F}_{\text{crit}}(t) + \sum_{n=1}^{\infty} \hat{F}_{\text{int},n}(t)$ .

For the aggregate gap  $\hat{X}_n(t)$ , a discrete time approximation of the integral in equation (39) treats the forcing as constant on each time interval and integrates the kernel exactly:

$$\hat{X}_n(t) \approx \sum_{j=0}^{\lfloor t/\Delta t \rfloor} e^{-\lambda_{KFE,n}(t-j\Delta t-\Delta t)} \varsigma(\lambda_{KFE,n}) \left( \xi_{F,n}\hat{F}(j\Delta t) + \xi_{x^*,n}\hat{x}^*(j\Delta t) + \xi_{\underline{x},n}\hat{\underline{x}}(j\Delta t) - \xi_{\bar{x},n}\hat{\bar{x}}(j\Delta t) \right)$$

<sup>23</sup>While the backward-looking KFE is approximated with a left-endpoint evaluation (including the current period flow), the forward-looking HJB is approximated with a right-endpoint evaluation (starting from the next period). This distinction ensures stability in the discrete time system.

<sup>24</sup>The choice to use  $\hat{F}(t)$  here versus  $\hat{F}(t-\Delta t)$  approximates the same continuous function, but is useful for both stability and so that the discrete time approximation of the vector representation follows naturally from the continuous time case.

Because of the exponential function, this equation is recursive backwards:

$$\hat{X}_n(t) \approx \varsigma(\lambda_{KFE,n}) \left( \xi_{F,n} \hat{F}(t) + \xi_{x^*,n} \hat{x}^*(t) + \xi_{\underline{x},n} \hat{\underline{x}}(t) - \xi_{\bar{x},n} \hat{\bar{x}}(t) \right) + e^{-\lambda_{KFE,n} \Delta t} \hat{X}_n(t - \Delta t)$$

The total average gap is  $\hat{X}(t) = \sum_{n=1}^{\infty} \hat{X}_n(t)$ .

Setting the step size to  $\Delta t = 1$  and adopting the discrete time notation gives the desired equations.  $\square$

## A.6 Proof of Theorem 2

*Proof.* The Optimal Price Setting equation follows from equation (47), with  $p_t^* = \alpha_{p^*} \hat{x}_{\hat{n},t}^*$  for some scalar  $\alpha_{p^*}$ :

$$p_t^* = \alpha_{p^*} \varsigma_{HJB,\hat{n}} (\chi_{x^*,\hat{n}} (-MC_t) + \Xi_{x^*,\hat{n}} V_t^*) + e^{-\lambda_{HJB,\hat{n}}} p_{t+1}^*$$

Following the value matching conditions (43), it is convenient to characterize  $\underline{V}_t$  instead of  $V_t^*$  directly. The primary eigenfunction approximation is

$$\hat{V}_{\hat{n},t} \equiv \underline{V}_t = \varsigma_{HJB,\hat{n}} \left( \Theta_{MC,\hat{n}}(\underline{x}) (-MC_t) + \Theta_{v,\hat{n}}(\underline{x}) \hat{V}_t^* \right) + e^{-\lambda_{HJB,\hat{n}}} \underline{V}_{t+1}$$

by Proposition 2. Observe that  $\Theta_{MC,n}(\underline{x}) = 0$  and  $\Theta_{v,n}(\underline{x}) = 0$ , because  $\gamma_{HJB,n}(\underline{x}, y) = 0$  for all  $n$  and  $y$ . Therefore  $\underline{V}_t = V_t^* = 0$  and the price setting equation reduces to

$$p_t^* = \alpha_{p^*} \varsigma_{HJB,\hat{n}} \chi_{x^*,\hat{n}} (-MC_t) + e^{-\lambda_{HJB,\hat{n}}} p_{t+1}^*$$

The effect on  $p_t^*$  of a permanent marginal cost change  $\kappa$  is

$$\frac{dp_t^*}{d\kappa} = \frac{\alpha_{p^*} \varsigma_{HJB,\hat{n}} \chi_{x^*,\hat{n}}}{1 - e^{-\lambda_{HJB,\hat{n}}}} \kappa$$

thus long-run neutrality requires  $\alpha_{p^*} \varsigma_{HJB,\hat{n}} \chi_{x^*,\hat{n}} = 1 - e^{-\lambda_{HJB,\hat{n}}}$ . Since  $\varsigma_{HJB,\hat{n}} = (1 - e^{-\lambda_{HJB,\hat{n}}}) / \lambda_{HJB,\hat{n}}$ , the  $1 - e^{-\lambda_{HJB,\hat{n}}}$  factors cancel, giving  $\alpha_{p^*} = \lambda_{HJB,\hat{n}} / \chi_{x^*,\hat{n}}$ . Use  $e^{-\lambda_{HJB,\hat{n}}} = e^{-\rho - \lambda_{KFE,\hat{n}}} = \theta\beta$  and note that  $\alpha_{p^*} \varsigma_{HJB,\hat{n}} \chi_{x^*,\hat{n}} = 1 - \theta\beta$  to write

$$p_t^* = (1 - \theta\beta) MC_t + \theta\beta p_{t+1}^*$$

Similarly, the other results from Proposition 2 give

$$\underline{p}_t = \alpha_{\underline{p}} \varsigma_{HJB,\hat{n}} \chi_{\underline{x},\hat{n}} (-MC_t) + e^{-\lambda_{HJB,\hat{n}}} \underline{p}_{t+1} \quad \bar{p}_t = \alpha_{\bar{p}} \varsigma_{HJB,\hat{n}} \chi_{\bar{x},\hat{n}} (-MC_t) + e^{-\lambda_{HJB,\hat{n}}} \bar{p}_{t+1}$$

and long-run neutrality requires

$$\alpha_{\underline{p}} \varsigma_{HJB, \hat{n}} \chi_{\underline{x}, \hat{n}} = (1 - e^{-\lambda_{HJB, \hat{n}}}) \quad \alpha_{\bar{p}} \varsigma_{HJB, \hat{n}} \chi_{\bar{x}, \hat{n}} = (1 - e^{-\lambda_{HJB, \hat{n}}})$$

which then imply  $p_t^* = \underline{p}_t = \bar{p}_t$ .

The Flow Determination equation follows from the critical-point component equation (51) and the modified interior component equation (57). In the single-eigenfunction approximation with  $p_t^* = \underline{p}_t = \bar{p}_t$ , the critical-point component is

$$\hat{F}_{\text{crit}, t} = \varphi_{p^*} p_t^*$$

where  $\varphi_{p^*} \equiv \varphi_{x^*} + \varphi_{\underline{x}} - \varphi_{\bar{x}}$  combines the critical-point coefficients (which do not depend on  $n$ ). The interior component satisfies

$$\hat{F}_{\text{int}, \hat{n}, t} = \varsigma_{KFE, \hat{n}} \left( \tilde{\varphi}_{F, \hat{n}} \hat{F}_t + \varphi'_{p^*, \hat{n}} \Delta p_t^* \right) + e^{-\lambda_{KFE, \hat{n}}} \hat{F}_{\text{int}, \hat{n}, t-1}$$

where  $\varphi'_{p^*, n} \equiv \varphi_{x^{*'}, n} + \varphi_{\underline{x}', n} - \varphi_{\bar{x}', n}$  involves the primed interior coefficients and  $\Delta p_t^* = p_t^* - p_{t-1}^*$ .

The total FPA perturbation is  $\hat{F}_t = \hat{F}_{\text{crit}, t} + \sum_{n=1}^{\infty} \hat{F}_{\text{int}, n, t}$ . In the PED, the FPA is up to scale in each component, i.e.

$$F_t = \alpha_{F, \text{crit}} \hat{F}_{\text{crit}, t} + \alpha_{F, \text{int}} \hat{F}_{\text{int}, \hat{n}, t}$$

for some coefficients  $\alpha_{F, \text{crit}}$  and  $\alpha_{F, \text{int}}$ . Substituting the expressions:

$$F_t = \alpha_{F, \text{crit}} \varphi_{p^*} p_t^* + \alpha_{F, \text{int}} \varsigma_{KFE, \hat{n}} \left( \tilde{\varphi}_{F, \hat{n}} \hat{F}_t + \varphi'_{p^*, \hat{n}} \Delta p_t^* \right) + e^{-\lambda_{KFE, \hat{n}}} \hat{F}_{\text{int}, \hat{n}, t-1}$$

FPA-consistency (Definition 3) requires that after a permanent  $\kappa$  marginal cost shock,  $F_t \rightarrow 0$  in the long-run.  $p_t^*$  permanently increases by  $\kappa$  to satisfy long-run neutrality, which implies  $\alpha_{F, \text{crit}} = 0$ . FPA-consistency also requires that  $\tilde{\varphi}_{F, n}$  coefficients sum to zero. Therefore the FPA equation reduces to

$$F_t = \alpha_{F, \text{int}} \varsigma_{KFE, \hat{n}} \varphi'_{p^*, \hat{n}} \Delta p_t^* + e^{-\lambda_{KFE, \hat{n}}} F_{t-1}$$

FPA-consistency also requires matching the impact effect  $\hat{F}_1 \kappa$  to a  $\Delta p_1^* = \kappa$  shock, which requires

$$\begin{aligned} F_1 \kappa &= \alpha_{F, \text{int}} \varsigma_{KFE, \hat{n}} \varphi'_{p^*, \hat{n}} \kappa \\ \implies \alpha_{F, \text{int}} &= \frac{\hat{F}_1}{\varsigma_{KFE, \hat{n}} \varphi'_{p^*, \hat{n}}} \end{aligned}$$

given these values for the scaling coefficients, use the  $\hat{F}_1$  value from Definition 3 (which implies  $\psi_{p^*} = \hat{F}_1$ )

and substitute back in with the  $\psi_{p^*}$  and  $\theta$  definitions to yield the Flow Determination equation:

$$F_t = \psi_{p^*} (p_t^* - p_{t-1}^*) + \theta F_{t-1}$$

The Price Level Law of Motion follows from the discretization (50), which holds up to scale with unknown coefficient  $\alpha_p$ . In the single-eigenfunction approximation with  $p_t^* = \underline{p}_t = \bar{p}_t$ , this reduces to

$$p_t = \alpha_p \varsigma_{KFE, \dot{n}} (\xi_{F, \dot{n}} F_t + \xi_{p^*, \dot{n}} p_t^*) + \theta p_{t-1}$$

where  $\xi_{p^*, n} \equiv \xi_{x^*, n} + \xi_{\underline{x}, n} - \xi_{\bar{x}, n}$ .

Long-run neutrality requires that a permanent  $\kappa$  increase in  $MC_t$  leads to a  $\kappa$  increase in the limit  $p_\infty$ . In the long run,  $\frac{dp_\infty^*}{d\kappa} = \kappa$  and  $\frac{dF_\infty}{d\kappa} = 0$  by construction. These limits imply

$$\frac{dp_\infty}{d\kappa} = \alpha_p \varsigma_{KFE, \dot{n}} \xi_{p^*, \dot{n}} \kappa + \theta \frac{dp_\infty}{d\kappa}$$

Impose neutrality ( $\frac{dp_\infty}{d\kappa} = \kappa$ ):

$$\alpha_p = \frac{1 - \theta}{\varsigma_{KFE, \dot{n}} \xi_{p^*, \dot{n}}}$$

thus the law of motion becomes

$$p_t = (1 - \theta) \frac{\xi_{F, \dot{n}}}{\xi_{p^*, \dot{n}}} F_t + (1 - \theta) p_t^* + \theta p_{t-1}$$

□

## A.7 Proof of Proposition 3

*Proof.* Begin by shifting forward the Price Level Law of Motion, multiply by  $\theta\beta$ , and subtract from the original equation:

$$p_t - \theta\beta p_{t+1} = \epsilon(F_t - \theta\beta F_{t+1}) + (1 - \theta)(p_t^* - \beta\theta p_{t+1}^*) + \theta(p_{t-1} - \theta\beta p_t)$$

substitute from the Optimal Price Setting equation and rearrange:

$$p_t - \theta\beta X_{t+1} = \epsilon(F_t - \theta\beta F_{t+1}) + (1 - \theta)(1 - \theta\beta)(mc_t + p_t) + \theta(p_{t-1} - \theta\beta p_t)$$

$$-\theta p_{t-1} + (1 - m + \theta^2\beta)p_t - \theta\beta X_{t+1} = \epsilon(F_t - \theta\beta F_{t+1}) + (1 - \theta)(1 - \theta\beta)mc_t + ((1 - \theta)(1 - \theta\beta) - m)p_t$$

for some  $m$ . Specifically, it will be helpful to chose an  $m$  such that the left hand side can be written in terms of inflations, i.e.  $\Pi_t = p_t - p_{t-1}$ .

$$-\theta p_{t-1} + (1 - m + \theta^2 \beta) p_t - \theta \beta X_{t+1} = \epsilon(F_t - \theta \beta F_{t+1}) + (1 - \theta)(1 - \theta \beta) m c_t + ((1 - \theta)(1 - \theta \beta) - m) p_t$$

$$\theta \Pi_t + (1 - m + \theta^2 \beta - \theta) p_t - \theta \beta X_{t+1} = \epsilon(F_t - \theta \beta F_{t+1}) + (1 - \theta)(1 - \theta \beta) m c_t + ((1 - \theta)(1 - \theta \beta) - m) p_t$$

$$\theta \Pi_t + (1 - m + \theta^2 \beta - \theta - \theta \beta) p_t - \theta \beta \Pi_{t+1} = \epsilon(F_t - \theta \beta F_{t+1}) + (1 - \theta)(1 - \theta \beta) m c_t + ((1 - \theta)(1 - \theta \beta) - m) p_t$$

which simplifies nicely if  $m = (1 - \theta)(1 - \theta \beta)$ . Using this value, divide by  $\theta$ :

$$\Pi_t - \beta \Pi_{t+1} = \frac{\epsilon}{\theta} (F_t - \theta \beta F_{t+1}) + \frac{(1 - \theta)(1 - \theta \beta)}{\theta} m c_t + \left( \frac{(1 - \theta)(1 - \theta \beta)}{\theta} - \frac{(1 - \theta)(1 - \theta \beta)}{\theta} \right) p_t$$

$$\Pi_t - \beta \Pi_{t+1} = \frac{\epsilon}{\theta} (F_t - \theta \beta F_{t+1}) + \frac{(1 - \theta)(1 - \theta \beta)}{\theta} m c_t$$

Substitute in the with  $\Lambda = \frac{(1 - \theta)(1 - \theta \beta)}{\theta}$  and rearrange:

$$\Pi_t = \Lambda m c_t + \beta \Pi_{t+1} + \frac{\epsilon}{\theta} (F_t - \theta \beta F_{t+1})$$

Differencing the Price Level Law of Motion gives

$$\pi_t = \epsilon(F_t - F_{t-1}) + (1 - \theta)(p_t^* - p_{t-1}^*) + \theta \pi_{t-1}$$

rearrange to isolate  $p_t^* - p_{t-1}^*$  and substitute into the FPA Determination equation

$$F_t = \frac{\psi_{p^*} \epsilon}{1 - \theta} (\pi_t - \theta \pi_{t-1} - \epsilon(F_t - F_{t-1})) + \theta F_{t-1}$$

Collect terms:

$$\left( 1 + \frac{\psi_{p^*} \epsilon}{1 - \theta} \right) F_t = \frac{\psi_{p^*}}{1 - \theta} (\pi_t - \theta \pi_{t-1}) + \left( \theta + \frac{\psi_{p^*} \epsilon}{1 - \theta} \right) F_{t-1}$$

$$F_t = \frac{\psi_{p^*}}{1 - \theta + \psi_{p^*} \epsilon} (\pi_t - \theta \pi_{t-1}) + \frac{\theta(1 - \theta) + \psi_{p^*} \epsilon}{1 - \theta + \psi_{p^*} \epsilon} F_{t-1}$$

Substitute with  $\psi_\pi$  to complete the proof. □

## A.8 Proof of Proposition 4

*Proof.* The PED Optimal Price Setting equation already matches the Calvo model, so it remains to show that the PED Price Level Law of Motion reduces to the Calvo law of motion with the appropriate  $\theta$  parameter.

The Calvo model is obtained as the limiting case of the menu cost model when the inaction region becomes large,  $\ell \equiv \bar{x} - \underline{x} \rightarrow \infty$ , keeping the random reset rate  $\zeta > 0$  fixed.

When  $\bar{\pi} = 0$ , the stationary pricing problem is symmetric, and the aggregate response to a (small) cost shock is anti-symmetric around the midpoint. (Alvarez et al., 2023) show that in this case only even-indexed eigenfunctions are relevant, so the PED eigenvalue index  $\hat{n}$  must also be even.

Lemma 4 implies that  $\epsilon = 0$  with zero trend inflation and  $\hat{n}$  even. Therefore the PED Price Level Law of Motion (Theorem 2) reduces to

$$p_t = (1 - \theta)p_t^* + \theta p_{t-1}$$

which is the Calvo law of motion.

Finally,  $\theta$  in the PED is defined as

$$\theta = e^{-\lambda_{KFE, \hat{n}}} = e^{-\zeta - \frac{n^2 \pi^2 \sigma^2}{2\ell^2}}$$

from the definition of  $\lambda_{KFE, n}$  in Lemma 2. Taking the limit as  $\ell \rightarrow \infty$  gives

$$\lim_{\ell \rightarrow \infty} \theta = e^{-\zeta} = \theta_{Calvo}$$

□

This proof relies on an intermediate result:

**Lemma 4.** *If trend inflation is zero ( $\bar{\pi} = 0$ ), then  $\xi_{F, n} = 0$  for any even eigenvalue index  $n$ .*

*Proof.* From Lemma 2,

$$\xi_{F, n} \equiv \int_{\underline{x}}^{\bar{x}} x \gamma_{KFE, n}(x, x^*) dx.$$

Using the explicit kernel definition (29), when  $\bar{\pi} = 0$  we have

$$\gamma_{KFE, n}(x, y) = \frac{2}{\ell} \sin\left(\frac{n\pi(x - \underline{x})}{\ell}\right) \sin\left(\frac{n\pi(y - \underline{x})}{\ell}\right), \quad \ell \equiv \bar{x} - \underline{x}.$$

Evaluating at  $y = x^*$  gives

$$\gamma_{KFE, n}(x, x^*) = \frac{2}{\ell} \sin\left(\frac{n\pi(x - \underline{x})}{\ell}\right) \sin\left(\frac{n\pi(x^* - \underline{x})}{\ell}\right).$$

Zero trend inflation implies that the inaction region is symmetric, so  $x^* = (\underline{x} + \bar{x})/2$  and  $(x^* - \underline{x})/\ell = 1/2$ , thus

$$\sin\left(\frac{n\pi(x^* - \underline{x})}{\ell}\right) = \sin\left(\frac{n\pi}{2}\right) = 0 \quad \text{for even } n.$$

Therefore  $\gamma_{KFE, n}(x, x^*) \equiv 0$  for even  $n$ , which implies  $\xi_{F, n} = 0$  and hence  $\epsilon = 0$ . □

## A.9 Proof of Proposition 5

*Proof.* Trend inflation is zero, so the PED eigenvalue index  $\hat{n}$  must be even (Alvarez et al., 2023). With an even eigenvalue index  $n$ , Lemma 4 implies  $\epsilon = 0$ .

Per Proposition 3, the Phillips curve is

$$\pi_t = \Lambda mc_t + \beta\pi_{t+1} + \frac{\epsilon}{\theta}(F_t - \theta\beta F_{t+1})$$

With  $\epsilon = 0$ , the  $\frac{\epsilon}{\theta}(F_t - \theta\beta F_{t+1})$  correction term vanishes, yielding the standard NKPC.  $\square$

## B Mathematical Appendix

**Property 3.** For a PDE of the form:

$$\partial_t f(x, t) = a\partial_x^2 f(x, t) + b\partial_x f(x, t) + cf(x, t) + \Phi(x, t)$$

on the interval  $x \in [0, \ell]$ ,  $t \geq 0$ , with Dirchlet boundary conditions  $f(0, t) = g_0(t)$  and  $f(\ell, t) = g_\ell(t)$ , and initial condition  $f(x, 0) = f_0(x)$ , the unique solution is given by:

$$f(x, t) = \int_0^\ell G(x, y, t)f_0(y)dy + \int_0^t \int_0^\ell G(x, y, t-\tau)\Phi(y, \tau)dyd\tau + a \int_0^t \partial_y G(x, 0, t-\tau)g_0(\tau)d\tau - a \int_0^t \partial_y G(x, \ell, t-\tau)g_\ell(\tau)d\tau$$

where  $G_{abc}(x, y, t)$  is the appropriate Green's function:

$$G_{abc}(x, y, t) = \frac{2}{\ell} e^{\left(\frac{b}{2a}(y-x) + \left(c - \frac{b^2}{4a}\right)t\right)} \sum_{n=1}^{\infty} \sin\left(\frac{n\pi x}{\ell}\right) \sin\left(\frac{n\pi y}{\ell}\right) e^{-\frac{an^2\pi^2}{\ell^2}t} \quad (69)$$

which is also written in terms of eigenfunctions and eigenvalues as

$$G_{abc}(x, y, t) = \sum_{n=1}^{\infty} \gamma_n(x, y) e^{-\lambda_n t} \quad (70)$$

where  $\lambda_n = \left(c - \frac{b^2}{4a}\right) + \frac{an^2\pi^2}{\ell^2}$  and  $\gamma_n(x, y) = \frac{2}{\ell} e^{\frac{b}{2a}(y-x)} \sin\left(\frac{n\pi x}{\ell}\right) \sin\left(\frac{n\pi y}{\ell}\right)$ .

**Lemma 5.** For a PDE of the form:

$$\partial_t f(x, t) = -a\partial_x^2 f(x, t) - b\partial_x f(x, t) - cf(x, t) - \Phi(x, t)$$

for  $x \in [0, \ell]$ ,  $t \in [0, T]$ , with Dirchlet boundary conditions  $f(0, t) = g_0(t)$  and  $f(\ell, t) = g_\ell(t)$ , and terminal

condition  $f(x, 0) = f_T(x)$ , the unique solution is given by:

$$f(x, t) = \int_0^\ell G_{abc}(x, y, T-t) f_T(y) dy + \int_t^T \int_0^\ell G_{abc}(x, y, \tau-t) \Phi(y, \tau) dy d\tau \\ + a \int_t^T \partial_y G_{abc}(x, 0, \tau-t) g_0(\tau) d\tau - a \int_t^T \partial_y G_{abc}(x, \ell, \tau-t) g_\ell(\tau) d\tau \quad (71)$$

where  $G_{abc}(x, y, t)$  is given by equation (69).

*Proof.* Use a change of variable to redefine the problem: let  $u = T - t$  and define

$$h(x, u) \equiv f(x, T - u)$$

Then the PDE becomes:

$$\partial_u h(x, u) = a \partial_x^2 h(x, u) + b \partial_x h(x, u) + c h(x, u) + \Phi(x, T - u)$$

with initial condition  $h(x, 0) = f_T(x)$ , and Dirchlet boundary conditions  $h(0, u) = g_0(T - u)$  and  $h(\ell, u) = g_\ell(T - u)$ .

Per Property 3, the unique solution is given by:

$$h(x, u) = \int_{-\infty}^{\infty} G_{abc}(x, y, u) f_T(y) dy + \int_0^u \int_{-\infty}^{\infty} G_{abc}(x, y, u - \omega) \Phi(y, T - \omega) dy d\omega \\ + a \int_0^u \partial_y G_{abc}(x, 0, u - \omega) g_0(T - \omega) d\omega - a \int_0^u \partial_y G_{abc}(x, \ell, u - \omega) g_\ell(T - \omega) d\omega$$

Transforming back to the original variables (using  $\omega = T - \tau$  and  $u = T - t$ ), we have

$$h(x, u) = \int_{-\infty}^{\infty} G_{abc}(x, y, u) f_T(y) dy + \int_{T-u}^T \int_{-\infty}^{\infty} G_{abc}(x, y, u - T + \tau) \Phi(y, \tau) dy d\tau \\ + a \int_{T-u}^T \partial_y G_{abc}(x, 0, u - T + \tau) g_0(\tau) d\tau - a \int_{T-u}^T \partial_y G_{abc}(x, \ell, u - T + \tau) g_\ell(\tau) d\tau \\ = \int_{-\infty}^{\infty} G_{abc}(x, y, T-t) f_T(y) dy + \int_t^T \int_{-\infty}^{\infty} G_{abc}(x, y, \tau-t) \Phi(y, \tau) dy d\tau \\ + a \int_t^T \partial_y G_{abc}(x, 0, \tau-t) g_0(\tau) d\tau - a \int_t^T \partial_y G_{abc}(x, \ell, \tau-t) g_\ell(\tau) d\tau \\ = h(x, T-t) = f(x, t)$$

□

## C Steady-State

### C.1 Steady-State Value Function

The firm's steady-state value function  $v_{ss}(x)$  solves the steady-state HJB

$$\rho v_{ss}(x) = -\mathbf{B}x^2 - \bar{\pi}v'_{ss}(x) + \nu v''_{ss}(x) + \zeta(v_{ss}(x^*) - v_{ss}(x)), \quad x \in (\underline{x}, \bar{x}), \quad (72)$$

which is a second-order ODE on the steady-state inaction interval. The free boundaries  $\underline{x}_{ss}$ ,  $x^*_{ss}$ , and  $\bar{x}_{ss}$  are determined jointly with  $v_{ss}(\cdot)$  by the usual value-matching and smooth-pasting conditions:

$$\begin{aligned} \text{Value-matching} & \quad v_{ss}(\underline{x}) = v_{ss}(x^*) + \Psi = v_{ss}(\bar{x}) \\ \text{Reset optimality} & \quad \partial_x v_{ss}(x^*) = 0 \\ \text{Smooth-pasting} & \quad \partial_x v_{ss}(\underline{x}) = 0 = \partial_x v_{ss}(\bar{x}) \end{aligned}$$

Rearrange the HJB (72) as

$$\nu v''_{ss}(x) - \bar{\pi}v'_{ss}(x) - (\rho + \zeta)v_{ss}(x) = \mathbf{B}x^2 - \zeta v_{ss}(x^*), \quad x \in (\underline{x}, \bar{x}). \quad (73)$$

The homogeneous part,

$$\nu v''_h(x) - \bar{\pi}v'_h(x) - (\rho + \zeta)v_h(x) = 0, \quad (74)$$

has exponential solutions. The characteristic equation

$$\nu r^2 - \bar{\pi}r - (\rho + \zeta) = 0$$

has two real roots

$$r_{1,2} = \frac{\bar{\pi} \pm \sqrt{\bar{\pi}^2 + 4\nu(\rho + \zeta)}}{2\nu}, \quad (75)$$

so the homogeneous solution is

$$v_h(x) = C_1 e^{r_1 x} + C_2 e^{r_2 x}, \quad (76)$$

for constants  $C_1, C_2$ . Given some particular solution  $v_p(x)$ , the value function solving the HJB is given by  $v_{ss}(x) = v_p(x) + v_h(x)$ .

The five boundary conditions pin down the five unknowns  $(x^*_{ss}, \underline{x}_{ss}, \bar{x}_{ss}, C_1, C_2)$ , which can be solved numerically.

## C.2 Steady-state Stationary Distribution

Write the steady-state Kolmogorov forward equation on the inaction region (set  $\partial_t h = 0$ ):

$$0 = \nu \partial_x^2 h_{ss}(x) + \bar{\pi} \partial_x h_{ss}(x) - \zeta h_{ss}(x) + F_{ss} \delta(x - x_{ss}^*), \quad x \in [\underline{x}, \bar{x}] \quad (77)$$

with absorbing boundary conditions

$$h_{ss}(\underline{x}) = 0 = h_{ss}(\bar{x}),$$

normalization

$$\int_{\underline{x}}^{\bar{x}} h_{ss}(x) dx = 1,$$

and the convention that  $h_{ss}(x) = 0$  for  $x \notin [\underline{x}, \bar{x}]$ .

Away from the reset point  $x_{ss}^*$ , the distribution is differentiable and the steady-state KFE on each open interval reduces to the homogeneous ODE

$$\nu h_{ss}''(x) + \bar{\pi} h_{ss}'(x) - \zeta h_{ss}(x) = 0, \quad x \in (\underline{x}, x_{ss}^*) \cup (x_{ss}^*, \bar{x}) \quad (78)$$

The characteristic equation is

$$\nu r^2 + \bar{\pi} r - \zeta = 0,$$

with explicit roots

$$r_{1,2} = \frac{-\bar{\pi} \pm \sqrt{\bar{\pi}^2 + 4\nu\zeta}}{2\nu} \quad (79)$$

Note that for the parameter values of interest ( $\nu > 0$ ,  $\zeta > 0$ ) the discriminant is strictly positive and the two roots are real.

Because the homogeneous coefficients are identical on both sides, the exponential basis given by  $r_1, r_2$  is shared. Thus the general piecewise form is

$$h_{ss}(x) = \begin{cases} h_L(x) = A_L e^{r_1 x} + B_L e^{r_2 x}, & x \in [\underline{x}, x_{ss}^*], \\ h_R(x) = A_R e^{r_1 x} + B_R e^{r_2 x}, & x \in [x_{ss}^*, \bar{x}], \end{cases}$$

The four coefficients ( $A_L, B_L, A_R, B_R$ ) are pinned down by four linear conditions: the two absorbing boundary conditions  $h_{ss}(\underline{x}) = 0$ ,  $h_{ss}(\bar{x}) = 0$ ; continuity at the reset point  $h_L(x_{ss}^*) = h_R(x_{ss}^*)$ ; and the normalization condition  $\int_{\underline{x}}^{\bar{x}} h_{ss}(x) dx = 1$ .

Two of the coefficients are easily determined from the absorbing boundary conditions. From  $h_{ss}(\underline{x}) = 0$ :

$$A_L = -B_L e^{(r_2 - r_1)\underline{x}} \quad (80)$$

From  $h_{ss}(\bar{x}) = 0$ :

$$A_R = -B_R e^{(r_2 - r_1)\bar{x}} \quad (81)$$

In the steady-state, the FPA is given by

$$F_{ss} = \nu h'_{ss}(\underline{x}) + \bar{\pi} h_{ss}(\underline{x}) - \nu h'_{ss}(\bar{x}) - \bar{\pi} h_{ss}(\bar{x}) + \zeta \quad (82)$$

Given the absorbing boundary conditions  $h_{ss}(\underline{x}) = h_{ss}(\bar{x}) = 0$ , this simplifies to  $F_{ss} = \nu h'_{ss}(\underline{x}) - \nu h'_{ss}(\bar{x}) + \zeta$ . This flow of firms re-enters the distribution at  $x_{ss}^*$ ; the of firms in either direction from this point must sum to  $F_{ss}$ :

$$F_{ss} = \nu (h'_L(x_{ss}^*) - h'_R(x_{ss}^*))$$

where now the drift terms disappear because the continuity condition implies  $\bar{\pi} (h_L(x^*) - h_R(x^*)) = 0$ .

In practice the small  $4 \times 4$  linear system for  $(A_L, B_L, A_R, B_R)$  is assembled and solved numerically (with attention to conditioning); once the coefficients are known the piecewise density is completely determined.

## D Lifting Functions

The eigenfunction expansion in Lemma 2 uses eigenfunctions satisfying homogeneous Dirichlet boundary conditions. Infinite sums of these eigenfunctions converge almost everywhere to the true solution. However, while they converge in a neighborhood around the boundary points, they do not converge at the boundaries themselves. For most features of the price gap distribution this distinction does not matter, but for the flow of firms out of the boundaries, which is determined by the distribution level and derivative at the critical points, it does.

This section constructs lifting functions that resolve these difficulties by solving the problematic terms with closed-form expressions.

### D.1 Lifting Function for Reset Point Perturbations

With the standard Green's function approach, the effects associated with changes the reset point  $x^*$  are problematic, with non-convergent coefficient series.

The key idea is to construct a ‘‘lifting function’’  $J_{x^*}(x)$  that solves the same spatial differential equation as the Green's function, but with a  $\delta'(x - x^*)$  source rather than a  $\delta(x - x^*)$  source. The contribution of this lifting function to the frequency perturbation  $\hat{F}$  can be computed in closed form, yielding a critical-point coefficient  $\varphi_{x^*}$  that captures the divergent part of the eigenfunction sum.

**Lemma 6.** *Let  $\mathcal{K} = \nu \partial_x^2 + \bar{\pi} \partial_x - \zeta$  be the KFE spatial operator with  $\zeta > 0$ . There exists a function  $J_{x^*} : [\underline{x}, \bar{x}] \rightarrow \mathbb{R}$  satisfying*

$$\mathcal{K} J_{x^*}(x) = -\delta'(x - x^*) \quad (83)$$

with homogeneous Dirichlet boundary conditions  $J_{x^*}(\underline{x}) = J_{x^*}(\bar{x}) = 0$ .

Define the characteristic roots

$$r_1 = \frac{-\bar{\pi} + \sqrt{\bar{\pi}^2 + 4\nu\zeta}}{2\nu} > 0, \quad r_2 = \frac{-\bar{\pi} - \sqrt{\bar{\pi}^2 + 4\nu\zeta}}{2\nu} < 0$$

and the Neumann basis functions

$$\psi_L(x) = r_2 e^{r_1(x-\underline{x})} - r_1 e^{r_2(x-\underline{x})}, \quad \psi_R(x) = r_2 e^{r_1(x-\bar{x})} - r_1 e^{r_2(x-\bar{x})}$$

which satisfy  $\mathcal{K}\psi_L = \mathcal{K}\psi_R = 0$  with  $\psi'_L(\underline{x}) = \psi'_R(\bar{x}) = 0$ . Then

$$J_{x^*}(x) = \begin{cases} -\frac{\psi_R(x^*)}{\nu W_N(x^*)} \psi'_L(x) & x < x^* \\ -\frac{\psi_L(x^*)}{\nu W_N(x^*)} \psi'_R(x) & x > x^* \end{cases} \quad (84)$$

where

$$W_N(x^*) = \psi_L(x^*)\psi'_R(x^*) - \psi'_L(x^*)\psi_R(x^*)$$

*Proof.* I construct a function  $j_{x^*}(x)$  satisfying  $\mathcal{K}j_{x^*} = -\delta(x - x^*)$  with Neumann boundary conditions  $j'_{x^*}(\underline{x}) = j'_{x^*}(\bar{x}) = 0$ . Constructing  $j_{x^*}$  requires basis functions satisfying  $\mathcal{K}\psi = 0$  with a zero-derivative condition at one boundary. For  $\psi_L(x) = a e^{r_1(x-\underline{x})} + b e^{r_2(x-\underline{x})}$ , the condition  $\psi'_L(\underline{x}) = ar_1 + br_2 = 0$  gives  $a/b = -r_2/r_1$ . Taking  $a = r_2$  and  $b = -r_1$  yields  $\psi_L(x) = r_2 e^{r_1(x-\underline{x})} - r_1 e^{r_2(x-\underline{x})}$ . Similarly,  $\psi_R(x) = r_2 e^{r_1(x-\bar{x})} - r_1 e^{r_2(x-\bar{x})}$  satisfies  $\psi'_R(\bar{x}) = 0$ .

The Neumann Green's function is  $j_{x^*}(x) = B_L \psi_L(x)$  for  $x < x^*$  and  $j_{x^*}(x) = B_R \psi_R(x)$  for  $x > x^*$ . The matching conditions at  $x^*$  are continuity of  $j_{x^*}$  and a jump of  $-1/\nu$  in  $j'_{x^*}$ :

$$B_L \psi_L(x^*) = B_R \psi_R(x^*), \quad B_R \psi'_R(x^*) - B_L \psi'_L(x^*) = -\frac{1}{\nu}$$

Solving gives  $B_L = -\psi_R(x^*)/[\nu W_N(x^*)]$  and  $B_R = -\psi_L(x^*)/[\nu W_N(x^*)]$ .

Finally let  $J_{x^*}(x) = j'_{x^*}(x)$ . Since  $\mathcal{K}$  has constant coefficients, differentiating  $\mathcal{K}j_{x^*} = -\delta(x - x^*)$  gives  $\mathcal{K}J_{x^*} = -\delta'(x - x^*)$ . The Dirichlet boundary conditions  $J_{x^*}(\underline{x}) = J_{x^*}(\bar{x}) = 0$  hold because  $j'_{x^*}(\underline{x}) = j'_{x^*}(\bar{x}) = 0$  by the Neumann conditions on  $j_{x^*}$ . Explicitly,  $J_{x^*}(x) = B_L \psi'_L(x)$  for  $x < x^*$  and  $J_{x^*}(x) = B_R \psi'_R(x)$  for  $x > x^*$ , which gives (84).  $\square$

**Lemma 7.** Let  $J_{x^*}$  be the lifting function from Lemma 6. Define the critical-point coefficient

$$\varphi_{x^*} \equiv -F_{ss}\nu (J'_{x^*}(\underline{x}) - J'_{x^*}(\bar{x}))$$

Then

$$\varphi_{x^*} = \frac{F_{ss}r_1r_2(r_1 - r_2)(\psi_R(x^*) - \psi_L(x^*))}{W_N(x^*)} \quad (85)$$

where  $\psi_L$ ,  $\psi_R$ , and  $W_N$  are defined in Lemma 6.

*Proof.* From (84),  $J'_{x^*}(\underline{x}) = B_L\psi_L''(\underline{x})$  where  $B_L = -\psi_R(x^*)/[\nu W_N(x^*)]$ . Computing the derivative,  $\psi'_L(x) = r_1r_2(e^{r_1(x-\underline{x})} - e^{r_2(x-\underline{x})})$ , so  $\psi_L''(\underline{x}) = r_1r_2(r_1 - r_2)$ . Therefore

$$J'_{x^*}(\underline{x}) = -\frac{\psi_R(x^*) \cdot r_1r_2(r_1 - r_2)}{\nu W_N(x^*)}$$

Similarly,  $J'_{x^*}(\bar{x}) = B_R\psi_R''(\bar{x}) = -\psi_L(x^*) \cdot r_1r_2(r_1 - r_2)/[\nu W_N(x^*)]$ . Substituting:

$$\varphi_{x^*} = -F_{ss}\nu(J'_{x^*}(\underline{x}) - J'_{x^*}(\bar{x})) = \frac{F_{ss}r_1r_2(r_1 - r_2)}{W_N(x^*)}(\psi_R(x^*) - \psi_L(x^*))$$

□

## D.2 Lifting Functions for Boundary Perturbations

When the inaction boundaries move, the absorbing boundary conditions for the distribution become inhomogeneous:  $\hat{h}(\underline{x}, t) = -h'_{ss}(\underline{x})\hat{x}(t)$  and  $\hat{h}(\bar{x}, t) = -h'_{ss}(\bar{x})\hat{x}(t)$ . Rather than expanding these inhomogeneous conditions directly in eigenfunctions (which diverges), we construct harmonic lifting functions that satisfy the boundary conditions exactly and contribute algebraically to the aggregate quantities.

**Lemma 8.** *Let  $\mathcal{K} = \nu\partial_x^2 + \bar{\pi}\partial_x - \zeta$  be the KFE spatial operator with  $\zeta > 0$ . Define the characteristic roots*

$$r_1 = \frac{-\bar{\pi} + \sqrt{\bar{\pi}^2 + 4\nu\zeta}}{2\nu} > 0, \quad r_2 = \frac{-\bar{\pi} - \sqrt{\bar{\pi}^2 + 4\nu\zeta}}{2\nu} < 0 \quad (86)$$

and let  $\ell = \bar{x} - \underline{x}$  denote the width of the inaction region.

There exist harmonic lifting functions  $H_{\underline{x}} : [\underline{x}, \bar{x}] \rightarrow \mathbb{R}$  and  $H_{\bar{x}} : [\underline{x}, \bar{x}] \rightarrow \mathbb{R}$  satisfying

$$\mathcal{K}H_{\underline{x}}(x) = 0, \quad H_{\underline{x}}(\underline{x}) = 1, \quad H_{\underline{x}}(\bar{x}) = 0 \quad (87)$$

$$\mathcal{K}H_{\bar{x}}(x) = 0, \quad H_{\bar{x}}(\underline{x}) = 0, \quad H_{\bar{x}}(\bar{x}) = -1 \quad (88)$$

The explicit solutions are

$$H_{\underline{x}}(x) = \frac{e^{r_2(x-\underline{x})} - e^{r_1(x-\underline{x})} \cdot e^{(r_2-r_1)\ell}}{1 - e^{(r_2-r_1)\ell}} \quad (89)$$

$$H_{\bar{x}}(x) = \frac{e^{r_1(x-\underline{x})} - e^{r_2(x-\underline{x})}}{e^{r_2\ell} - e^{r_1\ell}} \quad (90)$$

*Proof.* The general solution to  $\mathcal{K}u = 0$  is  $u(x) = C_1e^{r_1(x-\underline{x})} + C_2e^{r_2(x-\underline{x})}$ .

For  $H_{\underline{x}}$ : The boundary conditions  $H_{\underline{x}}(\underline{x}) = 1$  and  $H_{\underline{x}}(\bar{x}) = 0$  give

$$\begin{aligned} C_1 + C_2 &= 1 \\ C_1 e^{r_1 \ell} + C_2 e^{r_2 \ell} &= 0 \end{aligned}$$

Solving:  $C_1 = -e^{r_2 \ell} / (e^{r_1 \ell} - e^{r_2 \ell})$  and  $C_2 = e^{r_1 \ell} / (e^{r_1 \ell} - e^{r_2 \ell})$ . Substituting and simplifying yields (89).

For  $H_{\bar{x}}$ : The boundary conditions  $H_{\bar{x}}(\underline{x}) = 0$  and  $H_{\bar{x}}(\bar{x}) = -1$  give

$$\begin{aligned} C_1 + C_2 &= 0 \\ C_1 e^{r_1 \ell} + C_2 e^{r_2 \ell} &= -1 \end{aligned}$$

Solving:  $C_1 = -1 / (e^{r_1 \ell} - e^{r_2 \ell})$  and  $C_2 = 1 / (e^{r_1 \ell} - e^{r_2 \ell})$ . Substituting yields (90). □

**Lemma 9.** *The derivatives of the harmonic lifting functions at the boundaries are:*

$$H'_{\underline{x}}(\underline{x}) = \frac{r_2 - r_1 e^{(r_2 - r_1)\ell}}{1 - e^{(r_2 - r_1)\ell}} \quad (91)$$

$$H'_{\underline{x}}(\bar{x}) = \frac{(r_2 - r_1) e^{r_2 \ell}}{1 - e^{(r_2 - r_1)\ell}} \quad (92)$$

$$H'_{\bar{x}}(\underline{x}) = \frac{r_1 - r_2}{e^{r_2 \ell} - e^{r_1 \ell}} \quad (93)$$

$$H'_{\bar{x}}(\bar{x}) = \frac{r_1 e^{r_1 \ell} - r_2 e^{r_2 \ell}}{e^{r_2 \ell} - e^{r_1 \ell}} \quad (94)$$

*Proof.* Direct differentiation of (89) and (90). For  $H_{\underline{x}}$ :

$$H'_{\underline{x}}(x) = \frac{r_2 e^{r_2(x-\underline{x})} - r_1 e^{r_1(x-\underline{x})} \cdot e^{(r_2 - r_1)\ell}}{1 - e^{(r_2 - r_1)\ell}}$$

Evaluating at  $x = \underline{x}$  gives (91); at  $x = \bar{x}$  gives (92). The formulas for  $H'_{\bar{x}}$  follow similarly. □

**Lemma 10.** *Let  $H_{\underline{x}}$  and  $H_{\bar{x}}$  be the harmonic lifting functions from Lemma 8. The critical-point coefficients for the aggregate gap are*

$$\xi_{\underline{x}} \equiv -h'_{ss}(\underline{x}) \int_{\underline{x}}^{\bar{x}} x H_{\underline{x}}(x) dx \quad (95)$$

$$\xi_{\bar{x}} \equiv -h'_{ss}(\bar{x}) \int_{\underline{x}}^{\bar{x}} x H_{\bar{x}}(x) dx \quad (96)$$

*These integrals are well-defined and finite since  $H_{\underline{x}}$  and  $H_{\bar{x}}$  are smooth on  $[\underline{x}, \bar{x}]$ .*

Explicitly, using the exponential forms (89)–(90):

$$\int_{\underline{x}}^{\bar{x}} x H_{\underline{x}}(x) dx = \frac{1}{1 - e^{(r_2 - r_1)\ell}} [I_2 - e^{(r_2 - r_1)\ell} I_1] \quad (97)$$

$$\int_{\underline{x}}^{\bar{x}} x H_{\bar{x}}(x) dx = \frac{1}{e^{r_2\ell} - e^{r_1\ell}} [I_1 - I_2] \quad (98)$$

where

$$I_k \equiv \int_{\underline{x}}^{\bar{x}} x e^{r_k(x - \underline{x})} dx = \frac{1}{r_k^2} [(r_k \bar{x} - 1)e^{r_k \ell} - (r_k \underline{x} - 1)], \quad k = 1, 2$$

*Proof.* The definitions (95)–(96) follow from the critical-point decomposition (27): the boundary contribution to  $\hat{h}_{\text{crit}}$  is  $-h'_{ss}(\underline{x})\hat{x}(t)H_{\underline{x}}(x) + h'_{ss}(\bar{x})\hat{x}(t)H_{\bar{x}}(x)$ , and the aggregate gap contribution is  $\hat{X}_{\text{crit,bc}}(t) = \int x (-h'_{ss}(\underline{x})\hat{x}(t)H_{\underline{x}}(x) + h'_{ss}(\bar{x})\hat{x}(t)H_{\bar{x}}(x)) dx$ .

The integrals  $I_k$  are computed by integration by parts:

$$\int_{\underline{x}}^{\bar{x}} x e^{r_k(x - \underline{x})} dx = \left[ \frac{x}{r_k} e^{r_k(x - \underline{x})} \right]_{\underline{x}}^{\bar{x}} - \frac{1}{r_k} \int_{\underline{x}}^{\bar{x}} e^{r_k(x - \underline{x})} dx$$

which yields the stated formula after simplification.  $\square$

**Lemma 11.** *Let  $H_{\underline{x}}$  and  $H_{\bar{x}}$  be the harmonic lifting functions from Lemma 8. The critical-point coefficients for the frequency of price adjustment are*

$$\varphi_{\underline{x}} \equiv -h'_{ss}(\underline{x}) \left[ \nu (H'_{\underline{x}}(\underline{x}) - H'_{\underline{x}}(\bar{x})) + \bar{\pi} \right] \quad (99)$$

$$\varphi_{\bar{x}} \equiv -h'_{ss}(\bar{x}) \left[ \nu (H'_{\bar{x}}(\underline{x}) - H'_{\bar{x}}(\bar{x})) + \bar{\pi} \right] \quad (100)$$

Using the derivatives from Lemma 9:

$$\varphi_{\underline{x}} = -h'_{ss}(\underline{x}) \left[ \nu \cdot \frac{(r_2 - r_1)(1 - e^{r_2\ell})}{1 - e^{(r_2 - r_1)\ell}} + \bar{\pi} \right] \quad (101)$$

$$\varphi_{\bar{x}} = -h'_{ss}(\bar{x}) \left[ \nu \cdot \frac{(r_1 - r_2)(1 - e^{r_1\ell})}{e^{r_2\ell} - e^{r_1\ell}} + \bar{\pi} \right] \quad (102)$$

*Proof.* The frequency perturbation from the boundary-lifting function is

$$\hat{F}_{\text{bc}}(t) = \nu \partial_x \hat{h}_{\text{bc}}(\underline{x}, t) + \bar{\pi} \hat{h}_{\text{bc}}(\underline{x}, t) - \nu \partial_x \hat{h}_{\text{bc}}(\bar{x}, t) - \bar{\pi} \hat{h}_{\text{bc}}(\bar{x}, t)$$

Substituting  $\hat{h}_{\text{bc}}(x, t) = -h'_{ss}(\underline{x})\hat{x}(t)H_{\underline{x}}(x) + h'_{ss}(\bar{x})\hat{x}(t)H_{\bar{x}}(x)$  and using the boundary values  $H_{\underline{x}}(\underline{x}) = 1$ ,

$$H_{\underline{x}}(\bar{x}) = 0, H_{\bar{x}}(\underline{x}) = 0, H_{\bar{x}}(\bar{x}) = -1:$$

$$\begin{aligned}\hat{F}_{bc}(t) &= -h'_{ss}(\underline{x})\hat{x}(t) \left[ \nu H'_{\underline{x}}(\underline{x}) + \bar{\pi} - \nu H'_{\underline{x}}(\bar{x}) \right] \\ &\quad + h'_{ss}(\bar{x})\hat{x}(t) \left[ \nu H'_{\bar{x}}(\underline{x}) - \nu H'_{\bar{x}}(\bar{x}) + \bar{\pi} \right]\end{aligned}$$

This gives  $\hat{F}_{bc}(t) = \varphi_{\underline{x}}\hat{x}(t) - \varphi_{\bar{x}}\hat{x}(t)$  with coefficients as defined.

The explicit formulas follow by substituting the derivatives from Lemma 9 and simplifying:

$$\begin{aligned}H'_{\underline{x}}(\underline{x}) - H'_{\underline{x}}(\bar{x}) &= \frac{r_2 - r_1 e^{(r_2 - r_1)\ell} - (r_2 - r_1)e^{r_2\ell}}{1 - e^{(r_2 - r_1)\ell}} \\ &= \frac{(r_2 - r_1)(1 - e^{r_2\ell})}{1 - e^{(r_2 - r_1)\ell}}\end{aligned}$$

and similarly for  $H'_{\bar{x}}(\underline{x}) - H'_{\bar{x}}(\bar{x})$ . □

## E Dynamic Distribution in Discrete Time

This section derives the discrete-time dynamics of the distribution perturbation  $\hat{h}(x, t)$ , building on the continuous-time solution in Lemma 2. These results are used to construct the plot in Figure 1.

### E.1 Discrete-Time Recursion for the Distribution

**Proposition 8.** *The discrete time approximation of the interior distribution perturbation from Lemma 2 is*

$$\hat{h}_{\text{int}}(x, t) = \sum_{n=1}^{\infty} \hat{h}_{\text{int},n}(x, t)$$

where each modal contribution admits the recursive approximation (with unit time step)

$$\hat{h}_{\text{int},n}(x, t) \approx \varpi_{F,n}(x) \hat{F}_t + \varpi_{x^*,n}(x) \Delta \hat{x}_t^* + h'_{ss}(\underline{x}) \varpi_{H,\underline{x},n}(x) \Delta \hat{x}_t - h'_{ss}(\bar{x}) \varpi_{H,\bar{x},n}(x) \Delta \hat{x}_t + \theta_n \hat{h}_{\text{int},n}(x, t-1) \quad (103)$$

where  $\theta_n \equiv e^{-\lambda_{KFE,n}}$  and  $\Delta \hat{y}_t \equiv \hat{y}_t - \hat{y}_{t-1}$  denotes the first difference. The coefficient functions are

$$\varpi_{F,n}(x) \equiv \gamma_{KFE,n}(x, x^*) \quad (104)$$

$$\varpi_{x^*,n}(x) \equiv F_{ss} \varpi_{J,n}(x) + F_{ss} \lambda_{KFE,n} \int_{\underline{x}}^{\bar{x}} \gamma_{KFE,n}(x, y) J_{x^*}(y) dy \quad (105)$$

$$\varpi_{H,\underline{x},n}(x) \equiv \frac{\nu}{\lambda_{KFE,n}} \partial_y \gamma_{KFE,n}(x, \underline{x}) \quad (106)$$

$$\varpi_{H,\bar{x},n}(x) \equiv \frac{\nu}{\lambda_{KFE,n}} \partial_y \gamma_{KFE,n}(x, \bar{x}) \quad (107)$$

with  $\varpi_{J,n}(x)$  as defined in Lemma 2.

*Proof.* Lemma 2 gives the interior component as an integral over time-derivatives of the forcing variables. To convert to a recursion in levels, apply integration by parts to each term.

Consider the boundary term  $\int_0^t e^{-\lambda(t-\tau)} h'_{ss}(\underline{x}) \hat{x}'(\tau) \varpi_{H,\underline{x},n}(x) d\tau$  where  $\varpi_{H,\underline{x},n}(x) = \frac{\nu}{\lambda} \partial_y \gamma_{KFE,n}(x, \underline{x})$ . Integration by parts with  $u = \hat{x}(\tau)$  and  $dv = e^{-\lambda(t-\tau)} d\tau$  yields

$$\begin{aligned} & \int_0^t e^{-\lambda(t-\tau)} h'_{ss}(\underline{x}) \hat{x}'(\tau) \cdot \frac{\nu}{\lambda} \partial_y \gamma_{KFE,n}(x, \underline{x}) d\tau \\ &= h'_{ss}(\underline{x}) \nu \partial_y \gamma_{KFE,n}(x, \underline{x}) \cdot \frac{1}{\lambda} \left[ e^{-\lambda(t-\tau)} \hat{x}(\tau) \right]_0^t + (\text{decayed integral}) \\ &= h'_{ss}(\underline{x}) \nu \partial_y \gamma_{KFE,n}(x, \underline{x}) \cdot \left( \hat{x}(t) - e^{-\lambda t} \hat{x}(0) + \int_0^t e^{-\lambda(t-\tau)} \hat{x}(\tau) d\tau \right) / \lambda \end{aligned}$$

Combined with the initial condition term  $h'_{ss}(\underline{x}) \hat{x}(0) \varpi_{H,\underline{x},n}(x) e^{-\lambda t}$  from Lemma 2, the  $e^{-\lambda t} \hat{x}(0)$  terms cancel, leaving an integral over levels.

The discrete-time approximation (Riemann sum with step  $\Delta t = 1$ ) of an integral  $\int_0^t e^{-\lambda(t-\tau)} y(\tau) d\tau$  is

$$\sum_{s=0}^{t-1} e^{-\lambda(t-s)} y(s) \approx y(t) + e^{-\lambda} \sum_{s=0}^{t-2} e^{-\lambda(t-1-s)} y(s)$$

Recognizing the second term as  $\theta_n$  times the integral at  $t-1$ , and noting that the cumulative sum can be written in terms of differences:

$$\sum_{s=0}^t e^{-\lambda(t-s)} y(s) = \sum_{s=0}^t e^{-\lambda(t-s)} \Delta y_s + \theta_n \sum_{s=0}^{t-1} e^{-\lambda(t-1-s)} y(s)$$

where the first-difference formulation isolates the new contribution at time  $t$ . This yields the recursion (103).  $\square$

## E.2 Mass Conservation

The distribution perturbation  $\hat{h}(x, t)$  represents the change in the density of firms at each price gap  $x$ . Since the total mass of firms is fixed at unity, the perturbation must integrate to zero for all  $t$ :

$$\hat{M}(t) \equiv \int_{\underline{x}}^{\bar{x}} \hat{h}(x, t) dx = 0 \quad (108)$$

The mass decomposes into critical-point and interior components:

$$\hat{M}(t) = \hat{M}_{\text{crit}}(t) + \hat{M}_{\text{int}}(t) \quad (109)$$

where

$$\hat{M}_{\text{crit}}(t) = -h'_{ss}(\underline{x}) \hat{x}(t) \vartheta_{H,\underline{x}} + h'_{ss}(\bar{x}) \hat{x}(t) \vartheta_{H,\bar{x}} - F_{ss} \hat{x}^*(t) \vartheta_J \quad (110)$$

and the critical-point mass coefficients are

$$\vartheta_{H,\underline{x}} \equiv \int_{\underline{x}}^{\bar{x}} H_{\underline{x}}(x) dx, \quad \vartheta_{H,\bar{x}} \equiv \int_{\underline{x}}^{\bar{x}} H_{\bar{x}}(x) dx, \quad \vartheta_J \equiv \int_{\underline{x}}^{\bar{x}} J_{x^*}(x) dx \quad (111)$$

The interior mass decomposes as  $\hat{M}_{\text{int}}(t) = \sum_n \hat{M}_{\text{int},n}(t)$ , where each component satisfies the recursion

$$\hat{M}_{\text{int},n,t} = \Delta t \vartheta_{F,n} \hat{F}_t + \vartheta_{x^{*'},n} \Delta \hat{x}_t^* + \vartheta_{\underline{x}',n} \Delta \hat{x}_t - \vartheta_{\bar{x}',n} \Delta \hat{x}_t + \theta_n \hat{M}_{\text{int},n,t-\Delta t} \quad (112)$$

with interior mass coefficients

$$\vartheta_{F,n} \equiv \int_{\underline{x}}^{\bar{x}} \varpi_{F,n}(x) dx, \quad \vartheta_{x^{*'},n} \equiv F_{ss} \int_{\underline{x}}^{\bar{x}} \varpi_{J,n}(x) dx, \quad \vartheta_{\underline{x}',n} \equiv h'_{ss}(\underline{x}) \int_{\underline{x}}^{\bar{x}} \varpi_{H,\underline{x},n}(x) dx, \quad \vartheta_{\bar{x}',n} \equiv h'_{ss}(\bar{x}) \int_{\underline{x}}^{\bar{x}} \varpi_{H,\bar{x},n}(x) dx \quad (113)$$

### E.2.1 Determining F via Mass Conservation

The constraint  $\hat{M}(t) = 0$  provides an alternative method for computing the frequency of price adjustment. Imposing  $\hat{M}_{\text{crit}}(t) + \sum_n \hat{M}_{\text{int},n}(t) = 0$  and solving for  $\hat{F}_t$ :

**Proposition 9** (F from mass conservation). *The frequency of price adjustment satisfies*

$$\hat{F}_t = \frac{-\hat{M}_{\text{crit},t} - \sum_n \left[ \vartheta_{x^{*'},n} \Delta \hat{x}_t^* + \vartheta_{\underline{x}',n} \Delta \hat{x}_t - \vartheta_{\bar{x}',n} \Delta \hat{x}_t + \theta_n \hat{M}_{\text{int},n,t-\Delta t} \right]}{\Delta t \sum_n \vartheta_{F,n}} \quad (114)$$

where  $\hat{M}_{\text{crit},t} = -h'_{ss}(\underline{x}) \hat{x}_t \vartheta_{H,\underline{x}} + h'_{ss}(\bar{x}) \hat{x}_t \vartheta_{H,\bar{x}} - F_{ss} \hat{x}_t^* \vartheta_J$ .

*Proof.* From (108),  $\hat{M}_{\text{crit},t} + \sum_n \hat{M}_{\text{int},n,t} = 0$ . Substituting (112) and collecting  $\hat{F}_t$  terms:

$$\hat{M}_{\text{crit},t} + \Delta t \hat{F}_t \sum_n \vartheta_{F,n} + \sum_n \left[ \vartheta_{x^{*'},n} \Delta \hat{x}_t^* + \vartheta_{\underline{x}',n} \Delta \hat{x}_t - \vartheta_{\bar{x}',n} \Delta \hat{x}_t + \theta_n \hat{M}_{\text{int},n,t-\Delta t} \right] = 0$$

Solving for  $\hat{F}_t$  yields (114). □

**Lemma 12** (Completeness relation for primed mass coefficients). *The primed interior mass coefficients satisfy the completeness relations*

$$\sum_{n=1}^{\infty} \vartheta_{x^{*'},n} = F_{ss} \vartheta_J, \quad \sum_{n=1}^{\infty} \vartheta_{\underline{x}',n} = h'_{ss}(\underline{x}) \vartheta_{H,\underline{x}}, \quad \sum_{n=1}^{\infty} \vartheta_{\bar{x}',n} = h'_{ss}(\bar{x}) \vartheta_{H,\bar{x}} \quad (115)$$

where  $\vartheta_J, \vartheta_{H,\underline{x}}, \vartheta_{H,\bar{x}}$  are the critical-point mass coefficients from (111).

*Proof.* The mass conservation constraint  $\hat{M}_{\text{crit},t} + \sum_n \hat{M}_{\text{int},n,t} = 0$  must hold for arbitrary boundary perturbations. Consider a step change in boundaries at  $t = 0$  starting from steady state, so that  $\Delta \hat{x}_0^* = \hat{x}_0^*$ ,  $\Delta \hat{x}_0 = \hat{x}_0$ ,  $\Delta \hat{x}_0 = \hat{x}_0$ , and  $\hat{M}_{\text{int},n,-\Delta t} = 0$ . Set  $\hat{F}_0 = 0$  (no flow perturbation at impact).

The interior mass at  $t = 0$  is:

$$\hat{M}_{\text{int},0} = \sum_n \hat{M}_{\text{int},n,0} = \sum_n \vartheta_{x^{*'},n} \hat{x}_0^* + \sum_n \vartheta_{\underline{x}',n} \hat{\underline{x}}_0 - \sum_n \vartheta_{\bar{x}',n} \hat{\bar{x}}_0$$

The critical mass at  $t = 0$  from (110) is:

$$\hat{M}_{\text{crit},0} = -h'_{ss}(\underline{x}) \vartheta_{H,\underline{x}} \hat{\underline{x}}_0 + h'_{ss}(\bar{x}) \vartheta_{H,\bar{x}} \hat{\bar{x}}_0 - F_{ss} \vartheta_J \hat{x}_0^*$$

Imposing  $\hat{M}_{\text{crit},0} + \hat{M}_{\text{int},0} = 0$  and collecting terms by boundary variable:

$$\begin{aligned} \hat{x}_0^* : \quad & -F_{ss} \vartheta_J + \sum_n \vartheta_{x^{*'},n} = 0 \\ \hat{\underline{x}}_0 : \quad & -h'_{ss}(\underline{x}) \vartheta_{H,\underline{x}} + \sum_n \vartheta_{\underline{x}',n} = 0 \\ \hat{\bar{x}}_0 : \quad & h'_{ss}(\bar{x}) \vartheta_{H,\bar{x}} - \sum_n \vartheta_{\bar{x}',n} = 0 \end{aligned}$$

Since mass conservation must hold for arbitrary  $(\hat{x}_0^*, \hat{\underline{x}}_0, \hat{\bar{x}}_0)$ , each coefficient equation must vanish separately, yielding (115).  $\square$

## E.2.2 Relating Mass Coefficients to Frequency Coefficients

The mass-based approach is connected to the flux-based  $\varphi$  coefficients through spatial integration.

**Lemma 13** (Relationship between  $\vartheta$  and  $\xi$  coefficients). *The mass coefficients satisfy*

$$\vartheta_{x^{*'},n} = \xi_{x^{*'},n}|_{x \rightarrow 1}, \quad \vartheta_{\underline{x}',n} = \xi_{\underline{x}',n}|_{x \rightarrow 1}, \quad \vartheta_{\bar{x}',n} = \xi_{\bar{x}',n}|_{x \rightarrow 1} \quad (116)$$

where the notation  $\xi|_{x \rightarrow 1}$  means replacing the  $x$  weighting in the integral by 1.

*Proof.* By definition,  $\xi_{x^{*'},n} = F \int_{\underline{x}}^{\bar{x}} x \varpi_{J,n}(x) dx$  while  $\vartheta_{x^{*'},n} = F \int_{\underline{x}}^{\bar{x}} \varpi_{J,n}(x) dx$ . The relation is the same with and without the  $x$  weighting.  $\square$

**Lemma 14** (Relationship between  $\vartheta_F$  and  $\varphi_F$ ). *The frequency forcing coefficients satisfy*

$$\sum_{n=1}^{\infty} \vartheta_{F,n} = 1 \quad (117)$$

*Proof.* By definition,  $\vartheta_{F,n} = \int_{\underline{x}}^{\bar{x}} \varpi_{F,n}(x) dx = \int_{\underline{x}}^{\bar{x}} \gamma_{KFE,n}(x, x^*) dx$ . By the eigenfunction completeness relation  $\sum_n \gamma_{KFE,n}(x, y) = \delta(x - y)$ :

$$\sum_n \vartheta_{F,n} = \int_{\underline{x}}^{\bar{x}} \sum_n \gamma_{KFE,n}(x, x^*) dx = \int_{\underline{x}}^{\bar{x}} \delta(x - x^*) dx = 1$$

□

The mass conservation approach (114) and the flux-based approach are equivalent. The KFE flux condition at the boundaries gives

$$\hat{F}(t) = \nu \left( \partial_x \hat{h}(\underline{x}, t) - \partial_x \hat{h}(\bar{x}, t) \right) + \bar{\pi} \left( h'_{ss}(\bar{x}) \hat{x}(t) - h'_{ss}(\underline{x}) \hat{x}(t) \right)$$

Integrating the KFE  $\partial_t \hat{h} = \nu \partial_x^2 \hat{h} - \bar{\pi} \partial_x \hat{h} - \zeta \hat{h} + \hat{F} \delta(x - x^*)$  over  $[\underline{x}, \bar{x}]$  and using mass conservation  $\int \hat{h} dx = 0$ :

$$0 = \nu \left( \partial_x \hat{h}(\bar{x}) - \partial_x \hat{h}(\underline{x}) \right) - \bar{\pi} \left( \hat{h}(\bar{x}) - \hat{h}(\underline{x}) \right) + \hat{F}$$

With the linearized boundary conditions  $\hat{h}(\underline{x}) = -h'_{ss}(\underline{x}) \hat{x}$  and  $\hat{h}(\bar{x}) = -h'_{ss}(\bar{x}) \hat{x}$ , this recovers the flux formula. The two approaches encode the same physical constraint from different perspectives: mass conservation versus boundary flux balance.

### E.2.3 Analytical Formulas for Mass Coefficients

The mass coefficients (113) require spatial integrals over the eigenfunction projections without the  $x$ -weighting used in the  $\xi$  coefficients. Define the fundamental integral

$$\mathcal{I}_n \equiv \int_{\underline{x}}^{\bar{x}} e^{-\alpha x} \sin(\omega_n(x - \underline{x})) dx \quad (118)$$

where  $\alpha = \bar{\pi}/(2\nu)$  and  $\omega_n = n\pi/\ell$ .

**Lemma 15.** *The integral  $\mathcal{I}_n$  has the closed form*

$$\mathcal{I}_n = \frac{\omega_n}{\alpha^2 + \omega_n^2} \left( e^{-\alpha \underline{x}} - (-1)^n e^{-\alpha \bar{x}} \right) \quad (119)$$

*Proof.* Using the standard integral  $\int e^{ax} \sin(bx) dx = \frac{e^{ax}}{a^2 + b^2} (a \sin(bx) - b \cos(bx))$ :

$$\begin{aligned} \mathcal{I}_n &= \int_{\underline{x}}^{\bar{x}} e^{-\alpha x} \sin(\omega_n(x - \underline{x})) dx \\ &= \left[ \frac{e^{-\alpha x}}{\alpha^2 + \omega_n^2} (-\alpha \sin(\omega_n(x - \underline{x})) - \omega_n \cos(\omega_n(x - \underline{x}))) \right]_{\underline{x}}^{\bar{x}} \end{aligned}$$

At  $x = \underline{x}$ :  $\sin(0) = 0$ ,  $\cos(0) = 1$ , giving  $-\omega_n e^{-\alpha \underline{x}}/(\alpha^2 + \omega_n^2)$ . At  $x = \bar{x}$ :  $\sin(\omega_n \ell) = \sin(n\pi) = 0$ ,  $\cos(\omega_n \ell) = (-1)^n$ , giving  $-\omega_n (-1)^n e^{-\alpha \bar{x}}/(\alpha^2 + \omega_n^2)$ . The result follows. □

**Proposition 10.** *The interior mass coefficients (113) are:*

$$\vartheta_{F,n} = \frac{2}{\ell} \sin(\omega_n(x^* - \underline{x})) e^{\alpha x^*} \mathcal{I}_n \quad (120)$$

$$\vartheta_{\underline{x}',n} = h'_{ss}(\underline{x}) \frac{\nu}{\lambda_{KFE,n}} \frac{2\omega_n}{\ell} e^{\alpha \underline{x}} \mathcal{I}_n \quad (121)$$

$$\vartheta_{\bar{x}',n} = h'_{ss}(\bar{x}) \frac{\nu}{\lambda_{KFE,n}} \frac{2\omega_n}{\ell} (-1)^n e^{\alpha \bar{x}} \mathcal{I}_n \quad (122)$$

The coefficient  $\vartheta_{x^{*'},n}$  requires numerical integration over the lifting function  $J_{x^*}$ .

*Proof.* By definition,

$$\vartheta_{F,n} = \int_{\underline{x}}^{\bar{x}} \gamma_{KFE,n}(x, x^*) dx = \int_{\underline{x}}^{\bar{x}} \frac{2}{\ell} e^{\alpha(x^* - x)} \sin(\omega_n(x - \underline{x})) \sin(\omega_n(x^* - \underline{x})) dx$$

Factoring out terms independent of  $x$ :

$$\vartheta_{F,n} = \frac{2}{\ell} \sin(\omega_n(x^* - \underline{x})) e^{\alpha x^*} \int_{\underline{x}}^{\bar{x}} e^{-\alpha x} \sin(\omega_n(x - \underline{x})) dx = \frac{2}{\ell} \sin(\omega_n(x^* - \underline{x})) e^{\alpha x^*} \mathcal{I}_n$$

The projection kernel is  $\varpi_{H,\underline{x},n}(x) = \frac{\nu}{\lambda_{KFE,n}} \partial_y \gamma_{KFE,n}(x, y) \Big|_{y=\underline{x}}$ . From

$$\partial_y \gamma_{KFE,n}(x, y) = \frac{2}{\ell} e^{\alpha(y-x)} \sin(\omega_n(x - \underline{x})) (\alpha \sin(\omega_n(y - \underline{x})) + \omega_n \cos(\omega_n(y - \underline{x})))$$

evaluating at  $y = \underline{x}$  where  $\sin(0) = 0$  and  $\cos(0) = 1$ :

$$\partial_y \gamma_{KFE,n}(x, \underline{x}) = \frac{2\omega_n}{\ell} e^{\alpha(\underline{x}-x)} \sin(\omega_n(x - \underline{x}))$$

Thus

$$\vartheta_{\underline{x}',n} = h'_{ss}(\underline{x}) \frac{\nu}{\lambda_{KFE,n}} \int_{\underline{x}}^{\bar{x}} \frac{2\omega_n}{\ell} e^{\alpha(\underline{x}-x)} \sin(\omega_n(x - \underline{x})) dx = h'_{ss}(\underline{x}) \frac{\nu}{\lambda_{KFE,n}} \frac{2\omega_n}{\ell} e^{\alpha \underline{x}} \mathcal{I}_n$$

Similarly, at  $y = \bar{x}$  where  $\sin(\omega_n \ell) = 0$  and  $\cos(\omega_n \ell) = (-1)^n$ :

$$\partial_y \gamma_{KFE,n}(x, \bar{x}) = \frac{2\omega_n}{\ell} (-1)^n e^{\alpha(\bar{x}-x)} \sin(\omega_n(x - \underline{x}))$$

giving

$$\vartheta_{\bar{x}',n} = h'_{ss}(\bar{x}) \frac{\nu}{\lambda_{KFE,n}} \frac{2\omega_n}{\ell} (-1)^n e^{\alpha \bar{x}} \mathcal{I}_n$$

□

## F Impact Effects

This section derives the analytical instantaneous responses of aggregate variables to marginal cost shocks.

## F.1 Initial Condition and Boundary Discontinuity

The initial condition  $\hat{h}(x, 0) = 0$  holds on the *interior* of the inaction region, i.e., for  $x \in (\underline{x}, \bar{x})$ . However, the linearized absorbing boundary conditions (21) require  $\hat{h}(\underline{x}, t) = -h'_{ss}(\underline{x})\hat{x}(t)$  and  $\hat{h}(\bar{x}, t) = -h'_{ss}(\bar{x})\hat{x}(t)$  for  $t > 0$ . When  $\hat{x}(0) \neq 0$  or  $\hat{\bar{x}}(0) \neq 0$ , these boundary values are non-zero while the interior remains at zero, creating a discontinuity between the interior and the boundaries as  $t \rightarrow 0$ , which I denote as  $t = 0^+$ .

Since  $\hat{h}(x, 0^+) = 0$  almost everywhere, the Lebesgue integral  $\int_{\underline{x}}^{\bar{x}} x \hat{h}(x, 0) dx = 0$ , so  $\hat{X}(0) = 0$ .

When the aggregate shock arrives at  $t = 0$ , no firm has yet had time to adjust its price, so  $\hat{h}(x, 0) = 0$  on the open interior as stated in (23). Because this exact initial condition is uniformly zero, it is uninformative about the subsequent dynamics. Therefore this section characterizes the limiting initial condition at  $t = 0^+$ , which is zero almost everywhere, but with three spatial discontinuities corresponding to the three critical points.

At each boundary, the linearized Dirichlet condition (21) imposes  $\hat{h}(\underline{x}, t) = -h'_{ss}(\underline{x})\hat{x}(t)$  and  $\hat{h}(\bar{x}, t) = -h'_{ss}(\bar{x})\hat{\bar{x}}(t)$  for  $t > 0$ . These values are nonzero while the interior remains at zero as  $t \rightarrow 0$ , producing two spatial discontinuities:

$$\hat{h}(\underline{x}, 0^+) = -h'_{ss}(\underline{x})\hat{x}(0), \quad \hat{h}(\underline{x}^+, 0^+) = 0; \quad \hat{h}(\bar{x}^-, 0^+) = 0, \quad \hat{h}(\bar{x}, 0^+) = -h'_{ss}(\bar{x})\hat{\bar{x}}(0) \quad (123)$$

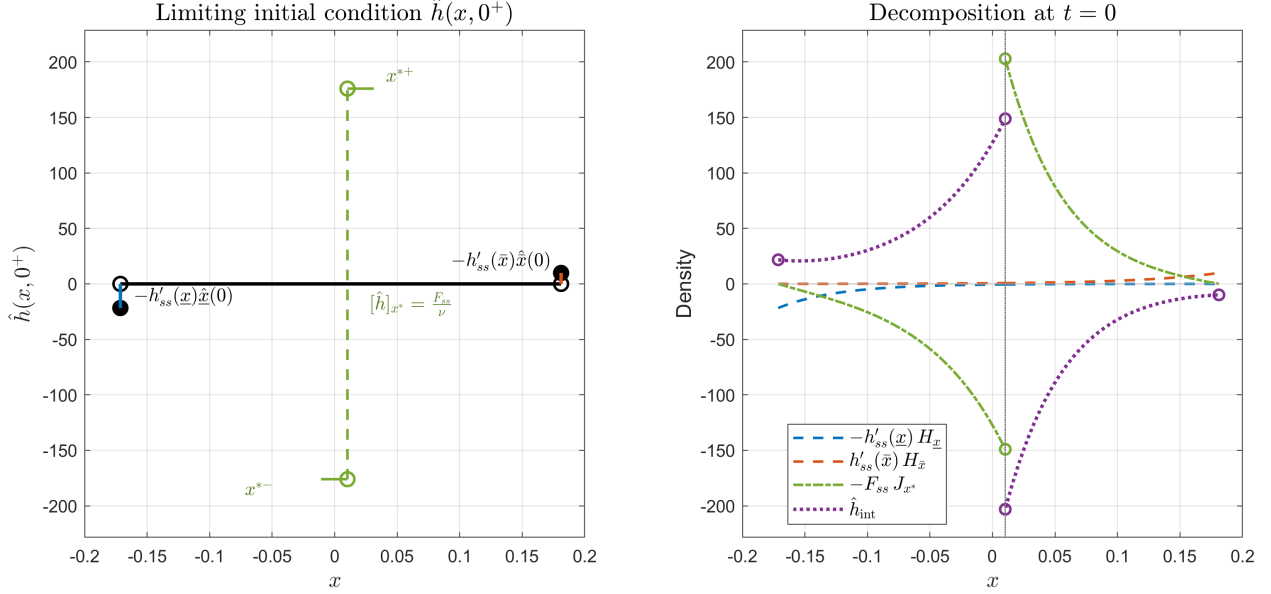
Why? If a shock causes the lower boundary to shift right ( $\hat{x}(0) > 0$ ), the old boundary point  $\underline{x}$  is now outside the inaction region, and the density will fall in the neighborhood of that point as firms exit. But this linearization corresponds to a marginal change in the boundary, so on impact that marginal change only affects the density at the boundary itself. A symmetric argument applies at  $\bar{x}$ : the new boundary shifts to the right, so the density increases. Figure 9 demonstrates by plotting a hypothetical example under the baseline Calvo-plus calibration where all critical points shift to the right by the same quantity. In the left panel, the initial condition (in black) has discontinuities at the boundaries.

At the reset point, the perturbation  $\hat{x}^*(0) > 0$  means that adjusting firms now reset to a location slightly right of the old  $x^*$ . Since a flow  $F_{ss}$  of firms per unit time resets to  $x^*$ , the perturbation removes density just below  $x^*$  and deposits it just above. This effect shows up as the  $\delta'(x - x^*)$  term in the KFE (20). Again, Figure 9 plots this discontinuity in the  $t = 0^+$  initial condition, except the discontinuity at  $x^*$  is different when taking the limit from the right versus from the left.

To understand this dipole structure, consider again the distribution's decomposition in Lemma 2. The critical-point component (27) carries the lifting function  $J_{x^*}$  from Lemma 6, which jumps at  $x^*$  by  $[J_{x^*}]_{x^*} = -1/\nu$ . The boundary-harmonic functions  $H_{\underline{x}}$  and  $H_{\bar{x}}$  are smooth at  $x^*$ , so  $\hat{h}_{\text{crit}}$  inherits the full jump:

$$[\hat{h}_{\text{crit}}]_{x^*}(t) = -F_{ss}\hat{x}^*(t) [J_{x^*}]_{x^*} = \frac{F_{ss}\hat{x}^*(t)}{\nu} \quad (124)$$

Meanwhile, the interior component  $\hat{h}_{\text{int}}(x, t)$  is smooth at  $x^*$  for all  $t > 0$ . Therefore the total jump remains



Notes: Left panel: the distribution perturbation at  $t = 0^+$ , showing all three spatial discontinuities. Boundary values (filled circles) from the linearized absorbing conditions (123); the dipole at  $x^*$  (open circles with directional whiskers) has different one-sided limits; vertical bars mark each discontinuity. Right panel: the three components of  $\hat{h}_{\text{crit}}(x, 0)$  from (27) together with the interior component  $\hat{h}_{\text{int}}(x, 0)$ . The steady state corresponds to the Calvo-plus calibration. All quantities normalized by a unit shock ( $\hat{x}(0) = \hat{x}^*(0) = \hat{x}^*(0) = 1$ ).

Figure 9: Limiting initial condition  $\hat{h}(x, 0^+)$  and its critical-point decomposition

$$[\hat{h}]_{x^*}(t) = [\hat{h}_{\text{crit}}]_{x^*}(t) = F_{ss}\hat{x}^*(t)/\nu \text{ for } t > 0.$$

## F.2 Impact Effect on the Frequency of Price Adjustment

The impact effect on the FPA requires careful treatment because the spatial derivatives appearing in the flux formula (22) become singular when boundary conditions jump discontinuously.

For computing the singular part of the diffusive flux  $\nu\partial_x\hat{h}$ , it is helpful to focus on the limiting behavior near each boundary separately, because for a small time interval  $t = \Delta t$  after the shock, the distribution's behavior at each critical point has negligible effects on the others. Thus, for small  $\Delta t$ , away from  $x^*$  the distribution is well described by the homogeneous component of the perturbed KFE:

$$[t \approx 0, x \ll x^*, x \gg x^*]: \quad \partial_t \hat{h}(x, t) \approx \nu \partial_x^2 \hat{h}(x, t) + \bar{\pi} \partial_x \hat{h}(x, t) - \zeta \hat{h}(x, t) \quad (125)$$

Then, it is useful to transform this homogeneous KFE into the canonical heat equation by substituting  $y = x - \underline{x}$  and writing

$$w(y, t) = e^{\bar{\pi}/(2\nu)y + (\bar{\pi}^2/(4\nu) + \zeta)t} \hat{h}(y + \underline{x}, t) \quad (126)$$

which satisfies  $\partial_t w(y, t) = \nu \partial_x^2 w(y, t)$  on  $[0, \bar{x} - \underline{x}]$ . Then in order to consider single boundaries alone, which is valid for  $\Delta t$  small, I will instead analyze this solution on the half line  $y \in [0, \infty)$  with boundary condition

$w(0, t) = -h'_{ss}(\underline{x})\hat{\underline{x}}(t)$ . This is a useful strategy because this PDE has a known solution:<sup>25</sup>

**Property 4** (Heat equation on the half-line). *If  $w(y, t)$  satisfies the heat equation  $\partial_t w = \nu \partial_y^2 w$  on the half-line  $y \geq 0$  with initial condition  $w(y, 0) = 0$  and constant Dirichlet boundary condition  $w(0, t) = w_0$  for  $t > 0$ . The solution is*

$$w(y, t) = w_0 \operatorname{erfc}\left(\frac{y}{\sqrt{4\nu t}}\right) \quad (127)$$

where  $\operatorname{erfc}(z) = \frac{2}{\sqrt{\pi}} \int_z^\infty e^{-\xi^2} d\xi$  is the complementary error function. The spatial derivative at the boundary is

$$\partial_y w(0, t) = -\frac{w_0}{\sqrt{\pi\nu t}} \quad (128)$$

Property 4 allows for straightforward characterization of the derivative in a neighborhood near the boundary. Lemma 16 follows:

**Lemma 16.** *If the boundary perturbations  $\hat{\underline{x}}(t)$  and  $\hat{\bar{x}}(t)$  are continuous with  $\hat{\underline{x}}(0)$  and  $\hat{\bar{x}}(0)$  finite, and  $\Delta t$  is sufficiently small, then the FPA at time  $\Delta t$  is approximately*

$$\hat{F}(\Delta t) \approx \sqrt{\frac{\nu}{\pi\Delta t}} (h'_{ss}(\underline{x})\hat{\underline{x}}(\Delta t) + h'_{ss}(\bar{x})\hat{\bar{x}}(\Delta t)) + \frac{\bar{\pi}}{2} (h'_{ss}(\bar{x})\hat{\bar{x}}(\Delta t) - h'_{ss}(\underline{x})\hat{\underline{x}}(\Delta t)) \quad (129)$$

*Proof.* Near the lower boundary, for small time  $t = \Delta t$ , the transformed distribution  $w(x, t)$  satisfies (by Property 4)

$$w(x - \underline{x}, \Delta t) = -h'_{ss}(\underline{x})\hat{\underline{x}}(\Delta t) \operatorname{erfc}\left(\frac{x - \underline{x}}{\sqrt{4\nu\Delta t}}\right) + o(1)$$

The approximation error is only  $o(1)$  because of the continuity/finiteness assumption on  $\hat{\underline{x}}(t)$ . The spatial derivative is  $\partial_y w(0, \Delta t) = \frac{h'_{ss}(\underline{x})\hat{\underline{x}}(\Delta t)}{\sqrt{\pi\nu\Delta t}} + o(1)$ . The spatial derivative relates to the original distribution by

$$\begin{aligned} \partial_x \hat{h}(x, t) &= \partial_x \left( e^{-\bar{\pi}/(2\nu)(x-\underline{x}) - (\bar{\pi}^2/(4\nu) + \zeta)t} w(x - \underline{x}, t) \right) \\ &= -\frac{\bar{\pi}}{2\nu} e^{-\bar{\pi}/(2\nu)(x-\underline{x}) - (\bar{\pi}^2/(4\nu) + \zeta)t} w(x - \underline{x}, t) + e^{-\bar{\pi}/(2\nu)(x-\underline{x}) - (\bar{\pi}^2/(4\nu) + \zeta)t} \partial_y w(x - \underline{x}, t) \end{aligned}$$

Evaluate at the lower boundary:

$$\partial_x \hat{h}(\underline{x}, t) = -\frac{\bar{\pi}}{2\nu} e^{-(\bar{\pi}^2/(4\nu) + \zeta)t} (-h'_{ss}(\underline{x})\hat{\underline{x}}(t)) + e^{-(\bar{\pi}^2/(4\nu) + \zeta)t} \partial_y w(0, t)$$

which for small  $t = \Delta t$  is

$$\begin{aligned} \partial_x \hat{h}(\underline{x}, \Delta t) &= \frac{\bar{\pi}}{2\nu} e^{-(\bar{\pi}^2/(4\nu) + \zeta)\Delta t} h'_{ss}(\underline{x})\hat{\underline{x}}(\Delta t) + e^{-(\bar{\pi}^2/(4\nu) + \zeta)\Delta t} \frac{h'_{ss}(\underline{x})\hat{\underline{x}}(\Delta t)}{\sqrt{\pi\nu\Delta t}} + o(1) \\ &= h'_{ss}(\underline{x})\hat{\underline{x}}(\Delta t) \left( \frac{\bar{\pi}}{2\nu} + \frac{1}{\sqrt{\pi\nu\Delta t}} \right) + o(1) \end{aligned}$$

<sup>25</sup>See (Carslaw and Jaeger, 1959, Section 2.4) or (Polyanin, 2001, Section 3.1).

Near the upper boundary, instead use the change of variable  $y = \bar{x} - x \geq 0$  to write

$$\tilde{w}(y, t) = e^{-\bar{\pi}/(2\nu)y + (\bar{\pi}^2/(4\nu) + \zeta)t} \hat{h}(\bar{x} - y, t)$$

so that  $\partial_t \tilde{w} = \nu \partial_y^2 \tilde{w}$ . If  $y \geq 0$  with boundary condition  $\tilde{w}(0, t) = -h'_{ss}(\bar{x}) \hat{x}(t)$ , then for small time  $t = \Delta t$

$$\tilde{w}(\bar{x} - x, \Delta t) = -h'_{ss}(\bar{x}) \hat{x}(\Delta t) \operatorname{erfc} \left( \frac{\bar{x} - x}{\sqrt{4\nu\Delta t}} \right) + o(1)$$

with spatial derivative  $\partial_y \tilde{w}(0, \Delta t) = \frac{h'_{ss}(\bar{x}) \hat{x}(\Delta t)}{\sqrt{\pi\nu\Delta t}} + o(1)$ . The spatial derivative relates to the original distribution by

$$\begin{aligned} \partial_x \hat{h}(x, t) &= \partial_x \left( e^{\bar{\pi}/(2\nu)(\bar{x}-x) - (\bar{\pi}^2/(4\nu) + \zeta)t} \tilde{w}(\bar{x} - x, t) \right) \\ &= -\frac{\bar{\pi}}{2\nu} e^{\bar{\pi}/(2\nu)(\bar{x}-x) - (\bar{\pi}^2/(4\nu) + \zeta)t} \tilde{w}(\bar{x} - x, t) - e^{\bar{\pi}/(2\nu)(\bar{x}-x) - (\bar{\pi}^2/(4\nu) + \zeta)t} \partial_y \tilde{w}(\bar{x} - x, t) \end{aligned}$$

Evaluate at the upper boundary:

$$\partial_x \hat{h}(\bar{x}, t) = -\frac{\bar{\pi}}{2\nu} e^{-(\bar{\pi}^2/(4\nu) + \zeta)t} (-h'_{ss}(\bar{x})) \hat{x}(t) - e^{-(\bar{\pi}^2/(4\nu) + \zeta)t} \partial_y \tilde{w}(0, t)$$

which for small  $t = \Delta t$  is

$$\begin{aligned} \partial_x \hat{h}(\bar{x}, \Delta t) &= \frac{\bar{\pi}}{2\nu} e^{-(\bar{\pi}^2/(4\nu) + \zeta)\Delta t} h'_{ss}(\bar{x}) \hat{x}(\Delta t) - e^{-(\bar{\pi}^2/(4\nu) + \zeta)\Delta t} \frac{h'_{ss}(\bar{x}) \hat{x}(\Delta t)}{\sqrt{\pi\nu\Delta t}} + o(1) \\ &= h'_{ss}(\bar{x}) \hat{x}(\Delta t) \left( \frac{\bar{\pi}}{2\nu} - \frac{1}{\sqrt{\pi\nu\Delta t}} \right) + o(1) \end{aligned}$$

The FPA formula (22) is  $\hat{F}(t) = \nu \partial_x \hat{h}(\underline{x}, t) + \bar{\pi} \hat{h}(\underline{x}, t) - \nu \partial_x \hat{h}(\bar{x}, t) - \bar{\pi} \hat{h}(\bar{x}, t)$ . The diffusive contributions are:

$$\begin{aligned} \nu \partial_x \hat{h}(\underline{x}, \Delta t) &= h'_{ss}(\underline{x}) \hat{x}(\Delta t) \left( \frac{\bar{\pi}}{2} + \sqrt{\frac{\nu}{\pi\Delta t}} \right) + o(1) \\ -\nu \partial_x \hat{h}(\bar{x}, \Delta t) &= -h'_{ss}(\bar{x}) \hat{x}(\Delta t) \left( \frac{\bar{\pi}}{2} - \sqrt{\frac{\nu}{\pi\Delta t}} \right) + o(1) = h'_{ss}(\bar{x}) \hat{x}(\Delta t) \left( -\frac{\bar{\pi}}{2} + \sqrt{\frac{\nu}{\pi\Delta t}} \right) + o(1) \\ \nu \partial_x \hat{h}(\underline{x}, \Delta t) - \nu \partial_x \hat{h}(\bar{x}, \Delta t) &= h'_{ss}(\underline{x}) \hat{x}(\Delta t) \left( \frac{\bar{\pi}}{2} + \sqrt{\frac{\nu}{\pi\Delta t}} \right) - h'_{ss}(\bar{x}) \hat{x}(\Delta t) \left( -\frac{\bar{\pi}}{2} + \sqrt{\frac{\nu}{\pi\Delta t}} \right) + o(1) \end{aligned}$$

The drift terms follow from the boundary conditions:  $\bar{\pi} \hat{h}(\underline{x}, \Delta t) - \bar{\pi} \hat{h}(\bar{x}, \Delta t) = \bar{\pi} (-h'_{ss}(\underline{x}) \hat{x}(\Delta t) + h'_{ss}(\bar{x}) \hat{x}(\Delta t))$ .

Summing all contributions:

$$\begin{aligned} \hat{F}(\Delta t) &= h'_{ss}(\underline{x}) \hat{x}(\Delta t) \left( \frac{\bar{\pi}}{2} + \sqrt{\frac{\nu}{\pi\Delta t}} - \bar{\pi} \right) + h'_{ss}(\bar{x}) \hat{x}(\Delta t) \left( -\frac{\bar{\pi}}{2} + \sqrt{\frac{\nu}{\pi\Delta t}} + \bar{\pi} \right) + o(1) \\ &= h'_{ss}(\underline{x}) \hat{x}(\Delta t) \left( \sqrt{\frac{\nu}{\pi\Delta t}} - \frac{\bar{\pi}}{2} \right) + h'_{ss}(\bar{x}) \hat{x}(\Delta t) \left( \sqrt{\frac{\nu}{\pi\Delta t}} + \frac{\bar{\pi}}{2} \right) + o(1) \end{aligned}$$

Rearranging gives (129). □

Lemma 16 shows that the initial FPA is infinite:  $\lim_{\Delta t \rightarrow 0} \hat{F}(\Delta t) = \pm\infty$ , where the sign depends on the sign of  $(h'_{ss}(\underline{x})\hat{x}(0) + h'_{ss}(\bar{x})\hat{x}(0))$ . This is because the immediate shift of the boundaries causes firms to reset prices immediately. For large shocks, this leads to a non-zero mass of resetting firms. In this perturbed economy, the marginal shock causes a zero mass of firms to reset, but the rate remains infinite. However, it is only instantaneously singular; the FPA falls rapidly with  $\Delta t$ , and is integrable.

**Corollary 1.** *For a permanent marginal cost increase of size  $\kappa$ , if  $\Delta t$  and  $\bar{\pi}$  are sufficiently small, then the FPA at time  $\Delta t$  is approximately*

$$\hat{F}(\Delta t) \approx \left( \sqrt{\frac{\nu}{\pi\Delta t}} (h'_{ss}(\underline{x}) + h'_{ss}(\bar{x})) + \frac{\bar{\pi}}{2} (h'_{ss}(\bar{x}) - h'_{ss}(\underline{x})) \right) \kappa$$

and the average FPA over the interval is

$$\Upsilon(\Delta t) \equiv \left( 2\sqrt{\frac{\nu}{\pi\Delta t}} (h'_{ss}(\underline{x}) + h'_{ss}(\bar{x})) + \frac{\bar{\pi}}{2} (h'_{ss}(\bar{x}) - h'_{ss}(\underline{x})) \right) \kappa$$

*Proof.* When trend inflation is near zero, the value function perturbation at the critical points is zero (Alvarez et al., 2023) so the perturbed critical points (e.g. equation (47)) depend only on the present value of future marginal costs. The marginal cost change is permanent, so the critical points move permanently. Because of long-run neutrality (Definition 2) the critical points must all increase by  $\kappa$ .

Plug this change into the flow equation from Lemma 16:

$$\hat{F}(\Delta t) \approx \sqrt{\frac{\nu}{\pi\Delta t}} (h'_{ss}(\underline{x})\kappa + h'_{ss}(\bar{x})\kappa) + \frac{\bar{\pi}}{2} (h'_{ss}(\bar{x})\kappa - h'_{ss}(\underline{x})\kappa)$$

Collect terms to yield the desired expression.

Then, evaluate the integral:

$$\int_0^{\Delta t} \left( \sqrt{\frac{\nu}{\pi\Delta t}} (h'_{ss}(\underline{x}) + h'_{ss}(\bar{x})) + \frac{\bar{\pi}}{2} (h'_{ss}(\bar{x}) - h'_{ss}(\underline{x})) \right) \kappa d\tau = \left( 2\sqrt{\frac{\nu}{\pi\Delta t}} (h'_{ss}(\underline{x}) + h'_{ss}(\bar{x})) + \frac{\bar{\pi}}{2} (h'_{ss}(\bar{x}) - h'_{ss}(\underline{x})) \right) \Delta t \kappa$$

This is the cumulative price adjustment. Dividing by  $\Delta t$  gives the average FPA. □

## G Price Change Statistics

This section derives a number of price change statistics in the steady state, which are used for calibrating the model.

## G.1 Steady State Frequency of Price Adjustment

This subsection derives the components of the steady-state frequency of price adjustment  $F_{ss}$  in terms of primitive parameters and the steady-state distribution.

Per equation (82), the steady-state FPA is given by

$$F_{ss} = \nu h'_{ss}(\underline{x}) - \nu h'_{ss}(\bar{x}) + \zeta \quad (130)$$

Each component of this equation corresponds to a different type of price adjustment:  $F_{\underline{x}} \equiv \nu h'_{ss}(\underline{x})$  denotes resets from the lower boundary,  $F_{\bar{x}} \equiv -\nu h'_{ss}(\bar{x})$  denotes resets from the upper boundary, and  $F_{\zeta} \equiv \zeta$  denotes random resets. Together, the steady-state FPA is decomposed as

$$F_{ss} = F_{\underline{x}} + F_{\bar{x}} + F_{\zeta} \quad (131)$$

### G.1.1 General Case with Drift

For general  $\bar{\pi} \neq 0$ , the steady-state distribution has piecewise exponential form with shared roots  $r_1, r_2$  of the characteristic equation:

$$r_{1,2} = \frac{-\bar{\pi} \pm \sqrt{\bar{\pi}^2 + 4\nu\zeta}}{2\nu} \quad (132)$$

The absorbing boundary conditions yield (80) and (81), reducing the system to two unknowns ( $B_L, B_R$ ) determined by continuity at  $x^*$  and normalization.

Using (80), the derivative at the lower boundary simplifies:

$$h'_{ss}(\underline{x}) = A_L r_1 e^{r_1 \underline{x}} + B_L r_2 e^{r_2 \underline{x}} = B_L e^{r_2 \underline{x}} \left( r_2 - r_1 e^{(r_1 - r_2) \underline{x}} \right) \quad (133)$$

Similarly, using (81):

$$h'_{ss}(\bar{x}) = A_R r_1 e^{r_1 \bar{x}} + B_R r_2 e^{r_2 \bar{x}} = B_R e^{r_2 \bar{x}} \left( r_2 - r_1 e^{(r_1 - r_2) \bar{x}} \right) \quad (134)$$

The frequency components are:

$$F_{\underline{x}} = \nu B_L e^{r_2 \underline{x}} \left( r_2 - r_1 e^{(r_1 - r_2) \underline{x}} \right) \quad (135)$$

$$F_{\bar{x}} = -\nu B_R e^{r_2 \bar{x}} \left( r_2 - r_1 e^{(r_1 - r_2) \bar{x}} \right) \quad (136)$$

$$F_{\zeta} = \zeta \quad (137)$$

where the coefficients  $B_L$  and  $B_R$  are determined by the remaining two linear conditions. This decomposition shows how frequency depends on the distribution shape: when  $\zeta$  is small, most adjustments occur at the boundaries; when  $\zeta$  is large, random adjustments dominate.

### G.1.2 Zero-Drift Special Case

When  $\bar{\pi} = 0$ , symmetry implies  $x_{ss}^* = 0$  and  $\bar{x}_{ss} = -\underline{x}_{ss} \equiv \ell/2$ . The roots become  $r_{1,2} = \pm s_{zd}$  where  $s_{zd} = \sqrt{\zeta/\nu}$ . The distribution is symmetric:  $h'_{ss}(x) = -h'_{ss}(\bar{x})$ , so:

$$F_{\underline{x}} = F_{\bar{x}} = \nu h'_{ss}(\underline{x}), \quad F_{ss} = 2\nu h'_{ss}(\underline{x}) + \zeta \quad (138)$$

From the boundary condition  $h(-\ell/2) = 0$  with  $h_L(x) = A_L e^{s_{zd}x} + B_L e^{-s_{zd}x}$ :

$$A_L = -B_L e^{-s_{zd}\ell}$$

Thus  $h_L(x) = B_L (e^{-s_{zd}x} - e^{-s_{zd}\ell} e^{s_{zd}x}) = 2B_L e^{-s_{zd}\ell/2} \sinh(s_{zd}(x + \ell/2))$  for  $x \in [-\ell/2, 0]$ . The derivative at  $x = -\ell/2$  is:

$$h'(-\ell/2) = 2B_L e^{-s_{zd}\ell/2} s_{zd}$$

Normalization  $\int_{-\ell/2}^{\ell/2} h_{ss}(x) dx = 1$  and symmetry determine

$$B_L = \frac{s_{zd}}{4e^{-s_{zd}\ell/2}(\cosh(s_{zd}\ell/2) - 1)}$$

Therefore:

$$F_{ss} = 4\nu B_L e^{-s_{zd}\ell/2} s_{zd} + \zeta = \frac{\nu s_{zd}^2}{\cosh(s_{zd}\ell/2) - 1} + \zeta = \frac{\zeta \cosh(s_{zd}\ell/2)}{\cosh(s_{zd}\ell/2) - 1} \quad (139)$$

with components:

$$F_{\underline{x}} = F_{\bar{x}} = \frac{\zeta}{2(\cosh(s_{zd}\ell/2) - 1)}, \quad F_{\zeta} = \zeta \quad (140)$$

Note that these sum to  $F_{ss}$ :  $\frac{\zeta}{\cosh(s_{zd}\ell/2) - 1} + \zeta = \frac{\zeta \cosh(s_{zd}\ell/2)}{\cosh(s_{zd}\ell/2) - 1}$ . The fraction of adjustments from each boundary is:

$$\frac{F_{\underline{x}}}{F_{ss}} = \frac{F_{\bar{x}}}{F_{ss}} = \frac{1}{2 \cosh(s_{zd}\ell/2)}, \quad \frac{F_{\zeta}}{F_{ss}} = \frac{\cosh(s_{zd}\ell/2) - 1}{\cosh(s_{zd}\ell/2)} \quad (141)$$

## G.2 Average Price Adjustment

The adjustment from the lower boundary is always  $x^* - \underline{x}$ , while the adjustment from the upper boundary is always  $\bar{x} - x^*$ . These occur at frequencies  $F_{\underline{x}}$  and  $F_{\bar{x}}$  respectively. When a firm with price gap  $x$  receives a random adjustment opportunity at rate  $\zeta$ , then its adjustment is  $x^* - x$ .

Therefore, the mean adjustment is

$$\begin{aligned} \mu_{1,\text{adj}} &\equiv \mathbb{E}[x - x^* | \text{adjust}] = \frac{1}{F_{ss}} \left( F_{\underline{x}}(x^* - \underline{x}) + F_{\bar{x}}(x^* - \bar{x}) + \zeta \int_{\underline{x}}^{\bar{x}} (x^* - x) h_{ss}(x) dx \right) \\ &= \frac{1}{F_{ss}} (F_{\underline{x}}(x^* - \underline{x}) + F_{\bar{x}}(x^* - \bar{x}) + \zeta(x^* - X)) \end{aligned} \quad (142)$$

where  $X$  is the average price gap.

In special case of zero drift ( $\bar{\pi} = 0$ ), the distribution is symmetric so the average price adjustment is zero.

### G.3 Variance of Price Adjustments

The second moment of price adjustment is

$$\mu_{2,\text{adj}} \equiv \mathbb{E}[(x^* - x)^2 | \text{adjust}] = \frac{1}{F_{ss}} \left( F_{\underline{x}}(x^* - \underline{x})^2 + F_{\bar{x}}(x^* - \bar{x})^2 + \zeta \int_{\underline{x}}^{\bar{x}} (x^* - x)^2 h_{ss}(x) dx \right) \quad (143)$$

The variance of price adjustments is then

$$\text{Var}(x^* - x | \text{adjust}) = \mu_{2,\text{adj}} - \mu_{1,\text{adj}}^2 \quad (144)$$

For algebraic purposes, we can decompose the weighted second moment contributions:

$$\mu_{2,\text{adj},\underline{x}} \equiv \frac{F_{\underline{x}}}{F_{ss}} (x - x^*)^2 \quad (145)$$

$$\mu_{2,\text{adj},\bar{x}} \equiv \frac{F_{\bar{x}}}{F_{ss}} (\bar{x} - x^*)^2 \quad (146)$$

$$\mu_{2,\text{adj},\zeta} \equiv \frac{\zeta}{F_{ss}} \int_{\underline{x}}^{\bar{x}} (x - x^*)^2 h_{ss}(x) dx \quad (147)$$

so that  $\mathbb{E}[(x^* - x)^2 | \text{adjust}] = \mu_{2,\text{adj},\underline{x}} + \mu_{2,\text{adj},\bar{x}} + \mu_{2,\text{adj},\zeta}$ .

#### G.3.1 Zero-Drift Special Case

When  $\bar{\pi} = 0$ , symmetry gives  $x^* = 0$ ,  $\bar{x} = -\underline{x} = \ell/2$ , and  $F_{\underline{x}} = F_{\bar{x}}$ . The mean adjustment vanishes by symmetry:

$$\mu_{1,\text{adj}} = \frac{1}{F_{ss}} [F_{\underline{x}}(0 - (-\ell/2)) + F_{\bar{x}}(0 - \ell/2) + \zeta(0 - 0)] = 0 \quad (148)$$

where the average price gap  $X = \int_{-\ell/2}^{\ell/2} x h_{ss}(x) dx = 0$  by symmetry. Therefore, the variance equals the second moment.

The second moment contributions from boundaries are equal. Using (141),  $F_{\underline{x}}/F_{ss} = 1/(2 \cosh(s_{zd}\ell/2))$ :

$$\mu_{2,\text{adj},\underline{x}} = \mu_{2,\text{adj},\bar{x}} = \frac{F_{\underline{x}}}{F_{ss}} (\ell/2)^2 = \frac{(\ell/2)^2}{2 \cosh(s_{zd}\ell/2)} = \frac{\ell^2}{8 \cosh(s_{zd}\ell/2)} \quad (149)$$

For the random adjustment term, using the symmetric density  $h_L(x) = \frac{s_{zd}}{2(\cosh(s_{zd}\ell/2)-1)} \sinh(s_{zd}(x+\ell/2))$ :

$$\mu_{2,\text{adj},\zeta} = \frac{\zeta}{F_{ss}} \int_{-\ell/2}^{\ell/2} x^2 h_{ss}(x) dx = \frac{2\zeta}{F_{ss}} \int_{-\ell/2}^0 x^2 h_L(x) dx$$

Substituting  $u = x + \ell/2$  so that  $x = u - \ell/2$  and integrating from  $u = 0$  to  $u = \ell/2$ :

$$\int_{-\ell/2}^0 x^2 h_L(x) dx = \frac{s_{zd}}{2(\cosh(s_{zd}\ell/2) - 1)} \int_0^{\ell/2} (u - \ell/2)^2 \sinh(s_{zd}u) du$$

Using integration by parts twice, this evaluates to:

$$\int_{-\ell/2}^0 x^2 h_L(x) dx = \frac{1}{s_{zd}^2} - \frac{\ell^2}{8(\cosh(s_{zd}\ell/2) - 1)} \quad (150)$$

Therefore, the random adjustment contribution is:

$$\mu_{2,\text{adj},\zeta} = \frac{\zeta}{F_{ss}} \left[ \frac{2}{s_{zd}^2} - \frac{\ell^2}{4(\cosh(s_{zd}\ell/2) - 1)} \right] \quad (151)$$

where  $\zeta/F_{ss} = (\cosh(s_{zd}\ell/2) - 1)/\cosh(s_{zd}\ell/2) = 1 - \text{sech}(s_{zd}\ell/2)$ .

The variance (which equals the second moment in this symmetric case) simplifies elegantly. Using  $s_{zd}^2 = \zeta/\nu$  and writing  $C \equiv \cosh(s_{zd}\ell/2)$  for brevity:

$$\begin{aligned} \mu_{2,\text{adj}} &= \frac{\ell^2}{4C} + \frac{C-1}{C} \left[ \frac{2}{s_{zd}^2} - \frac{\ell^2}{4(C-1)} \right] \\ &= \frac{\ell^2}{4C} + \frac{2(C-1)}{s_{zd}^2 C} - \frac{\ell^2}{4C} = \frac{2(\cosh(s_{zd}\ell/2) - 1)}{s_{zd}^2 \cosh(s_{zd}\ell/2)} \end{aligned} \quad (152)$$

or equivalently:

$$\text{Var}(x^* - x|\text{adjust}) = \frac{2\nu}{\zeta} (1 - \text{sech}(s_{zd}\ell/2)) \quad (153)$$

This decomposition is useful for calibrating the model to microdata on the distribution of price changes, distinguishing between adjustments driven by boundary crossings versus random opportunities.

## G.4 Kurtosis of Price Adjustments

The kurtosis of price adjustments characterizes the tail behavior of the distribution of price changes. The kurtosis is given by

$$\text{Kurt}(x - x^*|\text{adjust}) = \frac{\mathbb{E}[(x^* - x - \mu_{1,\text{adj}})^4|\text{adjust}]}{\text{Var}(x^* - x|\text{adjust})} \quad (154)$$

The denominator is given by equation (144) while the numerator is

$$\begin{aligned} &\mathbb{E}[(x^* - x - \mu_{1,\text{adj}})^4|\text{adjust}] = \\ &\frac{1}{F_{ss}} \left( F_{\underline{x}}(x^* - \underline{x} - \mu_{1,\text{adj}})^4 + F_{\bar{x}}(x^* - \bar{x} - \mu_{1,\text{adj}})^4 + \zeta \int_{\underline{x}}^{\bar{x}} (x^* - x - \mu_{1,\text{adj}})^4 h_{ss}(x) dx \right) \end{aligned} \quad (155)$$

### G.4.1 Zero-Drift Special Case

When  $\bar{\pi} = 0$ , symmetry gives  $x^* = 0$ ,  $\bar{x} = -\underline{x} = \ell/2$ , and  $F_{\underline{x}} = F_{\bar{x}}$ . Since  $\mu_{1,\text{adj}} = 0$  by symmetry, the centered moments equal the raw moments. The kurtosis simplifies to:

$$\text{Kurt}(x^* - x|\text{adjust}) = \frac{\mu_{4,\text{adj}}}{\mu_{2,\text{adj}}^2} \quad (156)$$

The fourth moment contributions from boundaries are equal. Using (141):

$$\mu_{4,\text{adj},\underline{x}} = \mu_{4,\text{adj},\bar{x}} = \frac{F_{\underline{x}}}{F_{ss}} (\ell/2)^4 = \frac{(\ell/2)^4}{2 \cosh(s_{zd}\ell/2)} = \frac{\ell^4}{32 \cosh(s_{zd}\ell/2)} \quad (157)$$

For the random adjustment term, using the symmetric density:

$$\mu_{4,\text{adj},\zeta} = \frac{\zeta}{F_{ss}} \int_{-\ell/2}^{\ell/2} x^4 h_{ss}(x) dx = \frac{2\zeta}{F_{ss}} \int_{-\ell/2}^0 x^4 h_L(x) dx$$

Using the same integration by parts technique as for the second moment:

$$\int_{-\ell/2}^0 x^4 h_L(x) dx = \frac{12}{s_{zd}^4} - \frac{\ell^4}{32(\cosh(s_{zd}\ell/2) - 1)} - \frac{3\ell^2}{2s_{zd}^2(\cosh(s_{zd}\ell/2) - 1)} \quad (158)$$

Therefore, the random adjustment contribution is:

$$\mu_{4,\text{adj},\zeta} = \frac{\zeta}{F_{ss}} \left[ \frac{24}{s_{zd}^4} - \frac{\ell^4}{16(\cosh(s_{zd}\ell/2) - 1)} - \frac{3\ell^2}{s_{zd}^2(\cosh(s_{zd}\ell/2) - 1)} \right] \quad (159)$$

where  $\zeta/F_{ss} = (\cosh(s_{zd}\ell/2) - 1)/\cosh(s_{zd}\ell/2)$ .

The total fourth moment simplifies similarly to the variance. Writing  $C \equiv \cosh(s_{zd}\ell/2)$  as before:

$$\mu_{4,\text{adj}} = \frac{\ell^4}{16C} + \frac{C-1}{C} \left[ \frac{24}{s_{zd}^4} - \frac{\ell^4}{16(C-1)} - \frac{3\ell^2}{s_{zd}^2(C-1)} \right] \quad (160)$$

which simplifies to:

$$\mu_{4,\text{adj}} = \frac{24(\cosh(s_{zd}\ell/2) - 1)}{s_{zd}^4 \cosh(s_{zd}\ell/2)} - \frac{3\ell^2}{s_{zd}^2 \cosh(s_{zd}\ell/2)} = \frac{24\nu^2}{\zeta^2} (1 - \text{sech}(s_{zd}\ell/2)) - \frac{3\ell^2\nu}{\zeta \cosh(s_{zd}\ell/2)} \quad (161)$$

The kurtosis depends on the relative importance of boundary versus random adjustments. When  $\zeta$  is small (mostly boundary adjustments), the distribution has mass concentrated at  $\pm\ell/2$ , yielding high kurtosis. When  $\zeta$  is large (mostly random adjustments from the interior), kurtosis is lower.

## H Computational Appendix

This appendix describes the numerical implementation of the model solution. For the purposes of speed and clarity, it derives a number of integrals analytically. Then it lays out the computational algorithm.

### H.1 Analytical integrals against the stationary distribution

This subsection records the closed-form integral formulas used to calculate moments from the piecewise-exponential stationary density. These solutions take the value function's piecewise coefficients  $(A_L, B_L, A_R, B_R)$  and shared roots  $(r_1, r_2)$  as known.

The common building blocks for integrals appearing in Lemma 1 and subsequent propositions are

1. mass on a subinterval:  $\Omega_0[a, b] = \int_a^b h_{ss}(x) dx$
2. first moment:  $\Omega_1[a, b] = \int_a^b x h_{ss}(x) dx$
3. second moment (quadratic kernel):  $\Omega_2[a, b] = \int_a^b x^2 h_{ss}(x) dx$

All of these are linear combinations of the basic exponential moments on an interval  $[a, b]$ . For  $r \in \mathbb{R}$  define

$$I_0(r; a, b) \equiv \int_a^b e^{rx} dx = \begin{cases} \frac{e^{rb} - e^{ra}}{r} & r \neq 0 \\ b - a & r = 0 \end{cases}$$

$$I_1(r; a, b) \equiv \int_a^b x e^{rx} dx = \frac{b e^{rb} - a e^{ra}}{r} - \frac{e^{rb} - e^{ra}}{r^2}$$

$$I_2(r; a, b) \equiv \int_a^b x^2 e^{rx} dx = \frac{b^2 e^{rb} - a^2 e^{ra}}{r} - 2 \frac{b e^{rb} - a e^{ra}}{r^2} + 2 \frac{e^{rb} - e^{ra}}{r^3}$$

For the full inaction region we simply sum the contributions from the left and right pieces. For example

$$\Omega_1[\underline{x}, \bar{x}] = A_L I_1(r_1; \underline{x}, x^*) + B_L I_1(r_2; \underline{x}, x^*) + A_R I_1(r_1; x^*, \bar{x}) + B_R I_1(r_2; x^*, \bar{x})$$

For a polynomial times an exponential,  $\int_a^b p(x) e^{rx} dx$  with  $p(x) = \alpha x^2 + \beta x + \gamma$ , the result is

$$\int_a^b p(x) e^{rx} dx = \alpha I_2(r; a, b) + \beta I_1(r; a, b) + \gamma I_0(r; a, b)$$

#### H.1.1 Analytical derivation of $\Theta_{MC,n}(x)$ and $\Theta_{v,n}(x)$

Recall from Lemma 1 that

$$\Theta_{MC,n}(x) = -2\mathbf{B} \int_{\underline{x}}^{\bar{x}} \gamma_{HJB,n}(x, y) y dy \quad \Theta_{v,n}(x) = -\zeta \int_{\underline{x}}^{\bar{x}} \gamma_{HJB,n}(x, y) dy + \nu \partial_y \gamma_{HJB,n}(x, \underline{x}) - \nu \partial_y \gamma_{HJB,n}(x, \bar{x})$$

From (29) and the relation  $\gamma_{HJB,n}(x, y) = \gamma_{KFE,n}(y, x)$  we have

$$\gamma_{HJB,n}(x, y) = \frac{2}{\bar{x} - \underline{x}} e^{\frac{\pi}{2\nu}(x-y)} \sin\left(\frac{n\pi(y - \underline{x})}{\bar{x} - \underline{x}}\right) \sin\left(\frac{n\pi(x - \underline{x})}{\bar{x} - \underline{x}}\right)$$

Separating the  $x$ - and  $y$ -dependence, define the constant (in  $y$ )

$$\mathcal{G}_n(x) \equiv \frac{2}{\bar{x} - \underline{x}} e^{\frac{\pi}{2\nu}x} \sin\left(\frac{n\pi(x - \underline{x})}{\bar{x} - \underline{x}}\right)$$

so that

$$\gamma_{HJB,n}(x, y) = \mathcal{G}_n(x) e^{-\frac{\pi}{2\nu}y} \sin\left(\frac{n\pi(y - \underline{x})}{\bar{x} - \underline{x}}\right)$$

We compute

$$\Theta_{MC,n}(x) = -2\mathbf{B}\mathcal{G}_n(x) \int_{\underline{x}}^{\bar{x}} e^{-\frac{\pi}{2\nu}y} \sin\left(\frac{n\pi(y - \underline{x})}{\bar{x} - \underline{x}}\right) y dy$$

This integral has the form

$$\int_{\underline{x}}^{\bar{x}} y e^{-\frac{\pi}{2\nu}y} \sin\left(\frac{n\pi(y - \underline{x})}{\bar{x} - \underline{x}}\right) dy$$

Using the identity  $\sin(\theta) = \frac{e^{i\theta} - e^{-i\theta}}{2i}$  with  $\theta = \frac{n\pi(y - \underline{x})}{\bar{x} - \underline{x}}$ , we obtain

$$\sin\left(\frac{n\pi(y - \underline{x})}{\bar{x} - \underline{x}}\right) = \frac{1}{2i} \left( e^{i\frac{n\pi}{\bar{x} - \underline{x}}(y - \underline{x})} - e^{-i\frac{n\pi}{\bar{x} - \underline{x}}(y - \underline{x})} \right) = \frac{e^{-i\frac{n\pi\underline{x}}{\bar{x} - \underline{x}}}}{2i} e^{i\frac{n\pi}{\bar{x} - \underline{x}}y} - \frac{e^{i\frac{n\pi\underline{x}}{\bar{x} - \underline{x}}}}{2i} e^{-i\frac{n\pi}{\bar{x} - \underline{x}}y}$$

Thus the integral becomes a linear combination of

$$\int_{\underline{x}}^{\bar{x}} y e^{(-\frac{\pi}{2\nu} \pm i\omega_n)y} dy, \quad \omega_n \equiv \frac{n\pi}{\bar{x} - \underline{x}}$$

which reduces to

$$\int_{\underline{x}}^{\bar{x}} y e^{sy} dy = I_1(s; \underline{x}, \bar{x})$$

where  $I_0$  and  $I_1$  are the elementary integrals defined above.

Specifically, with  $s_{\pm} = -\frac{\pi}{2\nu} \pm i\omega_n$  and the phase factors

$$\phi_{\pm} = e^{\mp i\omega_n \underline{x}},$$

we have

$$\Theta_{MC,n}(x) = -2\mathbf{B}\mathcal{G}_n(x) \cdot \text{Re} \left[ \frac{1}{2i} (\phi_- I_1(s_+; \underline{x}, \bar{x}) - \phi_+ I_1(s_-; \underline{x}, \bar{x})) \right]$$

Define the single integral (over the full domain  $[\underline{x}, \bar{x}]$ )

$$J_n^{\text{MC}} = \frac{1}{2i} \left[ e^{-i\omega_n \underline{x}} I_1(s_+; \underline{x}, \bar{x}) - e^{i\omega_n \underline{x}} I_1(s_-; \underline{x}, \bar{x}) \right]$$

where  $s_{\pm} = -\frac{\bar{\pi}}{2\nu} \pm i\omega_n$ . Then

$$\Theta_{MC,n}(x) = -2\mathbf{B}\mathcal{G}_n(x) \operatorname{Re} [J_n^{\text{MC}}]$$

Similarly for  $\Theta_{v,n}(x)$ , the integral term (without the stationary distribution  $h(y)$ ) is

$$\int_{\underline{x}}^{\bar{x}} \gamma_{HJB,n}(x, y) dy = \mathcal{G}_n(x) J_n^v$$

where

$$J_n^v = \frac{1}{2i} \left[ e^{-i\omega_n \underline{x}} I_0(s_+; \underline{x}, \bar{x}) - e^{i\omega_n \underline{x}} I_0(s_-; \underline{x}, \bar{x}) \right]$$

The boundary terms  $\partial_y \gamma_{HJB,n}(x, \underline{x})$  and  $\partial_y \gamma_{HJB,n}(x, \bar{x})$  are evaluated directly from the formula for  $\gamma_{HJB,n}$ .

### H.1.2 Analytical computation of $\chi$ and $\Xi$ coefficients

From Proposition 2, the boundary shift coefficients are

$$\chi_{x^*,n} = -\frac{1}{\partial_{\underline{x}}^2 v_{ss}(x^*)} \Theta'_{MC,n}(x^*), \quad \Xi_{x^*,n} = -\frac{1}{\partial_{\underline{x}}^2 v_{ss}(x^*)} \Theta'_{v,n}(x^*),$$

and similarly for  $\chi_{\underline{x},n}, \chi_{\bar{x},n}, \Xi_{\underline{x},n}, \Xi_{\bar{x},n}$ .

To compute  $\Theta'_{MC,n}(x)$ , differentiate the expression derived above with respect to  $x$ :

$$\Theta'_{MC,n}(x) = -2\mathbf{B}\mathcal{G}'_n(x) \operatorname{Re} [J_n^{\text{MC}}],$$

where

$$\mathcal{G}'_n(x) = \frac{2}{\bar{x} - \underline{x}} e^{\frac{\bar{\pi}}{2\nu} x} \left[ \frac{\bar{\pi}}{2\nu} \sin\left(\frac{n\pi(x - \underline{x})}{\bar{x} - \underline{x}}\right) + \frac{n\pi}{\bar{x} - \underline{x}} \cos\left(\frac{n\pi(x - \underline{x})}{\bar{x} - \underline{x}}\right) \right].$$

Similarly for  $\Theta'_{v,n}(x)$ .

### H.1.3 Analytical derivation of $\xi$ coefficients

This section derives analytical expressions for the  $\xi$  coefficients defined in Theorem 1. Throughout, let  $\ell = \bar{x} - \underline{x}$ ,  $\omega_n = n\pi/\ell$ , and  $\alpha = \bar{\pi}/(2\nu)$ .

**Lemma 17.** *The coefficients  $\xi_{F,n}$ ,  $\xi_{x^*,n}$ ,  $\xi_{\underline{x},n}$ , and  $\xi_{\bar{x},n}$  are given by*

$$\xi_{F,n} = \frac{2}{\ell} \mathcal{I}_n e^{\alpha x^*} \sin(\omega_n(x^* - \underline{x})) \tag{162}$$

$$\xi_{x^*,n} = F_{ss} \frac{2}{\ell} \mathcal{I}_n e^{\alpha x^*} [\alpha \sin(\omega_n(x^* - \underline{x})) + \omega_n \cos(\omega_n(x^* - \underline{x}))] \tag{163}$$

$$\xi_{\underline{x},n} = -\nu h'_{ss}(\underline{x}) \frac{2}{\ell} \mathcal{I}_n e^{\alpha \underline{x}} \omega_n \tag{164}$$

$$\xi_{\bar{x},n} = -\nu h'_{ss}(\bar{x}) \frac{2}{\ell} \mathcal{I}_n e^{\alpha \bar{x}} \omega_n (-1)^n \tag{165}$$

where  $\mathcal{I}_n \equiv \int_{\underline{x}}^{\bar{x}} x e^{-\alpha x} \sin(\omega_n(x - \underline{x})) dx$  has the closed-form expression

$$\mathcal{I}_n = \frac{e^{-\alpha \underline{x}}}{\alpha^2 + \omega_n^2} \left[ \left( \underline{x} + \frac{2\alpha}{\alpha^2 + \omega_n^2} \right) \omega_n (1 - (-1)^n e^{-\alpha \ell}) - \omega_n \ell (-1)^n e^{-\alpha \ell} \right] \quad (166)$$

*Proof.* From Proposition 2, the coefficients are defined as integrals of the KFE Green's function components. Recall the definition of the Green's function component from Lemma 2:

$$\gamma_{KFE,n}(x, y) = \frac{2}{\ell} e^{\alpha(y-x)} \sin(\omega_n(x - \underline{x})) \sin(\omega_n(y - \underline{x}))$$

using the definitions of  $\ell$ ,  $\omega_n$ , and  $\alpha$ .

The coefficient  $\xi_{F,n}$  is defined as  $\xi_{F,n} = \int_{\underline{x}}^{\bar{x}} x \gamma_{KFE,n}(x, x^*) dx$ . Substituting  $\gamma_{KFE,n}(x, x^*)$ :

$$\xi_{F,n} = \frac{2}{\ell} e^{\alpha x^*} \sin(\omega_n(x^* - \underline{x})) \int_{\underline{x}}^{\bar{x}} x e^{-\alpha x} \sin(\omega_n(x - \underline{x})) dx$$

The integral is exactly  $J_n$ , yielding the result.

The coefficient  $\xi_{x^*,n}$  is defined as  $\xi_{x^*,n} = F_{ss} \int_{\underline{x}}^{\bar{x}} x \partial_y \gamma_{KFE,n}(x, x^*) dx$ . Differentiating  $\gamma_{KFE,n}(x, y)$  with respect to  $y$ :

$$\partial_y \gamma_{KFE,n}(x, y) = \frac{2}{\ell} e^{-\alpha x} \sin(\omega_n(x - \underline{x})) [\alpha e^{\alpha y} \sin(\omega_n(y - \underline{x})) + e^{\alpha y} \omega_n \cos(\omega_n(y - \underline{x}))]$$

Evaluating at  $y = x^*$ :

$$\partial_y \gamma_{KFE,n}(x, x^*) = \frac{2}{\ell} e^{-\alpha x} \sin(\omega_n(x - \underline{x})) e^{\alpha x^*} [\alpha \sin(\omega_n(x^* - \underline{x})) + \omega_n \cos(\omega_n(x^* - \underline{x}))]$$

Substituting into the integral:

$$\xi_{x^*,n} = F_{ss} \frac{2}{\ell} e^{\alpha x^*} [\alpha \sin(\omega_n(x^* - \underline{x})) + \omega_n \cos(\omega_n(x^* - \underline{x}))] \int_{\underline{x}}^{\bar{x}} x e^{-\alpha x} \sin(\omega_n(x - \underline{x})) dx$$

which yields the result.

The coefficients  $\xi_{\underline{x},n}$  and  $\xi_{\bar{x},n}$  involve the derivative at the boundaries. At  $y = \underline{x}$ ,  $\sin(\omega_n(y - \underline{x})) = 0$  and  $\cos(\omega_n(y - \underline{x})) = 1$ , so

$$\partial_y \gamma_{KFE,n}(x, \underline{x}) = \frac{2}{\ell} e^{-\alpha x} \sin(\omega_n(x - \underline{x})) e^{\alpha \underline{x}} \omega_n$$

Substituting into  $\xi_{\underline{x},n} = -\nu h'_{ss}(\underline{x}) \int_{\underline{x}}^{\bar{x}} x \partial_y \gamma_{KFE,n}(x, \underline{x}) dx$  gives the result.

At  $y = \bar{x}$ ,  $\sin(\omega_n(y - \underline{x})) = 0$  and  $\cos(\omega_n(y - \underline{x})) = (-1)^n$ , so

$$\partial_y \gamma_{KFE,n}(x, \bar{x}) = \frac{2}{\ell} e^{-\alpha x} \sin(\omega_n(x - \underline{x})) e^{\alpha \bar{x}} \omega_n (-1)^n$$

Substituting into  $\xi_{\bar{x},n} = -\nu h'_{ss}(\bar{x}) \int_{\underline{x}}^{\bar{x}} x \partial_y \gamma_{KFE,n}(x, \bar{x}) dx$  gives the result.

To evaluate  $\mathcal{I}_n$ , substitute  $u = x - \underline{x}$  so that  $x = u + \underline{x}$  and the integral becomes

$$\mathcal{I}_n = e^{-\alpha \underline{x}} \int_0^\ell (u + \underline{x}) e^{-\alpha u} \sin(\omega_n u) du$$

This separates into two standard integrals. Using the formulas

$$\int_0^\ell e^{-\alpha u} \sin(\omega_n u) du = \frac{\omega_n}{\alpha^2 + \omega_n^2} (1 - (-1)^n e^{-\alpha \ell})$$

(since  $\sin(\omega_n \ell) = \sin(n\pi) = 0$  and  $\cos(\omega_n \ell) = (-1)^n$ ), and

$$\begin{aligned} \int_0^\ell u e^{-\alpha u} \sin(\omega_n u) du &= \left[ \frac{e^{-\alpha u}}{\alpha^2 + \omega_n^2} \left( (-\alpha \sin(\omega_n u) - \omega_n \cos(\omega_n u)) u + \frac{2\alpha \omega_n}{(\alpha^2 + \omega_n^2)} \sin(\omega_n u) \right. \right. \\ &\quad \left. \left. - \frac{\alpha^2 - \omega_n^2}{(\alpha^2 + \omega_n^2)} \cos(\omega_n u) \right) \right]_0^\ell \\ &= \frac{1}{\alpha^2 + \omega_n^2} \left[ -\omega_n \ell (-1)^n e^{-\alpha \ell} - \frac{\alpha^2 - \omega_n^2}{\alpha^2 + \omega_n^2} (-1)^n e^{-\alpha \ell} + \frac{\alpha^2 - \omega_n^2}{\alpha^2 + \omega_n^2} \right] \\ &= \frac{1}{\alpha^2 + \omega_n^2} \left[ -\omega_n \ell (-1)^n e^{-\alpha \ell} + \frac{\alpha^2 - \omega_n^2}{\alpha^2 + \omega_n^2} (1 - (-1)^n e^{-\alpha \ell}) \right] \end{aligned}$$

Combining and simplifying yields (166). □

**Lemma 18.** *The primed  $\xi$  coefficients are*

$$\xi_{\underline{x}', n} = h'_{ss}(\underline{x}) \frac{\nu}{\lambda_{KFE, n}} \frac{2\omega_n}{\ell} e^{\alpha \underline{x}} \mathcal{I}_n \quad (167)$$

$$\xi_{\bar{x}', n} = h'_{ss}(\bar{x}) \frac{\nu}{\lambda_{KFE, n}} \frac{2\omega_n}{\ell} (-1)^n e^{\alpha \bar{x}} \mathcal{I}_n \quad (168)$$

$$\xi_{x^{*'}, n} = F_{ss} \frac{2}{\ell} \mathcal{I}_n (\mathcal{K}_{L, n} + \mathcal{K}_{R, n}) \quad (169)$$

where  $\mathcal{I}_n$  is defined in Lemma 17, and

$$\mathcal{K}_{L, n} = B_L r_1 r_2 [e^{-r_1 \underline{x}} \mathcal{J}(r_1 + \alpha, \underline{x}, x^*) - e^{-r_2 \underline{x}} \mathcal{J}(r_2 + \alpha, \underline{x}, x^*)] \quad (170)$$

$$\mathcal{K}_{R, n} = B_R r_1 r_2 [e^{-r_1 \bar{x}} \mathcal{J}(r_1 + \alpha, x^*, \bar{x}) - e^{-r_2 \bar{x}} \mathcal{J}(r_2 + \alpha, x^*, \bar{x})] \quad (171)$$

with  $B_L = -\psi_R(x^*)/[\nu W_N(x^*)]$ ,  $B_R = -\psi_L(x^*)/[\nu W_N(x^*)]$  as defined in Lemma 6, and

$$\begin{aligned} \mathcal{J}(\beta, a, b) &\equiv \int_a^b e^{\beta y} \sin(\omega_n(y - \underline{x})) dy \\ &= \frac{e^{\beta b} (\beta \sin(\omega_n(b - \underline{x})) - \omega_n \cos(\omega_n(b - \underline{x}))) - e^{\beta a} (\beta \sin(\omega_n(a - \underline{x})) - \omega_n \cos(\omega_n(a - \underline{x})))}{\beta^2 + \omega_n^2} \end{aligned} \quad (172)$$

*Proof.* From Theorem 1 and Lemma 2, the  $\varpi_H$  functions are

$$\varpi_{H,\underline{x},n}(x) = \frac{\nu}{\lambda_{KFE,n}} \partial_y \gamma_{KFE,n}(x, \underline{x}), \quad \varpi_{H,\bar{x},n}(x) = \frac{\nu}{\lambda_{KFE,n}} \partial_y \gamma_{KFE,n}(x, \bar{x})$$

Computing  $\partial_y \gamma_{KFE,n}(x, y)$ :

$$\partial_y \gamma_{KFE,n}(x, y) = \frac{2}{\ell} e^{\alpha(y-x)} \sin(\omega_n(x - \underline{x})) [\alpha \sin(\omega_n(y - \underline{x})) + \omega_n \cos(\omega_n(y - \underline{x}))]$$

At  $y = \underline{x}$ :  $\sin(0) = 0$  and  $\cos(0) = 1$ , so

$$\partial_y \gamma_{KFE,n}(x, \underline{x}) = \frac{2\omega_n}{\ell} e^{\alpha(\underline{x}-x)} \sin(\omega_n(x - \underline{x}))$$

Thus

$$\varpi_{H,\underline{x},n}(x) = \frac{\nu}{\lambda_{KFE,n}} \frac{2\omega_n}{\ell} e^{\alpha\underline{x}} e^{-\alpha x} \sin(\omega_n(x - \underline{x}))$$

and from  $\xi_{\underline{x}',n} = h'_{ss}(\underline{x}) \int_{\underline{x}}^{\bar{x}} x \varpi_{H,\underline{x},n}(x) dx$ :

$$\xi_{\underline{x}',n} = h'_{ss}(\underline{x}) \frac{\nu}{\lambda_{KFE,n}} \frac{2\omega_n}{\ell} e^{\alpha\underline{x}} \int_{\underline{x}}^{\bar{x}} x e^{-\alpha x} \sin(\omega_n(x - \underline{x})) dx = h'_{ss}(\underline{x}) \frac{\nu}{\lambda_{KFE,n}} \frac{2\omega_n}{\ell} e^{\alpha\underline{x}} \mathcal{I}_n$$

At  $y = \bar{x}$ :  $\sin(n\pi) = 0$  and  $\cos(n\pi) = (-1)^n$ , so

$$\partial_y \gamma_{KFE,n}(x, \bar{x}) = \frac{2\omega_n}{\ell} (-1)^n e^{\alpha(\bar{x}-x)} \sin(\omega_n(x - \underline{x}))$$

and  $\xi_{\bar{x}',n}$  follows by the same calculation.

For  $\xi_{x^{*'},n}$ , from Theorem 1:

$$\xi_{x^{*'},n} = F_{ss} \int_{\underline{x}}^{\bar{x}} x \varpi_{J,n}(x) dx, \quad \varpi_{J,n}(x) = \int_{\underline{x}}^{\bar{x}} \gamma_{KFE,n}(x, y) J_{x^*}(y) dy$$

By Fubini's theorem, swapping the order of integration:

$$\xi_{x^{*'},n} = F_{ss} \int_{\underline{x}}^{\bar{x}} J_{x^*}(y) \left[ \int_{\underline{x}}^{\bar{x}} x \gamma_{KFE,n}(x, y) dx \right] dy$$

The inner integral evaluates to

$$\int_{\underline{x}}^{\bar{x}} x \gamma_{KFE,n}(x, y) dx = \frac{2}{\ell} \sin(\omega_n(y - \underline{x})) e^{\alpha y} \int_{\underline{x}}^{\bar{x}} x e^{-\alpha x} \sin(\omega_n(x - \underline{x})) dx = \frac{2}{\ell} \sin(\omega_n(y - \underline{x})) e^{\alpha y} \mathcal{I}_n$$

Therefore

$$\xi_{x^{*'},n} = F_{ss} \frac{2}{\ell} \mathcal{I}_n \int_{\underline{x}}^{\bar{x}} J_{x^*}(y) \sin(\omega_n(y - \underline{x})) e^{\alpha y} dy$$

Since  $J_{x^*}(y)$  is piecewise with  $J_{x^*}(y) = B_L \psi'_L(y)$  for  $y < x^*$  and  $J_{x^*}(y) = B_R \psi'_R(y)$  for  $y > x^*$  (from Lemma 6), and  $\psi'_L(y) = r_1 r_2 (e^{r_1(y-\underline{x})} - e^{r_2(y-\underline{x})})$ ,  $\psi'_R(y) = r_1 r_2 (e^{r_1(y-\bar{x})} - e^{r_2(y-\bar{x})})$ , the integral splits into  $\mathcal{K}_{L,n} + \mathcal{K}_{R,n}$ . Each term involves integrals of the form  $\int e^{\beta y} \sin(\omega_n(y-\underline{x})) dy$ , which evaluate to (172).  $\square$

**Lemma 19** (Sum of  $\xi_{F,n}/\lambda_{KFE,n}$ ). *The eigenvalue-weighted sum of the  $\xi_{F,n}$  coefficients equals the steady-state aggregate price gap divided by the steady-state frequency:*

$$\sum_{n=1}^{\infty} \frac{\xi_{F,n}}{\lambda_{KFE,n}} = \frac{\bar{X}}{F_{ss}}$$

where  $\bar{X} = \int_{\underline{x}}^{\bar{x}} x h_{ss}(x) dx$  is the steady-state aggregate price gap.

*Proof.* The steady-state distribution  $h_{ss}(x)$  satisfies the KFE

$$(\zeta - \mathcal{K}^*)h_{ss} = F_{ss} \delta(x - x^*)$$

where  $\mathcal{K}^* = \nu \partial_x^2 + \bar{\pi} \partial_x$  is the KFE differential operator. The Green's function (resolvent) satisfies  $(\zeta - \mathcal{K}^*)G(x, y) = \delta(x - y)$  with Dirichlet boundary conditions. Comparing these equations:

$$h_{ss}(x) = F_{ss} \cdot G_{KFE}(x, x^*)$$

The eigenfunction expansion of the time-dependent Green's function (from Lemma 2) is  $G_{KFE}(x, y, t) = \sum_{n=1}^{\infty} \gamma_{KFE,n}(x, y) e^{-\lambda_{KFE,n} t}$ . The resolvent (steady-state Green's function) is obtained by integrating over time:

$$G_{KFE}(x, y) = \int_0^{\infty} G_{KFE}(x, y, t) dt = \sum_{n=1}^{\infty} \frac{\gamma_{KFE,n}(x, y)}{\lambda_{KFE,n}}$$

Therefore  $h_{ss}(x)/F_{ss} = \sum_{n=1}^{\infty} \gamma_{KFE,n}(x, x^*)/\lambda_{KFE,n}$ . Integrating against  $x$ :

$$\frac{1}{F_{ss}} \int_{\underline{x}}^{\bar{x}} x h_{ss}(x) dx = \sum_{n=1}^{\infty} \frac{1}{\lambda_{KFE,n}} \int_{\underline{x}}^{\bar{x}} x \gamma_{KFE,n}(x, x^*) dx = \sum_{n=1}^{\infty} \frac{\xi_{F,n}}{\lambda_{KFE,n}}$$

$\square$

#### H.1.4 Analytical derivation of $\varphi$ coefficients

**Lemma 20** (Unprimed  $\varphi$  coefficients). *The coefficients  $\varphi_{F,n}$ ,  $\varphi_{x^*,n}$ ,  $\varphi_{\underline{x},n}$ , and  $\varphi_{\bar{x},n}$  are given by*

$$\varphi_{F,n} = \nu \frac{2}{\ell} \omega_n \sin(\omega_n(x^* - \underline{x})) [e^{-\alpha \underline{x}} - e^{-\alpha \bar{x}} (-1)^n] e^{\alpha x^*} \quad (173)$$

$$\begin{aligned} \varphi_{x^*,n} &= F_{ss} \nu \frac{2}{\ell} \omega_n [\alpha \sin(\omega_n(x^* - \underline{x})) + \omega_n \cos(\omega_n(x^* - \underline{x}))] e^{\alpha x^*} \\ &\quad \times [e^{-\alpha \underline{x}} - e^{-\alpha \bar{x}} (-1)^n] \end{aligned} \quad (174)$$

$$\varphi_{\underline{x},n} = -\nu^2 h'_{ss}(\underline{x}) \frac{2}{\ell} \omega_n^2 [1 - e^{\alpha(\underline{x} - \bar{x})} (-1)^n] \quad (175)$$

$$\varphi_{\bar{x},n} = -\nu^2 h'_{ss}(\bar{x}) \frac{2}{\ell} \omega_n^2 [e^{\alpha(\underline{x} - \bar{x})} (-1)^n - 1] \quad (176)$$

where  $\ell = \bar{x} - \underline{x}$ ,  $\omega_n = \frac{n\pi}{\ell}$ , and  $\alpha = \frac{\pi}{2\nu}$ .

*Proof.* From Theorem 1 and Lemma 2, the coefficients  $\varphi_{\cdot,n}$  are defined by

$$\varphi_{\cdot,n} \equiv \nu (\varpi'_{\cdot,n}(\underline{x}) - \varpi'_{\cdot,n}(\bar{x})) \quad (177)$$

where the  $\varpi_{\cdot,n}(x)$  functions are defined in terms of the KFE Green's function component:

$$\gamma_{KFE,n}(x, y) = \frac{2}{\ell} e^{\alpha(y-x)} \sin(\omega_n(x - \underline{x})) \sin(\omega_n(y - \underline{x}))$$

Lemma 2 gives  $\varpi_{F,n}(x) = \gamma_{KFE,n}(x, x^*)$ . Therefore

$$\varpi_{F,n}(x) = \frac{2}{\ell} e^{\alpha(x^* - x)} \sin(\omega_n(x - \underline{x})) \sin(\omega_n(x^* - \underline{x}))$$

Take the derivative with respect to  $x$ :

$$\varpi'_{F,n}(x) = \frac{2}{\ell} e^{\alpha(x^* - x)} \sin(\omega_n(x^* - \underline{x})) [-\alpha \sin(\omega_n(x - \underline{x})) + \omega_n \cos(\omega_n(x - \underline{x}))]$$

Evaluating at  $x = \underline{x}$  (where  $\sin(0) = 0$  and  $\cos(0) = 1$ ):

$$\varpi'_{F,n}(\underline{x}) = \frac{2}{\ell} e^{\alpha(x^* - \underline{x})} \sin(\omega_n(x^* - \underline{x})) \omega_n$$

Evaluating at  $x = \bar{x}$  (where  $\sin(n\pi) = 0$  and  $\cos(n\pi) = (-1)^n$ ):

$$\varpi'_{F,n}(\bar{x}) = \frac{2}{\ell} e^{\alpha(x^* - \bar{x})} \sin(\omega_n(x^* - \underline{x})) \omega_n (-1)^n$$

Substitute into equation (177):

$$\begin{aligned}\varphi_{F,n} &= \nu \frac{2}{\ell} e^{\alpha x^*} e^{-\alpha \underline{x}} \sin(\omega_n(x^* - \underline{x})) \omega_n - \nu \frac{2}{\ell} e^{\alpha x^*} e^{-\alpha \bar{x}} \sin(\omega_n(x^* - \underline{x})) \omega_n (-1)^n \\ &= \nu \frac{2}{\ell} \omega_n \sin(\omega_n(x^* - \underline{x})) e^{\alpha x^*} [e^{-\alpha \underline{x}} - e^{-\alpha \bar{x}} (-1)^n]\end{aligned}$$

Lemma 2 gives  $\varpi_{x^*,n}(x) = F_{ss} \partial_y \gamma_{KFE,n}(x, x^*)$ . Computing  $\partial_y \gamma_{KFE,n}(x, y)$ :

$$\partial_y \gamma_{KFE,n}(x, y) = \frac{2}{\ell} e^{-\alpha x} \sin(\omega_n(x - \underline{x})) e^{\alpha y} [\alpha \sin(\omega_n(y - \underline{x})) + \omega_n \cos(\omega_n(y - \underline{x}))]$$

At  $y = x^*$ :

$$\varpi_{x^*,n}(x) = F_{ss} \frac{2}{\ell} e^{-\alpha x} \sin(\omega_n(x - \underline{x})) e^{\alpha x^*} [\alpha \sin(\omega_n(x^* - \underline{x})) + \omega_n \cos(\omega_n(x^* - \underline{x}))]$$

Taking the derivative with respect to  $x$  and evaluating at the boundaries (using the same trigonometric identities as before):

$$\begin{aligned}\varpi'_{x^*,n}(\underline{x}) &= F_{ss} \frac{2}{\ell} e^{-\alpha \underline{x}} e^{\alpha x^*} [\alpha \sin(\omega_n(x^* - \underline{x})) + \omega_n \cos(\omega_n(x^* - \underline{x}))] \omega_n \\ \varpi'_{x^*,n}(\bar{x}) &= F_{ss} \frac{2}{\ell} e^{-\alpha \bar{x}} e^{\alpha x^*} [\alpha \sin(\omega_n(x^* - \underline{x})) + \omega_n \cos(\omega_n(x^* - \underline{x}))] \omega_n (-1)^n\end{aligned}$$

Substitute into equation (177):

$$\varphi_{x^*,n} = F_{ss} \nu \frac{2}{\ell} \omega_n [\alpha \sin(\omega_n(x^* - \underline{x})) + \omega_n \cos(\omega_n(x^* - \underline{x}))] e^{\alpha x^*} [e^{-\alpha \underline{x}} - e^{-\alpha \bar{x}} (-1)^n]$$

Lemma 2 gives  $\varpi_{\underline{x},n}(x) = -\nu h'_{ss}(\underline{x}) \partial_y \gamma_{KFE,n}(x, \underline{x})$ . At  $y = \underline{x}$ :

$$\partial_y \gamma_{KFE,n}(x, \underline{x}) = \frac{2}{\ell} e^{-\alpha x} \sin(\omega_n(x - \underline{x})) e^{\alpha \underline{x}} \omega_n$$

Therefore:

$$\varpi_{\underline{x},n}(x) = -\nu h'_{ss}(\underline{x}) \frac{2}{\ell} e^{\alpha \underline{x}} e^{-\alpha x} \sin(\omega_n(x - \underline{x})) \omega_n$$

Taking the derivative

$$\varpi'_{\underline{x},n}(x) = -\nu h'_{ss}(\underline{x}) \frac{2}{\ell} e^{\alpha \underline{x}} \omega_n e^{-\alpha x} [-\alpha \sin(\omega_n(x - \underline{x})) + \omega_n \cos(\omega_n(x - \underline{x}))]$$

Evaluating at the boundaries:

$$\varpi'_{\underline{x},n}(\underline{x}) = -\nu h'_{ss}(\underline{x}) \frac{2}{\ell} e^{\alpha \underline{x}} \omega_n e^{-\alpha \underline{x}} \omega_n = -\nu h'_{ss}(\underline{x}) \frac{2}{\ell} \omega_n^2$$

$$\varpi'_{\underline{x},n}(\bar{x}) = -\nu h'_{ss}(\underline{x}) \frac{2}{\ell} e^{\alpha \underline{x}} \omega_n e^{-\alpha \bar{x}} \omega_n (-1)^n$$

Substitute into equation (177)

$$\begin{aligned} \varphi_{\underline{x},n} &= -\nu^2 h'_{ss}(\underline{x}) \frac{2}{\ell} \omega_n^2 + \nu^2 h'_{ss}(\underline{x}) \frac{2}{\ell} e^{\alpha(\underline{x}-\bar{x})} \omega_n^2 (-1)^n \\ &= -\nu^2 h'_{ss}(\underline{x}) \frac{2}{\ell} \omega_n^2 \left[ 1 - e^{\alpha(\underline{x}-\bar{x})} (-1)^n \right] \end{aligned}$$

Lemma 2 gives  $\varpi_{\bar{x},n}(x) = -\nu h'_{ss}(\bar{x}) \partial_y \gamma_{KFE,n}(x, \bar{x})$ . At  $y = \bar{x}$ :

$$\partial_y \gamma_{KFE,n}(x, \bar{x}) = \frac{2}{\ell} e^{-\alpha x} \sin(\omega_n(x - \underline{x})) e^{\alpha \bar{x}} \omega_n (-1)^n$$

Following the same steps,

$$\varpi'_{\bar{x},n}(\underline{x}) = -\nu h'_{ss}(\bar{x}) \frac{2}{\ell} e^{\alpha(\bar{x}-\underline{x})} \omega_n^2 (-1)^n, \quad \varpi'_{\bar{x},n}(\bar{x}) = -\nu h'_{ss}(\bar{x}) \frac{2}{\ell} \omega_n^2$$

Substitute into equation (177)

$$\varphi_{\bar{x},n} = -\nu^2 h'_{ss}(\bar{x}) \frac{2}{\ell} \omega_n^2 \left[ e^{\alpha(\underline{x}-\bar{x})} (-1)^n - 1 \right]$$

□

**Lemma 21** (Primed  $\varphi$  coefficients). *The primed  $\varphi$  coefficients are*

$$\varphi_{\underline{x}',n} = h'_{ss}(\underline{x}) \frac{\nu^2}{\lambda_{KFE,n}} \frac{2}{\ell} \omega_n^2 \left[ 1 - (-1)^n e^{-\alpha \ell} \right] \quad (178)$$

$$\varphi_{\bar{x}',n} = h'_{ss}(\bar{x}) \frac{\nu^2}{\lambda_{KFE,n}} \frac{2}{\ell} \omega_n^2 \left[ (-1)^n e^{\alpha \ell} - 1 \right] \quad (179)$$

$$\varphi_{x^*,n} = F_{ss} \nu (\varpi'_{J,n}(\underline{x}) - \varpi'_{J,n}(\bar{x})) \quad (180)$$

where  $\varpi_{J,n}(x) = \int_{\underline{x}}^{\bar{x}} \gamma_{KFE,n}(x, y) J_{x^*}(y) dy$ . Since  $J_{x^*}(y)$  is piecewise (defined in (26)), this evaluates to

$$\varphi_{x^*,n} = F_{ss} \nu \frac{2\omega_n}{\ell} [\mathcal{K}_{L,n} + \mathcal{K}_{R,n}] \quad (181)$$

where

$$\mathcal{K}_{L,n} = -\frac{\psi_R(x^*)}{\nu W_N(x^*)} \int_{\underline{x}}^{x^*} \psi'_L(y) \left[ e^{\alpha(y-\underline{x})} - (-1)^n e^{\alpha(y-\bar{x})} \right] \sin(\omega_n(y - \underline{x})) dy \quad (182)$$

$$\mathcal{K}_{R,n} = -\frac{\psi_L(x^*)}{\nu W_N(x^*)} \int_{x^*}^{\bar{x}} \psi'_R(y) \left[ e^{\alpha(y-\underline{x})} - (-1)^n e^{\alpha(y-\bar{x})} \right] \sin(\omega_n(y - \underline{x})) dy \quad (183)$$

and the functions  $\psi_L, \psi_R, W_N$  are defined in Lemma 6.

*Proof.* For  $\varphi_{\underline{x}',n} = h'_{ss}(\underline{x})\nu(\varpi'_{H,\underline{x},n}(\underline{x}) - \varpi'_{H,\underline{x},n}(\bar{x}))$ , recall  $\varpi_{H,\underline{x},n}(x) = \frac{\nu}{\lambda_{KFE,n}}\partial_y\gamma_{KFE,n}(x,\underline{x})$ . Taking the derivative with respect to  $x$ :

$$\varpi'_{H,\underline{x},n}(x) = \frac{\nu}{\lambda_{KFE,n}}\frac{2}{\ell}\omega_n e^{\alpha\underline{x}}e^{-\alpha x} [-\alpha \sin(\omega_n(x - \underline{x})) + \omega_n \cos(\omega_n(x - \underline{x}))]$$

At  $x = \underline{x}$ :  $\varpi'_{H,\underline{x},n}(\underline{x}) = \frac{\nu}{\lambda_{KFE,n}}\frac{2}{\ell}\omega_n^2$ .

At  $x = \bar{x}$ :  $\varpi'_{H,\underline{x},n}(\bar{x}) = \frac{\nu}{\lambda_{KFE,n}}\frac{2}{\ell}\omega_n e^{\alpha(\underline{x}-\bar{x})}\omega_n(-1)^n$ .

Thus

$$\varphi_{\underline{x}',n} = h'_{ss}(\underline{x})\frac{\nu^2}{\lambda_{KFE,n}}\frac{2}{\ell}\omega_n^2 [1 - (-1)^n e^{-\alpha\ell}]$$

The derivation for  $\varphi_{\bar{x}',n}$  follows similarly using  $\varpi_{H,\bar{x},n}(x) = \frac{\nu}{\lambda_{KFE,n}}\partial_y\gamma_{KFE,n}(x,\bar{x})$ .

From the definition  $\varpi_{J,n}(x) = \int_{\underline{x}}^{\bar{x}} \gamma_{KFE,n}(x,y)J_{x^*}(y)dy$ , differentiating under the integral sign:

$$\varpi'_{J,n}(x) = \int_{\underline{x}}^{\bar{x}} \partial_x \gamma_{KFE,n}(x,y)J_{x^*}(y)dy$$

Computing  $\partial_x \gamma_{KFE,n}(x,y)$  from (29):

$$\partial_x \gamma_{KFE,n}(x,y) = \frac{2}{\ell}e^{\alpha(y-x)} \sin(\omega_n(y - \underline{x})) [-\alpha \sin(\omega_n(x - \underline{x})) + \omega_n \cos(\omega_n(x - \underline{x}))]$$

At the boundaries,  $\sin(\omega_n(\underline{x} - \underline{x})) = 0$ ,  $\cos(\omega_n(\underline{x} - \underline{x})) = 1$ , and  $\cos(\omega_n(\bar{x} - \underline{x})) = (-1)^n$ , so

$$\partial_x \gamma_{KFE,n}(\underline{x},y) = \frac{2\omega_n}{\ell}e^{\alpha(y-\underline{x})} \sin(\omega_n(y - \underline{x}))$$

$$\partial_x \gamma_{KFE,n}(\bar{x},y) = \frac{2\omega_n}{\ell}(-1)^n e^{\alpha(y-\bar{x})} \sin(\omega_n(y - \underline{x}))$$

Therefore

$$\varpi'_{J,n}(\underline{x}) - \varpi'_{J,n}(\bar{x}) = \frac{2\omega_n}{\ell} \int_{\underline{x}}^{\bar{x}} J_{x^*}(y) [e^{\alpha(y-\underline{x})} - (-1)^n e^{\alpha(y-\bar{x})}] \sin(\omega_n(y - \underline{x}))dy$$

The lifting function  $J_{x^*}(y)$  is piecewise, with  $J_{x^*}(y) = -\frac{\psi_R(x^*)}{\nu W_N(x^*)}\psi'_L(y)$  for  $y < x^*$  and  $J_{x^*}(y) = -\frac{\psi_L(x^*)}{\nu W_N(x^*)}\psi'_R(y)$  for  $y > x^*$ . Splitting the integral at  $x^*$  yields two terms of the form

$$\mathcal{K}_{n,j} = \int e^{(\alpha+r_j)y} \sin(\omega_n(y - \underline{x})) dy$$

where  $r_j$  is an exponent from the homogeneous solution  $\psi'_L$  or  $\psi'_R$ . Applying the standard identity

$$\int e^{ay} \sin(by + c) dy = \frac{e^{ay}}{a^2 + b^2} (a \sin(by + c) - b \cos(by + c))$$

with  $a = \alpha + r_j$ ,  $b = \omega_n$ , and  $c = -\omega_n\underline{x}$ , each  $\mathcal{K}_{n,j}$  evaluates to a closed-form expression in the model

parameters. □

**Lemma 22** (Sum of  $\varphi_{F,n}/\lambda_{KFE,n}$ ). *The eigenvalue-weighted sum of the  $\varphi_{F,n}$  coefficients is*

$$\sum_{n=1}^{\infty} \frac{\varphi_{F,n}}{\lambda_{KFE,n}} = 1 - \frac{\zeta}{F_{ss}}$$

where  $F_{ss}$  is the steady-state frequency of price adjustment.

*Proof.* From the definition  $\varphi_{F,n} = \nu(\varpi'_{F,n}(\underline{x}) - \varpi'_{F,n}(\bar{x}))$  where  $\varpi_{F,n}(x) = \gamma_{KFE,n}(x, x^*)$ :

$$\sum_{n=1}^{\infty} \frac{\varphi_{F,n}}{\lambda_{KFE,n}} = \nu \left( \sum_{n=1}^{\infty} \frac{\partial_x \gamma_{KFE,n}(x, x^*)}{\lambda_{KFE,n}} - \sum_{n=1}^{\infty} \frac{\partial_x \gamma_{KFE,n}(\bar{x}, x^*)}{\lambda_{KFE,n}} \right)$$

Using the resolvent representation from Lemma 19,  $\sum_{n=1}^{\infty} \gamma_{KFE,n}(x, x^*)/\lambda_{KFE,n} = h_{ss}(x)/F_{ss}$ . Differentiating with respect to  $x$ :

$$\sum_{n=1}^{\infty} \frac{\partial_x \gamma_{KFE,n}(x, x^*)}{\lambda_{KFE,n}} = \frac{h'_{ss}(x)}{F_{ss}}$$

Therefore

$$\sum_{n=1}^{\infty} \frac{\varphi_{F,n}}{\lambda_{KFE,n}} = \frac{\nu}{F_{ss}} (h'_{ss}(\underline{x}) - h'_{ss}(\bar{x}))$$

From the steady-state frequency formula (82) with absorbing boundary conditions  $h_{ss}(\underline{x}) = h_{ss}(\bar{x}) = 0$ :

$$F_{ss} = \nu h'_{ss}(\underline{x}) - \nu h'_{ss}(\bar{x}) + \zeta$$

Rearranging:  $\nu(h'_{ss}(\underline{x}) - h'_{ss}(\bar{x})) = F_{ss} - \zeta$ . Substituting:

$$\sum_{n=1}^{\infty} \frac{\varphi_{F,n}}{\lambda_{KFE,n}} = \frac{F_{ss} - \zeta}{F_{ss}} = 1 - \frac{\zeta}{F_{ss}}$$

□

## H.2 Dynamic Solution Algorithm

The discrete time partial equilibrium (Definition 1) is a series of forwards- and backwards-looking linear equations. The series is infinite, so in practice it must be truncated at a finite number of eigenvalues  $\bar{n}$ . For low levels of trend inflation, a small  $\bar{n}$  choice (e.g. 20) is sufficient to achieve high accuracy, but the algorithm is fast and higher trend inflation levels require higher truncation indices, so I use  $\bar{n} = 1000$  in the numerical examples.

For an arbitrary truncation  $\bar{n}$  on the solution order, any standard solution method for linear macroeconomic models (Uhlig, 2001; Sims, 2002) can be used to solve for the equilibrium processes. Instead, this appendix presents a more concrete algorithm that solves for each aggregate term sequentially. This can be

helpful for diagnosing problems and understanding the code.

The objective of the algorithm is to find the equilibrium sequence of price gaps  $\hat{X}_t$ , boundaries  $\hat{x}_t^*$ ,  $\hat{\underline{x}}_t$ ,  $\hat{\bar{x}}_t$ , values  $\hat{V}_t^*$ ,  $\hat{\underline{V}}_t$ ,  $\hat{\bar{V}}_t$ , and flows  $\hat{F}_t$ . It proceeds by:

1. Find  $\hat{V}_t^*$  by Proposition 2. In lag operator notation equation (44) becomes

$$\hat{V}_{n,t}^* = s_{HJB,n} \left( \Theta_{MC,n}(x^*) (-MC_t) + \Theta_{v,n}(x^*) \hat{V}_t^* \right) + \theta_n \beta L^{-1} \hat{V}_{n,t}^*$$

where  $\theta_n \beta = e^{-\lambda_{KFE,n}} e^{-\rho} = e^{-\lambda_{HJB,n}}$ . Aggregate over  $n$  and rearrange to obtain

$$\hat{V}_t^* = \sum_{n=1}^{\bar{n}} \frac{s_{HJB,n} \Theta_{MC,n}(x^*)}{1 - \theta_n \beta L^{-1}} (-MC_t) + \left( \sum_{n=1}^{\bar{n}} \frac{s_{HJB,n} \Theta_{v,n}(x^*)}{1 - \theta_n \beta L^{-1}} \right) \hat{V}_t^*$$

Write as a lag-operator polynomial and invert:

$$\hat{V}_t^* = \frac{1}{1 - \sum_{n=1}^{\bar{n}} \frac{s_{HJB,n} \Theta_{v,n}(x^*)}{1 - \theta_n \beta L^{-1}}} \left[ \sum_{n=1}^{\bar{n}} \frac{s_{HJB,n} \Theta_{MC,n}(x^*)}{1 - \theta_n \beta L^{-1}} (-MC_t) \right]$$

2. Given  $\hat{V}_t^*$ , find  $\hat{\underline{V}}_t$  and  $\hat{\bar{V}}_t$  by Proposition 2. In lag operator notation they become

$$\hat{\underline{V}}_{n,t} = s_{HJB,n} \left( -\Theta_{MC,n}(\underline{x}) MC_t + \Theta_{v,n}(\underline{x}) \hat{V}_t^* \right) + \theta_n \beta L^{-1} \hat{\underline{V}}_{n,t}$$

$$\hat{\bar{V}}_{n,t} = s_{HJB,n} \left( -\Theta_{MC,n}(\bar{x}) MC_t + \Theta_{v,n}(\bar{x}) \hat{V}_t^* \right) + \theta_n \beta L^{-1} \hat{\bar{V}}_{n,t}$$

thus the aggregate values are

$$\hat{\underline{V}}_t = \sum_{n=1}^{\bar{n}} \hat{\underline{V}}_{n,t} = \left( \sum_{n=1}^{\bar{n}} \frac{-s_{HJB,n} \Theta_{MC,n}(\underline{x})}{1 - \theta_n \beta L^{-1}} \right) MC_t + \left( \sum_{n=1}^{\bar{n}} \frac{s_{HJB,n} \Theta_{v,n}(\underline{x})}{1 - \theta_n \beta L^{-1}} \right) \hat{V}_t^*$$

$$\hat{\bar{V}}_t = \sum_{n=1}^{\bar{n}} \hat{\bar{V}}_{n,t} = \left( \sum_{n=1}^{\bar{n}} \frac{-s_{HJB,n} \Theta_{MC,n}(\bar{x})}{1 - \theta_n \beta L^{-1}} \right) MC_t + \left( \sum_{n=1}^{\bar{n}} \frac{s_{HJB,n} \Theta_{v,n}(\bar{x})}{1 - \theta_n \beta L^{-1}} \right) \hat{V}_t^*$$

3. Given  $\hat{V}_t^*$ , find  $(\hat{x}_t^*, \hat{\underline{x}}_t, \hat{\bar{x}}_t)$  by Proposition 2. In lag operator notation equations (47), (48), and (49) become

$$\hat{x}_{n,t}^* = s_{HJB,n} \left( \chi_{x^*,n} (-MC_t) + \Xi_{x^*,n} \hat{V}_t^* \right) + \theta_n \beta L^{-1} \hat{x}_{n,t}^*$$

$$\hat{\underline{x}}_{n,t} = s_{HJB,n} \left( \chi_{\underline{x},n} (-MC_t) + \Xi_{\underline{x},n} \hat{V}_t^* \right) + \theta_n \beta L^{-1} \hat{\underline{x}}_{n,t}$$

$$\hat{\bar{x}}_{n,t} = s_{HJB,n} \left( \chi_{\bar{x},n} (-MC_t) + \Xi_{\bar{x},n} \hat{V}_t^* \right) + \theta_n \beta L^{-1} \hat{\bar{x}}_{n,t}$$

thus the aggregate boundaries are

$$\begin{aligned}\hat{x}_t^* &= \sum_{n=1}^{\bar{n}} \hat{x}_{n,t}^* = \left( \sum_{n=1}^{\bar{n}} \frac{SHJB,n \chi_{x^*,n}}{1 - \theta_n \beta L^{-1}} \right) (-MC_t) + \left( \sum_{n=1}^{\bar{n}} \frac{SHJB,n \Xi_{x^*,n}}{1 - \theta_n \beta L^{-1}} \right) \hat{V}_t^* \\ \hat{x}_t &= \sum_{n=1}^{\bar{n}} \hat{x}_{n,t} = \left( \sum_{n=1}^{\bar{n}} \frac{SHJB,n \chi_{\underline{x},n}}{1 - \theta_n \beta L^{-1}} \right) (-MC_t) + \left( \sum_{n=1}^{\bar{n}} \frac{SHJB,n \Xi_{\underline{x},n}}{1 - \theta_n \beta L^{-1}} \right) \hat{V}_t^* \\ \hat{\bar{x}}_t &= \sum_{n=1}^{\bar{n}} \hat{\bar{x}}_{n,t} = \left( \sum_{n=1}^{\bar{n}} \frac{SHJB,n \chi_{\bar{x},n}}{1 - \theta_n \beta L^{-1}} \right) (-MC_t) + \left( \sum_{n=1}^{\bar{n}} \frac{SHJB,n \Xi_{\bar{x},n}}{1 - \theta_n \beta L^{-1}} \right) \hat{V}_t^*\end{aligned}$$

4. Given  $(\hat{x}_t^*, \hat{x}_t, \hat{\bar{x}}_t)$ , find  $\hat{F}_t$  by Proposition 2. In lag operator notation equation (52) becomes

$$\hat{F}_{n,t} = \varsigma_{KFE,n} \left( \varphi_{F,n} \hat{F}_t + \varphi_{x^*,n} \hat{x}_t^* + \varphi_{\underline{x},n} \hat{x}_t - \varphi_{\bar{x},n} \hat{\bar{x}}_t \right) + \theta_n L \hat{F}_{n,t}$$

Aggregate over  $n$  and rearrange to obtain

$$\hat{F}_t = \left( \sum_{n=1}^{\bar{n}} \frac{\varsigma_{KFE,n} \varphi_{F,n}}{1 - \theta_n L} \right) \hat{F}_t + \sum_{n=1}^{\bar{n}} \frac{\varsigma_{KFE,n} \varphi_{x^*,n}}{1 - \theta_n L} \hat{x}_t^* + \sum_{n=1}^{\bar{n}} \frac{\varsigma_{KFE,n} \varphi_{\underline{x},n}}{1 - \theta_n L} \hat{x}_t - \sum_{n=1}^{\bar{n}} \frac{\varsigma_{KFE,n} \varphi_{\bar{x},n}}{1 - \theta_n L} \hat{\bar{x}}_t$$

Write as a lag-operator polynomial and invert:

$$\hat{F}_t = \frac{1}{1 - \sum_{n=1}^{\bar{n}} \frac{\varsigma_{KFE,n} \varphi_{F,n}}{1 - \theta_n L}} \left[ \sum_{n=1}^{\bar{n}} \frac{\varsigma_{KFE,n} \varphi_{x^*,n}}{1 - \theta_n L} \hat{x}_t^* + \sum_{n=1}^{\bar{n}} \frac{\varsigma_{KFE,n} \varphi_{\underline{x},n}}{1 - \theta_n L} \hat{x}_t - \sum_{n=1}^{\bar{n}} \frac{\varsigma_{KFE,n} \varphi_{\bar{x},n}}{1 - \theta_n L} \hat{\bar{x}}_t \right]$$

5. Calculate the aggregate price gap  $\hat{X}_t$  by Proposition 2. In lag operator notation equation (50) becomes

$$\hat{X}_{n,t} = \varsigma_{KFE,n} \left( \xi_{F,n} \hat{F}_t + \xi_{x^*,n} \hat{x}_t^* + \xi_{\underline{x},n} \hat{x}_t - \xi_{\bar{x},n} \hat{\bar{x}}_t \right) + \theta_n L \hat{X}_{n,t}$$

thus the aggregate price gap is

$$\hat{X}_t = \sum_{n=1}^{\bar{n}} \hat{X}_{n,t} = \sum_{n=1}^{\bar{n}} \frac{\varsigma_{KFE,n} \xi_{F,n}}{1 - \theta_n L} \hat{F}_t + \sum_{n=1}^{\bar{n}} \frac{\varsigma_{KFE,n} \xi_{x^*,n}}{1 - \theta_n L} \hat{x}_t^* + \sum_{n=1}^{\bar{n}} \frac{\varsigma_{KFE,n} \xi_{\underline{x},n}}{1 - \theta_n L} \hat{x}_t - \sum_{n=1}^{\bar{n}} \frac{\varsigma_{KFE,n} \xi_{\bar{x},n}}{1 - \theta_n L} \hat{\bar{x}}_t$$

## I Summary of Mathematical Notation

Steady-state objects are denoted with subscript  $ss$  (e.g.,  $h_{ss}(x)$ ,  $v_{ss}(x)$ ,  $F_{ss}$ ,  $x_{ss}^*$ ,  $\underline{x}_{ss}$ ,  $\bar{x}_{ss}$ ). For brevity, I suppress  $ss$  in integration limits, domain specifications, eigenfunction arguments, and coefficient subscript labels.

Symbol	Description
$\rho$	Discount rate
$\Psi$	Menu cost (cost to adjust price)
$\zeta$	Rate of free price adjustment opportunities
$\nu$	Variance of idiosyncratic shocks
$\bar{\pi}$	Trend inflation rate
$\eta$	Elasticity of substitution
$\sigma$	Risk aversion parameter
$\alpha$	Disutility of labor parameter
$\mu$	Frictionless optimal markup
$\mathbf{B}$	Quadratic profit loss parameter

Table 3: Fixed parameter values.

Symbol	Description
$h_{ss}(x)$	Steady-state density of firms over price gaps
$v_{ss}(x)$	Steady-state firm value function
$F_{ss}$	Steady-state frequency of price adjustment
$x_{ss}^*$	Steady-state reset point
$\underline{x}_{ss}$	Steady-state lower inaction boundary
$\bar{x}_{ss}$	Steady-state upper inaction boundary

Table 4: Primary steady-state objects.

Symbol	Description
$t$	Continuous time
$i$	Firm index
$C(t)$	Aggregate consumption at time $t$
$L(t)$	Aggregate labor at time $t$
$M(t)$	Money balances at time $t$
$P(t)$	Aggregate price level at time $t$
$W(t)$	Nominal wage at time $t$
$R(t)$	Nominal interest rate at time $t$
$D(t)$	Aggregate dividends at time $t$
$Q(t)$	Price of nominal bond at time $t$
$A_i(t)$	Idiosyncratic preference shifter at time $t$
$Y_i(t)$	Output of firm $i$ at time $t$
$Z_i(t)$	Idiosyncratic productivity of firm $i$ at time $t$
$L_i(t)$	Labor input of firm $i$ at time $t$

Table 5: Primitive aggregate and firm-level variables.

Symbol	Description	Formula
$x$	Price gap (firm state variable)	$x_i(t) = \log P_i(t) - \log Z_i(t) - \log W(t) - \mu$
$\underline{x}(t, \kappa), \bar{x}(t, \kappa)$	Lower/upper bounds of inaction region	—
$x^*(t, \kappa)$	Optimal reset value for price gap	—
$v(x, t, \kappa)$	Value function for firm with gap $x$	—
$h(x, t, \kappa)$	Density of firms over price gaps	—
$MC(t, \kappa)$	Aggregate marginal cost deviation	$MC(t, \kappa) = \log W(t) - \log \bar{W}(t)$
$F(t, \kappa)$	Frequency of price adjustment	—
$\phi(x)$	Initial distribution of price gaps	—
$\varphi(x)$	Terminal condition for value function	—

Notes: The aggregate shock size  $\kappa$  is included as an argument where relevant.

Table 6: Mean field game variables and definitions.

Symbol	Description	Formula
$\hat{x}^*(t)$	Derivative of optimal reset value w.r.t. shock	$\hat{x}^*(t) = \partial_\kappa x^*(t, 0)$
$\hat{\underline{x}}(t), \hat{\bar{x}}(t)$	Derivatives of inaction region bounds	$\hat{\underline{x}}(t) = \partial_\kappa \underline{x}(t, 0), \hat{\bar{x}}(t) = \partial_\kappa \bar{x}(t, 0)$
$\hat{v}(x, t)$	Derivative of value function	$\hat{v}(x, t) = \partial_\kappa v(x, t, 0)$
$\hat{h}(x, t)$	Derivative of price gap density	$\hat{h}(x, t) = \partial_\kappa h(x, t, 0)$
$\hat{F}(t)$	Derivative of frequency of price adjustment	$\hat{F}(t) = \partial_\kappa F(t, 0)$
$\hat{X}(t)$	Derivative of average price gap	$\hat{X}(t) = \partial_\kappa X(t, 0)$

Notes: Hatted objects denote derivatives with respect to aggregate shock size, evaluated at  $\kappa = 0$ .

Table 7: Perturbed mean field game variables.

Symbol	Description	Formula / Definition
$\lambda_{KFE,n}$	$n$ -th KFE eigenvalue	$\lambda_{KFE,n} = \zeta + \frac{\bar{\pi}^2}{4\nu} + \frac{\nu n^2 \pi^2}{(\bar{x}-\underline{x})^2}$
$\lambda_{HJB,n}$	$n$ -th HJB eigenvalue	$\lambda_{HJB,n} = \rho + \lambda_{KFE,n}$
$\gamma_{KFE,n}(x, y)$	KFE Green's component	$\frac{2}{\bar{x}-\underline{x}} e^{\frac{\bar{\pi}}{2\nu}(y-x)} \sin\left(\frac{n\pi(x-\underline{x})}{\bar{x}-\underline{x}}\right) \sin\left(\frac{n\pi(y-\underline{x})}{\bar{x}-\underline{x}}\right)$
$\gamma_{HJB,n}(x, y)$	HJB Green's component	$\gamma_{KFE,n}(y, x)$
$\varpi_{S,n}(x)$	KFE shock coefficient	$\int_{\underline{x}}^{\bar{x}} \gamma_{KFE,n}(x, y) h'_{ss}(y) dy$
$\varpi_{F,n}(x)$	KFE FPA coefficient	$\gamma_{KFE,n}(x, x^*)$
$\varpi_{J,n}(x)$	KFE reset-point lifting coeff.	$\int_{\underline{x}}^{\bar{x}} \gamma_{KFE,n}(x, y) J_{x^*}(y) dy$
$\varpi_{H,\underline{x},n}(x)$	KFE lower-bound lifting coeff.	$\frac{\nu}{\lambda_{KFE,n}} \partial_y \gamma_{KFE,n}(x, \underline{x})$
$\varpi_{H,\bar{x},n}(x)$	KFE upper-bound lifting coeff.	$\frac{\nu}{\lambda_{KFE,n}} \partial_y \gamma_{KFE,n}(x, \bar{x})$
$\xi_{0,n}$	Price gap shock coefficient	$\int_{\underline{x}}^{\bar{x}} \int_{\underline{x}}^{\bar{x}} x h'_{ss}(y) \gamma_{KFE,n}(x, y) dy dx$
$\xi_{F,n}$	Price gap FPA coefficient	$\int_{\underline{x}}^{\bar{x}} x \gamma_{KFE,n}(x, x^*) dx$
$\xi_{x^*,n}$	Price gap reset coefficient	$F_{ss} \int_{\underline{x}}^{\bar{x}} x \partial_y \gamma_{KFE,n}(x, x^*) dx$
$\xi_{\underline{x},n}$	Price gap lower boundary coeff.	$-\nu h'_{ss}(\underline{x}) \int_{\underline{x}}^{\bar{x}} x \partial_y \gamma_{KFE,n}(x, \underline{x}) dx$
$\xi_{\bar{x},n}$	Price gap upper boundary coeff.	$-\nu h'_{ss}(\bar{x}) \int_{\underline{x}}^{\bar{x}} x \partial_y \gamma_{KFE,n}(x, \bar{x}) dx$
$\Theta_{MC,n}(x)$	HJB MC coefficient	$-2\mathbf{B} \int_{\underline{x}}^{\bar{x}} \gamma_{HJB,n}(x, y) y dy$
$\Theta_{v,n}(x)$	HJB value coefficient	$-\zeta \int_{\underline{x}}^{\bar{x}} \gamma_{HJB,n}(x, y) dy + \nu \partial_y \gamma_{HJB,n}(x, \underline{x}) - \nu \partial_y \gamma_{HJB,n}(x, \bar{x})$
$\chi_{x^*,n}$	Reset boundary MC coeff.	$-\frac{1}{\partial_x^2 v_{ss}(x^*)} \Theta'_{MC,n}(x^*)$
$\Xi_{x^*,n}$	Reset boundary value coeff.	$-\frac{1}{\partial_x^2 v_{ss}(x^*)} \Theta'_{v,n}(x^*)$
$\chi_{\underline{x},n}$	Lower boundary MC coeff.	$-\frac{1}{\partial_x^2 v_{ss}(\underline{x})} \Theta'_{MC,n}(\underline{x})$
$\Xi_{\underline{x},n}$	Lower boundary value coeff.	$-\frac{1}{\partial_x^2 v_{ss}(\underline{x})} \Theta'_{v,n}(\underline{x})$
$\chi_{\bar{x},n}$	Upper boundary MC coeff.	$-\frac{1}{\partial_x^2 v_{ss}(\bar{x})} \Theta'_{MC,n}(\bar{x})$
$\Xi_{\bar{x},n}$	Upper boundary value coeff.	$-\frac{1}{\partial_x^2 v_{ss}(\bar{x})} \Theta'_{v,n}(\bar{x})$
$\varphi_{\cdot,n}$	FPA coefficients	$\nu \varpi'_{\cdot,n}(\underline{x}) + \bar{\pi} \varpi_{\cdot,n}(\underline{x}) - \nu \varpi'_{\cdot,n}(\bar{x}) - \bar{\pi} \varpi_{\cdot,n}(\bar{x})$

Notes: Steady-state objects use  $ss$  notation. For compactness,  $ss$  is suppressed in integration limits and eigenfunction arguments.

Table 8: Intermediate constructed variables and coefficients.

Symbol	Description	Notes
$p_t$	Aggregate price gap (PED)	$p_t \propto \hat{X}_{\text{crit},t} + \hat{X}_{\text{int},\hat{n},t}$
$p_t^*$	Optimal reset price gap (PED)	$p_t^* \propto \hat{x}_{\hat{n},t}^*$
$\underline{p}_t$	Lower inaction boundary (PED)	$\underline{p}_t \propto \hat{x}_{\hat{n},t}$
$\bar{p}_t$	Upper inaction boundary (PED)	$\bar{p}_t \propto \hat{x}_{\hat{n},t}$
$V_t^*$	Value at reset point (PED)	$V_t^* = \hat{V}_{\hat{n},t}^*$
$\underline{V}_t$	Value at lower boundary (PED)	$\underline{V}_t = \hat{V}_{\hat{n},t}$
$\bar{V}_t$	Value at upper boundary (PED)	$\bar{V}_t = \hat{V}_{\hat{n},t}$
$F_t$	Frequency of price adjustment (PED)	$F_t \propto \hat{F}_{\text{crit},t} + \hat{F}_{\text{int},\hat{n},t}$
$MC_t$	Aggregate marginal cost (discrete time)	Exogenous or from GE
$\xi_{p^*,n}$	Composite price gap coefficient	$\xi_{x^*,n} + \xi_{\underline{x},n} - \xi_{\bar{x},n}$
$\varphi_{p^*,n}$	Composite FPA coefficient	$\varphi_{x^*,n} + \varphi_{\underline{x},n} - \varphi_{\bar{x},n}$

*Notes:* Subscript  $\hat{n}$  denotes the primary eigenfunction index. The critical-point components  $\hat{X}_{\text{crit},t}$  and  $\hat{F}_{\text{crit},t}$  are algebraic, while interior components  $\hat{X}_{\text{int},\hat{n},t}$  and  $\hat{F}_{\text{int},\hat{n},t}$  are dynamic states.

Table 9: Primary Eigenfunction Discretization (PED) variables.